ACTIVE VIBRATION CONTROL OF SMART BEAM AND CIRCULAR PLATE

A DISSERTATION

Submitted in partial fulfillment of the requirements for the award of the degree of

MASTER OF TECHNOLOGY

in

MECHANICAL ENGINEERING

(With Specialization in Machine Design Engineering)

By

CHANDRA BAHADUR KHATRI

DEPARTMENT OF MECHANICAL AND INDUSTRIAL ENGINEERING
INDIAN INSTITUTE OF TECHNOLOGY ROORKEE
ROORKEE - 247 667 (INDIA)

JUNE, 2011

INDIAN INSTITUTE OF TECHNOLOGY ROORKEE
ROORKEE

CANDIDATE'S DECLARATION

I hereby declare that the work carried out in this project report entitled "**ACTIVE VIBRATION CONTROL OF SMART BEAM AND CIRCULAR PLATE**" is presented on behalf of partial fulfillment of the requirement for the award of the degree of **Master of Technology** with specialization in **Machine Design Engineering**, submitted to the **Mechanical & Industrial Engineering Indian Institute of Technology Roorkee, India**, under the supervision of Dr. B.K. Mishra, Professor and Dr. I.V. SINGH, Assistant Professor, MIED, IIT Roorkee, India.

I have not submitted the matter embodied in this report for the award of any other degree or diploma.

Date: 30-June-2011
Place: **Roorkee**

CHANDRA BAHADUR KHATRI

CERTIFICATION

This is to certify that the above statement made by the candidate is correct to the best of our knowledge and belief.

Dr. B. K. MISHRA
Professor,
M.I.E.D.
IIT Roorkee, India

Dr. I.V. SINGH
Assistant Professor,
M.I.E.D
IIT Roorkee, India

ACKNOWLEDGEMENT

I wish to express immense pleasure and sincere thanks to **Dr. B.K. MISHRA, professor**, and, **Dr. I.V. SINGH, Assistant professor** in the Department of **Mechanical & Industrial** Engineering, IIT Roorkee for their valuable guidance and support. This work is simply the reflection of their thoughts, ideas and concepts and about their efforts. Working under their guidance was a privilege and an excellent learning experience that I will cherish for a long time.

I also express my heartful thanks to **Dr. S.C. SHARMA, Professor & Head Of Department, Mechanical & Industrial** Engineering for his encouragement and overall supervision in bringing out this dissertation report.

I also thank **Dr. S. P. Harsha,** Assistant Professor, MIED for his valuable suggestions and fruitful discussions related to this work and also for providing me a chance to work in vibrations and automation laboratory. I would also like to thanks the technical as well as non technical staff of vibrations and automation laboratory and tin smithy shop, Mechanical & Industrial Engineering for all their help and support.

I express my regards to my parents who have been a constant source of inspiration to me. Finally I would like to thank all my friends, for their help and encouragement at the hour of need.

JUNE 2011

Place: Roorkee

Chandra Bahadur Khatri
Enrollment No-09539004
M.Tech-II year
Machine Design Engg.
M.I.E.D.
I.I.T. Roorkee

ABSTRACT

Recent advances in materials science have led to the development of a range of functional materials which when embedded into a structure can produce and monitor structural deformations. These structures have been labeled 'smart structures' and such materials are known as 'smart materials'. Smart materials have the ability to change shape or size simply by adding or removing a little bit of energy. Thus, they have the capability to 'feel' a stimulus and suitably react to it just like any living organism. Each individual type of smart material has a different property which can be significantly altered, such as viscosity, volume, and conductivity. The field of smart structures and its control has come up as an emerging area of research especially in aerospace industry. This dissertation deals with the experimental and numerical assessment of the vibration suppression of smart structures using piezoelectric materials. These materials are usually thin wafers, which are poled in the thickness direction and bonded to the surfaces of the host structures. Piezoelectric material such as PZT patch (Piezoceramic patch) is equally effective as sensor and actuator. PZT patch is useful in vibration control because of advantages of high stiffness, light weight, low power consumption and easy implementation.

Active control methods use external active devices to generate a second set of disturbance of equal amplitude but opposite phase to cancel the targeted unwanted disturbance. Unlike passive control, active control needs an external power supply to its control system. A typical active control system is composed of three basic component; sensors, actuators and controller.

An experimental setup is developed to measure and control the vibration of a cantilevered aluminum straight beam (L=263mm, W=29mm & T= 1.5mm). One pair of piezoelectric patches of size (25 x 25 x 0.5) is mounted on the beam near the fixed side and other pair of piezoelectric patches is mounted on the beam near the midpoint. The patches are bonded in a symmetrical fashion on the opposite sides of the beam. One of the patch acts as a sensor and the other acts as an actuator. The experimental setup consist of piezoelectric material, i.e., PZT patches, an Aluminium cantilever beam, Vibration control unit (Piezo sensing and actuation system), USB based Data acquisition card (NI make), a function generator and a computer with LAB View software version 8.6. The beam is excited by

function generator at the free end in order to vibrate it in the first mode. As the beam deforms, an electric potential difference develops across the thickness of the sensor patch. The electric signal from the sensor is amplified by the control system to obtain the feedback voltage. This feedback voltage is supplied to the actuator patch. The force applied by the actuator induces a counteractive deformation to the beam structure and the amplitude of vibration is suppressed. Using this setup, Proportional Feedback Control was investigated for the cantilever beam, and a close co-relation was found between the theoretical predictions and experimental observations, thus establishing the authenticity of the theoretical derivations.

Further, the experimental work was extended to investigate the behavior of an axially clamped circular plate (outer radius=300mm, inner radius=90mm and thickness=0.5mm) to peripheral vibrations. Such thin disks find a wide range of uses in engineering applications. Using experimental data, an expression was obtained for vibration reduction as a function of the angular distance between exciting force and the sensor, thereby making it possible to achieve angular optimization. Further the vibration control of beam and circular plate is obtained through multiple patches which show that vibration control increases with increase in number of patches and also increases with increase in area covered by the patches.

CONTENTS

NOMENCLATURE

Notation	Definition
DSP	: Digital Signal Processing
PZT	: Piezo-electric (Lead Zirconate titanate)
PVDF	: Polyvinylidene fluoride
SMA	: Shape Memory Alloy
LQG	: Linear Quadratic Gaussian
SSA	: Self Sensing Actuator
LQR	: Linear Quadratic Regulator
CPT	: Classical Plate theory
MIMO	: Multi-input and multi-output
GA	: Genetic algorithms
VEM	: Viscoelastic material
PCLD	: Passive constrained layer damping
h	: Plate thickness
q	: Distributed transverse load
u	: Displacement vector (in x-axis)
v	: Displacement vector (in y- axis)
w	: Displacement vector (in z-axis)
t	: Time
γ	: Shear stain
G	: Control gain
N	: Force resultant
M	: Moment resultant
P	: Load
F_s	: Reaction force of elastic foundation
D_{ij}	: Bending stiffness
D	: Flexural stiffness
I_o	: Principal inertia
I_2	: Rotary Inertia

J_n : Bessel function of first kind

Y_n : Bessel function of second kind

I_n : Modified Bessel function of first kind

K_n : Modified Bessel function of second kind

V : Shear force

R_o : Outer radius

R_i : Inner radius

k : Elastic foundation modulus

Greek symbols:

Ω_o : Mid-plane of the plate

ε : Strain field

σ : Stress field

υ : Poisson ratio

α : Co-efficient of thermal expansion

ω : Angular frequency

ρ : Mass density

ϵ : Permittivity coefficient

Subscripts:

r : Refers to r direction

o : Refers to a point on the mid plane(i.e. Z=0)

θ : Refers to Θ direction

z : Refers to Z direction

S : No of nodal circle

s : Refers to sensor

a : Refers to actuator

$\acute{\emptyset}$: Electric

u : Elastic

LIST OF FIGURES

LIST OF TABLES

CHAPTER1 INTRODUCTION

1.1 Motivation

Vibration analysis and control of a structure are among the major research subjects in mechanical, aerospace, civil engineering and other related disciplines and are vital for many industrial applications. Structural damping refers to the capacity of a structure or structural component to dissipate energy or to its capacity for removing, from the structural vibration, some of the energy associated with that vibration. This removed energy may be converted directly to heat and transferred to connected structure or to the ambient media.

Flexible mechanical systems experience undesirable vibration in response to environmental and operational forces. The very existence of vibrations can limit the accuracy of sensitive instruments or cause significant error in applications where high-precision positioning is essential. In many scientific and engineering applications, vibrations control is a necessity. Structural vibration suppression has attracted the attention of engineers since machines with moving parts and vehicles were invented.

Control has been of great interest due to applications requiring low weight, lower energy consumption, ease of handling, safer operation due to reduced inertia, and high speed applications. Flexible structure control is extensively used in space applications such as potential solar power satellites, large antennas, and large space robots, but is of equal interest for terrestrial applications, such as high speed robots, large bridges, and others. Despite some of the merits listed above, light weight generally implies flimsiness with attendant difficulties such as long decay of vibration, fatigue and instability, and difficulty of accurate position and force tracking which are very important in vibration, position, shape, and force control. The use of highly flexible structures demands sophisticated controllers to overcome these problems.

Control of flexible structures has been an ongoing field of research for the past few decades. Among different control problems, "Vibration Control" is not only intrinsically important, but also is an issue of importance as it relates to many other flexible structural

tasks such as position, shape, and force control.

There are two major approaches for vibration control: passive and active. In passive control technique, the material properties of structures such as damping and stiffness are modified so as to change the response of structures. The two most essential components of passive vibration isolator are its load-supporting means (stiffness) and its energy dissipating means (damping). Typical passive isolator employs metallic springs, elastomers, wire cables, pneumatic springs. They don't require external power in order to function properly. They are very effective in the middle to high frequency range. However, passive control approaches become ineffective when the dynamics of the system and/or the frequencies of the disturbance vary with time. They are often impractical to implement in the low frequency range, where the disturbance wavelength is relatively long and the passive control methods require bulky/heavy installations. In many applications, such as in aeronautical industries, where minimizing the structural weight is paramount in the system designs involving large and heavy passive control appendages are impractical. Hence due to theses drawbacks active vibration control technique is frequently used in order to eliminate the undesired vibration. Particularly in recent years, due to the progresses in electronic technology and the availability of low cost electronic components, they experienced a dramatic gain in interest.

Active vibration control techniques have experienced rapid developments in last thirty years in industries like aerospace and automotive industry. It is mostly governed by the need of lightweight solutions for the aerospace technology. When traditional passive vibration control techniques fail to meet the requirements, active vibration control using smart materials in conjunction with various control strategy can be used to suppress vibrations in an effective way. A conventional approach with passive damping materials minimizes the structural vibrations but they add substantial amount of weight to the structure and thus minimize their performance. However, active vibration techniques using smart materials offer light weight high performance solutions to the vibration problems. Rising costs for gasoline and increased environmental concerns have compelled the automotive and aircraft industries to search for lighter damping solutions for their products. Automotive and

aircraft industries are spending millions of dollars every year on research for new lighter materials and new technologies like active vibration damping strategy. Decreasing the mass of passive damping materials in today's automobiles could lead to better fuel economy and hence to lower emission of greenhouse gases and pollution. Smart material based actuators and sensors are generally small and lightweight and hardly contribute to the mass of the structure.

An important issue in active control systems is sensor and actuator selection. In the recent years, there has been great interest among engineers to build "smart" structure that have capability to adjust their properties and shapes to the changing environment. Smart structure can be defined as structures that are capable of sensing and actuating in a controlled manner in response to a given input. The adjustments in such structures are made through the use of actuators. Different materials can be used as sensor and actuator elements. They are controlled through electric, magnetic, thermal or light energy. Some of the common actuator and sensor materials include: Piezoelectric materials, and electro-rheological fluids. Piezoelectric transducers have become increasingly popular in vibration control applications. They provide excellent actuation and sensing capabilities. The ability of piezoelectric materials to transform mechanical energy into electrical energy and vice versa makes them suitable for both sensor and actuator applications. Other advantages include: simple integration into the structure; a readily obtainable commercial supply of piezopolymers and Piezoceramic. The two common types of piezoelectric materials are lead zirconate titanate (PZT) ceramics and polyvinylidene fluoride (PVDF) polymers.

Among the different types of smart transducers, distributed piezoelectric sensors and actuators have received the most attention because of certain features such as: low mass and passive dynamic effect, high bandwidth, low cost, ease of bonding onto or embedding within flexible structures, capability of a wide frequency range of control etc.

Recent studies in the areas of smart structures inclined more attention towards piezoelectric materials as compared to conventional discrete sensing and control systems. Piezoelectric materials act as a coupling between mechanical and electrical properties which convert electrical to mechanical energy and vice-versa. This makes them suitable as

actuators and sensors. Bonded piezoelectric patches in a structure act as sensor to monitor or as actuator to control the response of the structure. In addition to these properties piezoelectric materials have several other characteristics such as quick response, lower power consumption, high efficiency and compactness, easily mounted on the structures and low weight etc. Piezoelectric patches are available in two forms: multi layered active materials and multi phase active materials [34]. Multi layered active materials are stack of active materials in which large fields are obtained with the moderate level of input voltage. It is manufactured by tape casting technology and electrodes are embedded in several different ways. The multi layered composite system is also amenable to miniaturization in order to decrease the thickness of active multi layers.

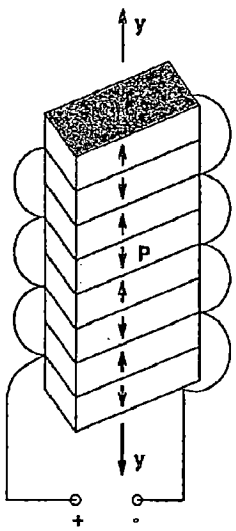

Figure 1.1: A multi-layer actuator [34]

Multi-phase composite systems consist of an active phase embedded in a passive matrix (e.g. PZT rods in a polymer matrix). Different connectivity schemes are possible in a two-phase system. The multi-phase composites are most often useful when there are conflicting requirements on the active material system. This type of active-passive phase combinations helps in achieving multifunctionality.

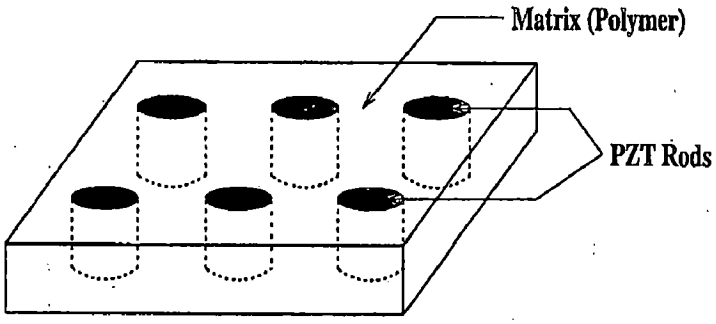

Figure 1.2: A schematic of a 1-3 connectivity composite [34]

The piezoelectric materials are frequently used as sensor/ actuator in the smart structure for vibration suppression. In the smart structures, sensing and actuation mechanism become parts of the structure itself. However, for the complex structure, it is very much costly to implement smart materials over the entire surface. Hence sensor and actuator are distributed discretely over the entire structure. One of the main limitations of the piezoelectric actuator is the amount of force it exerts. Hence, actuator should be placed at the optimal location in order to minimize the control effort. Hence, optimization of the placement of the sensor and actuator over the structure is one of the challenging tasks in the suppression of the vibration of structure. The problem becomes so much critical when the no of sensor/actuator increases and the mode shape becomes complicated. Due to these problems optimization technique has to be used in order to investigate a good set of sensor/actuator position. Several optimization techniques such as Genetic Algorithms, Tabu Search, Simulated Annealing and Hill Climbing may be used for this purpose.

1.2 Preamble

The primary objective of this study is to develop an experimental setup to demonstrate the use of piezoelectric material like PZT patch in the active vibration control application. This setup includes the piezoelectric material i.e. PZT patches, data acquisition card, signal conditioner and a computer with Lab VIEW software. An aluminum beam is mounted in the cantilever configuration and an aluminum circular plate mounted in axially clamped configuration are both excited by using a function generator. The vibration of the

beam is controlled by the using multi-piezo actuation system by increasing the gain. As the structures deforms, due to external applied loads, the bonded piezoelectric film (sensor) also deforms, and due to its constitutive behavior, it develops a voltage proportional to the strain. The voltage is then amplified by a control system, to obtain the feedback voltage. This feedback voltage is supplied to the other piezoelectric film (actuator) that induces a counteractive deformation to the structures and the amplitude of vibration is suppressed.

1.3 Organization of the thesis

Chapter 2 explains the background of the smart materials and piezoelectric material. Strategies of the active vibration control have been discussed.

Chapter 3 contains a brief discussion regarding the previous work that has been done in this field. A Summary of work carried out by different authors, their objectives and conclusions are presented in this chapter.

Chapter 4 details the development of the finite element model. The derivation of the equations of motion with sensor and actuator equations are given in detail. Control strategies used in the present work are also discussed.

Chapter 5 describes the experimental setup for the active vibration control. This includes the specification of the apparatus used in the experimental setup and their uses in the experiment. Procedure of active vibration control is also explained.

Chapter 6 presents the results and discussion of the present work. The controlled and uncontrolled responses of cantilever beam and axially clamped circular plate are compared numerically and experimentally.

Chapter 7 presents the conclusion of the present work.

Chapter 8 presents the scope for future work.

CHAPTER 2 BACKGROUND

This chapter gives an introduction of the smart material in general along with a description of piezoelectric material. It also covers the active vibration control strategies for vibration suppression.

2.1 Perspectives in smart Structure

A structure is an assembly that performs engineering function e.g. building, bridge, power plant, ship, Jet engine and space craft etc. It is reasonable to expect that all engineering design should be smart and not dumb. But one can still make a distinction between smartly designed structures and smart structures. The latter term has acquired a specific technical meaning over the last few decades. Smart structures are structures that are capable of sensing their environment and take suitable corrective measures in a predictable and desired manner through the integration of various elements such as sensors, actuators, power sources, signal processors and communication network etc. The integrated structure is called smart structure because it has ability to sense, measure, process and diagnoses at critical locations for any change in selected variables and to command suitable action to restore structural integrity and continue to perform the required function. The variable may be deformation, change in temperature and pressure, and change in state and phase and may be optical, electrical, magnetic, chemical or biological. In addition to carrying mechanical loads, smart structures may alleviate vibration, reduce acoustic noise, and monitor their own condition and environment, automatically perform precision alignments, or change their shape or mechanical properties [39].The development in the field of smart structures totally depends on the development of material science and the control logic. In the field of material science, various new smart materials are developed that allow them to be used for sensing and actuation in an efficient and controlled manner. Smart materials, similar to living beings, have the ability to perform both sensing and actuating functions and are capable of adapting to changes in the environment. In other words, smart materials call change themselves in response to an outside stimulus or respond to the stimulus by producing a signal of some sort. By utilizing these materials, a complicated part in a system consisting of individual structural, sensing, and actuating components can now exist in a

single component, thereby reducing overall size and complexity of the system.

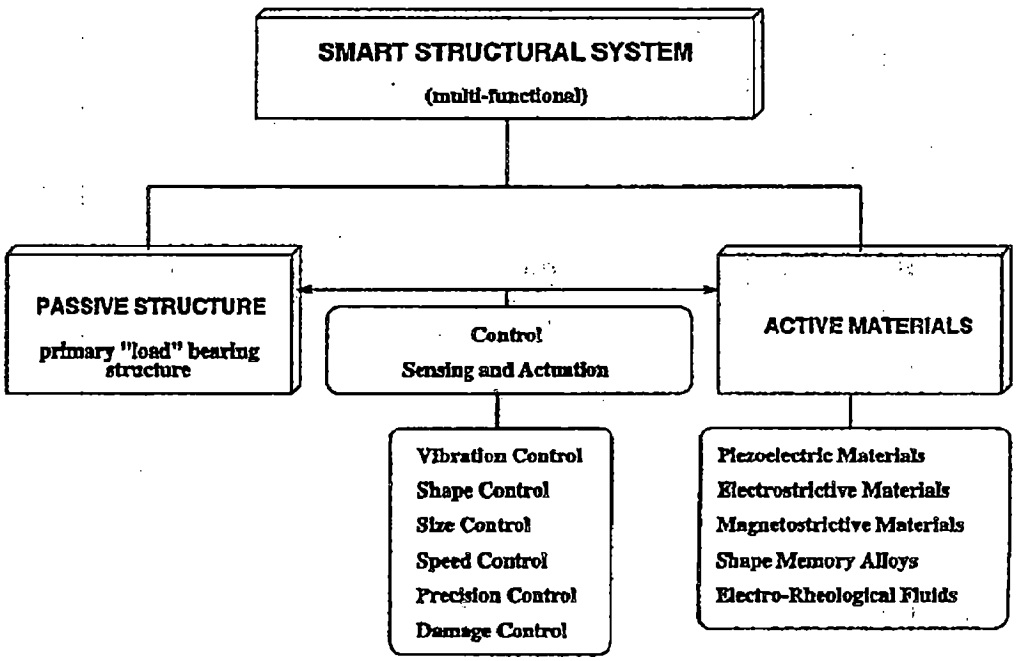

Figure 2.1 (a): Components of smart structure system [34]

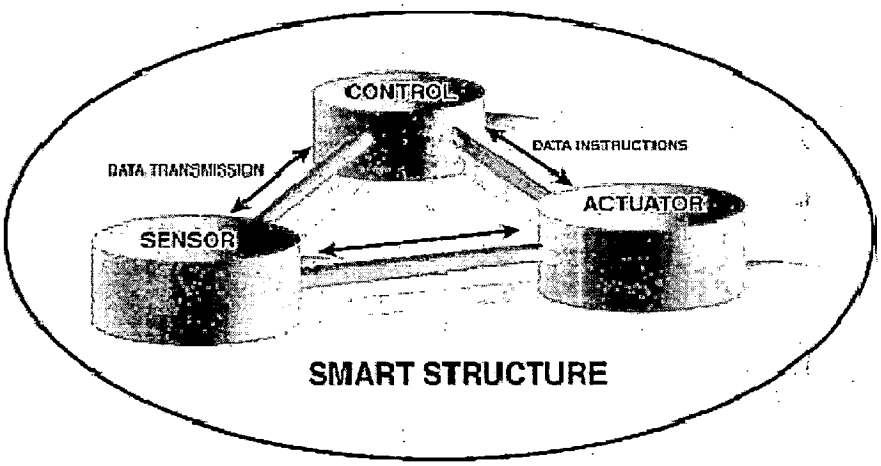

Figure 2.1 (b): Components of smart structure system [2]

Smart materials are thus defined as having the capability to 'feel' a stimulus and suitably react to it just like any living organism. Each individual type of smart material has a different property which can be significantly altered, such as viscosity, volume, and

conductivity. The property that can be altered influences the likely types of applications of the smart material. In the recent years, there has been great interest among engineers to builds "smart" structure that have capability to adjust their properties and shapes to the changing environment. The adjustments in such structures may be made through the use of actuators. The attenuation of vibrations is a problem of primary importance in many engineering fields, particularly so in aerospace applications.

Smart materials can be conveniently subdivided into passively and actively smart materials. A passively smart material responds to an external change without thought or signal processing while an actively smart material analyzes the sensed signal, perhaps for its frequency components, and then makes a choice as to what type of response to make.

A variety of smart material already exists, and is being researched extensively Theses includes shape memory alloy, piezoelectric material, magnetostrictive material, electrostrictive material, ferromagnetic shape memory alloy, electrorheologlcal and magnetorehological fluids and fiber optics etc.

2.1.1 Shape Memory Alloy (SMA)

Shape memory alloys (SMAs) are the most common group of metallic materials that can be deformed and can revert back to their original (undeformed) shapes when heated above their transformation temperatures. The first developed SMA was an alloy of nickel and titanium called Nitinol, which was discovered by scientists at the U S Naval Ordnance Laboratory in 1965. This alloy can deform up to 10 % and still regain its original form. Beyond this limit, it deforms plastically and does not regain its ordinal shape. SMAs are mostly used as actuators; SMAs are materials that "change shape, stiffness, position, natural frequency, and other mechanical characteristics in response to temperature or electromagnetic fields". The potential uses for SMAs especially as actuators have broadened the spectrum of many scientific fields. The study of the history and development of SMAs can provide an insight into a material involved in cutting-edge technology. SMA are deformed from their original atomic configuration, it regains its original geometry by itself during heating (one-way effect) or, at higher ambient temperatures, simply during unloading

(pseudo-elasticity or super elasticity). A remarkable characteristic of SMA material is its large change of modulus of elasticity with heating. The newest types of SMAs are combinations of copper and zinc that are alloyed with other metals such as aluminum. The shape memory effect is shown in Figure 2.2. Basically, shape recovery is due to solid-to-solid phase transformation from martensite to austenite [47].

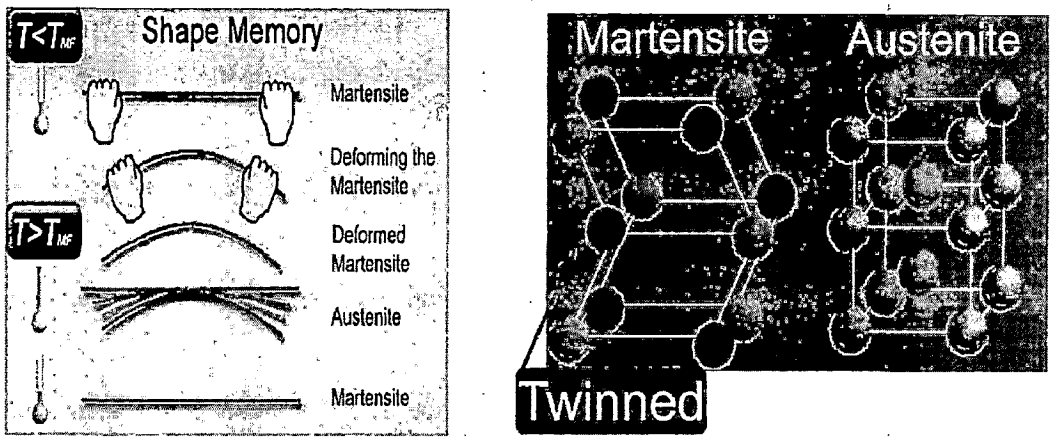

Figure 2.2: Shape memory effect [48].

The main use of SMA is especially as actuators but it has little use in vibration control. Following materials shows the SMA characteristics.

Commercially available shape memory alloys:

- Nickel/Titanium alloys such as Nitinol and Tinel
- Copper/Zinc/Aluminum Alloys
- Copper/Aluminum/Nickel Alloys

Other alloys that are known to display shape memory properties are:

- Silver/Cadmium Alloys
- Gold / Cadmium alloys
- Copper / Tin alloys
- Copper / Zinc alloys
- Indium / Titanium alloys
- Nickel / Aluminum alloys
- Iron / Platinum alloys
- Manganese / copper alloys
- Iron / Manganese / Silicon alloys

2.1.2 Piezoelectric Materials

Piezoelectric materials have two interrelated unique properties. When a piezoelectric material is deformed, it gives off a small but measurable electrical discharge. Alternately, when an electrical current is passed through a piezoelectric material it experiences a significant increase in size. Piezoelectric materials are most widely used as sensors in different environments. They are often used to measure fluid compositions, fluid density, fluid viscosity, or the force of an impact. Piezoelectric material can be broadly classified into two groups i.e. crystalline and ceramics. In the category of crystalline, Quartz (SiO_2), Aluminum Orthophosphate- Berlinite ($AlPO_4$), Gallium Orthophosphate ($GaPO_4$), and Tourmaline etc are available. In the field of ceramics, Barium Titanate ($BaTiO_3$) and Lead zirconate Titanate (PZT) are available. Several other materials also show piezoelectric effect to certain extent, such as Zinc oxide (ZnO), Aluminum nitride (AIN), Polyvinylidene fluoride (PVDF), Lithium tantalite, Lanthanum gallium silicate, Potassium sodium tartrate etc [49].

2.1.3 Electro-Rheostatic(ER) and Magneto-Rheostatic Materials (MR)

Electro-rheostatic (ER) and magneto-rheostatic (MR) materials are fluids. When external electric field is applied, the viscosity of these fluid increases, and when the electric field is taken away, the viscosity of the fluid goes back to original value. This characteristic is called ER effect. MR fluids experience a viscosity change when exposed to a magnetic field, while ER fluids experience similar changes in an electric field. These fluids can change from a thick fluid (similar to motor oil) to nearly a solid substance within the span of a millisecond when exposed to a magnetic or electric field; the effect can be completely reversed just as quickly when the field is removed. The composition of each type of smart fluid varies widely. The most common form of MR fluid consists of tiny iron particles suspended in oil, while ER fluids can be as simple as milk chocolate or cornstarch and oil. MR fluids are being developed for use in car shock absorbers, damping washing machine vibration, prosthetic limbs, exercise equipment, and surface polishing of machine parts. ER fluids have mainly been developed for use in clutches and valves, as well as engine mounts designed to reduce noise and vibration in vehicles.

2.1.4 Electrostrictive Materials

These materials are very similar to the piezoelectric material with better strain capability, but very much sensitive to temperature. The major difference between them is that piezoelectric materials will elongate or get compressed, whereas electrostrictive material will elongate only, irrespective of the direction of the applied electric field. Generally this property is found in all materials in very small quantity (approximately 10E-5 to 10E-7 % strain). Electrostrictive ceramics, based on a class of materials known as relaxor ferroelectrics, however show strains comparable to piezoelectric. Most commercial Electrostrictive ceramics are based upon the classical relaxor ferroelectric PMN (lead magnesium niobate) [50].

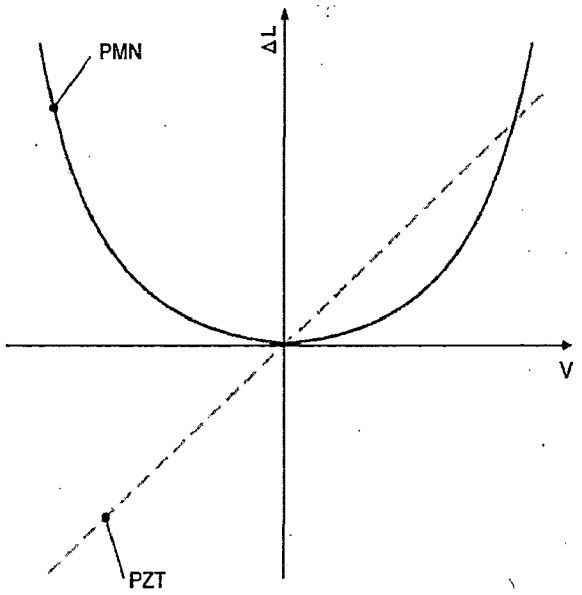

Figure 2.3: Displacement Vs Voltage behavior of piezoelectric and electrostrictive materials [50].

2.1.5 Magnetostrictive Materials

Magnetostrictive materials transduce or convert magnetic energy to mechanical energy and vice versa. As a magnetostrictive material is magnetized, it strains; that is it exhibits a change in length per unit length. Conversely, if an external force produces a strain in a magnetostrictive material the material's magnetic state will change. This bi-directional coupling between the magnetic and mechanical states of a magnetostrictive material,

provides a transduction capability that is used for both actuation and sensing devices. Magnetostrictive Materials were discovered in the 1840s by James Prescott Joule, when he noticed that iron changed length in response to changes in magnetism and named the phenomenon the Joule Effect.

Magnetostrictive materials can operate at higher temperatures than piezoelectric and electrostrictive actuators. They can also undergo higher strains and lower input voltages that most piezoelectric and electrostrictive materials can. However, magnetostrictive materials are not easily embedded in control structures. Some kinds of magnetostrictive materials are cobalt, iron, nickel, ferrite, terbium Alloys (Terfenol-D) and metglass etc [51].

2.1.6 Fiber Optics

An optical fiber is a glass or plastic fiber designed to guide light along its length by confining as much light as possible in a propagating form. In fibers with large core diameter, the confinement is based on total internal reflection. In smaller diameter core fibers, (widely used for most communication links longer than 200m) the confinement relies on establishing a waveguide. Fiber optics is the overlap of applied science and engineering concerned, with the design and application of optical fibers. Optical fibers are widely used in fiber-optic communications, which permits transmission over longer distance and at higher data rates than other forms of communications. Fibers are used instead of metal wires because signals travel along them with low loss, and they are immune to electromagnetic interference. Optical fibers are also used to form sensors and in a variety of other applications. The fiber optic sensors (FOSs) provide several advantages over their electrical counterparts, viz high bandwidth, small size, low weight, corrosion resistance, geometrical flexibility and an inherent immunity to electromagnetic interference (EMI). FOSs can be embedded in composite materials in a non-obtrusive manner that does not degrade structural integrity. In general, the embedded fiber optic sensors can monitor the health of the structures in service condition.

2.2 Piezoelectric Materials

Piezoelectricity ("Piezo" is a Greek term which means "to squeez) was discovered by Pierre and Jacques Curie in the 1880s. The Curies noticed two things: Firstly, applying mechanical stress on certain natural non-symmetrical crystals changes their internal electric polarization in proportion to the stress. Secondly, the same crystals deform when they are subjects to an electric field. These unique properties are known as the direct and converse piezoelectric effects respectively. The piezoelectric effect is practically linear and direction-dependent. As shown in Figure. 2.4, compressive and tensile stresses applied along the polarization direction of the material, will generate electric fields and hence voltages of opposite polarity. The phenomenon is also reciprocal so that upon application of electric fields of opposite polarity, the material will expand and contract in accordance with the applied fields. While these direct and converse effects are mostly used in sensors/generators and actuators/motors respectively, this dual functional ability enables piezoelectric to be employed as transducers, converting electrical energy into mechanical energy and vice-versa [47].

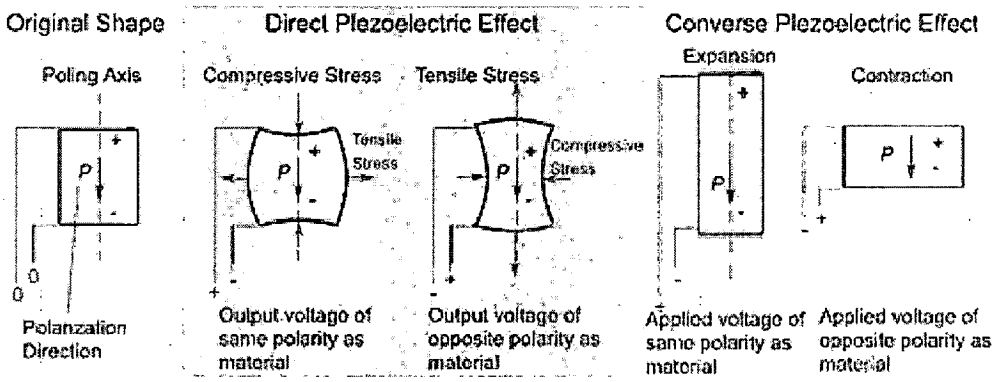

Figure 2.4: Piezoelectric effect [47].

For a material to exhibit the piezoelectric effect, its structure should have no center of symmetry (non Centro-symmetric). That is, the material has anisotropic characteristics, i.e. its properties differ according to the direction of measurement. Consequently, piezoelectricity is an anisotropic characteristic. Figure 2.5 shows the change in crystal structures of a PZT upon temperature change. Above the Curie temperature (*Tc*), the ceramic has a cubic (Centro-symmetric) structure with no electric dipole moment within its

unit cell. Below *Tc*, however, the positively charged Ti/Zr ion shifted from its central location along one of the several allowed directions, thereby distorting the crystal lattice into perovskite (non Centro-symmetric) structure and producing an electric dipole with a single axis of symmetry.

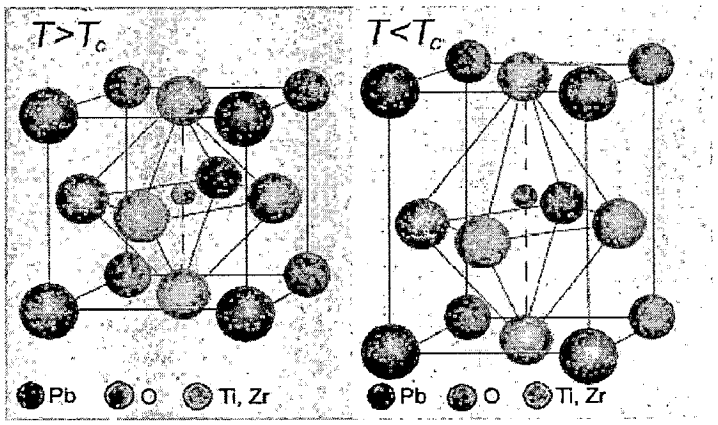

Figure 2.5: Crystal structures of PZT ceramics above and below their *Tc*[50].

This dipole form regions of local alignment called domains. The alignment gives a net dipole moment to the domain, and thus a net polarization. The direction of polarization among neighboring domains is random, so the ceramic element has no overall polarization (Figure 2. 6).

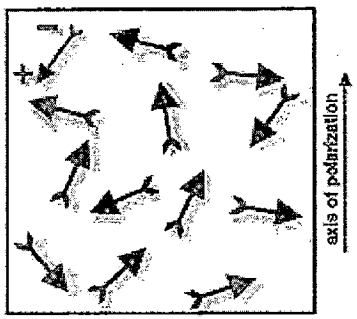

Figure 2.6: Random orientation of polar domain prior to polarization [50].

The domains in a ceramic element are aligned by exposing the element to a strong direct current electric field (more than 1KV/mm), usually at a temperature slightly below the Curie point (Figure 2.7). Through this polarizing (poling) treatment, domains most nearly aligned with the electric field expand at the expense of domains that are not aligned with the

field, and the element lengthens in the direction of the field. When the electric field is removed most of the dipoles are locked into a configuration of near alignment (Figure 2. 8). The element now has a permanent polarization, the remanent polarization, and is permanently elongated [50].

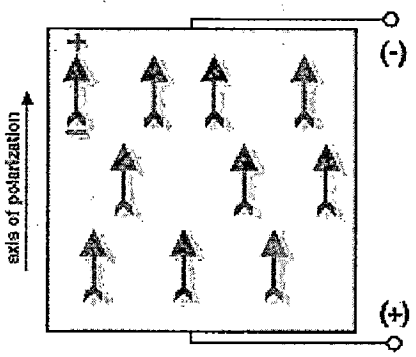

Figure 2.7: polarization in DC electric field

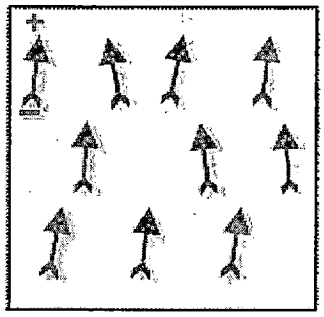

Figure 2.8: Remanent polarization after electric field is removed

The ability of piezoelectric materials is to exchange energy from the electrical to mechanical domain and vice-versa make them suitable as sensors and actuators. If piezoelectric material is bonded properly to the structure, deformation of the structure will be sensed properly, because deformation of the structure would cause the deformed piezoelectric material to produce an electric voltage. This is a sensor application. On the other side, structural deformation can be induced by applying a voltage to the piezoelectric material. Then it works as an actuator. Naturally occurring crystals show very weak piezoelectric effect, so they cannot be directly used as the sensor and actuator. But exponential developments in the field of material science have provided piezoelectric materials, which show very good inter-relation between electrical and mechanical domain. There are various piezoelectric materials such as Polyvinyllidene fluoride (PVDF) (semi crystalline polymer film) and lead zirconate titanate (PZT) [Pb (Zr, Ti) O_3] (piezoelectric ceramic material) which are commonly used in practice. PZT apply larger forces or moments on structure as compared to PVDF because it has larger value of electromechanical coupling coefficient. But, PZT is relatively brittle in nature while PVDF is flexible and can be cut into any desired shape. PVDF shows excellent sensing properties so it is commonly used as sensors. But they have some limitations also like applied voltage is limited in the

range of -500 V to 1500 V, piezo materials cannot be used above 200 °C to 300 °C due to possibility of depolarization. Piezoelectric materials are mostly used as actuators, for large range of frequency including ultrasonic application.

For the vibration suppression of thin structures, piezoelectric materials are widely used due to their following characteristics:

- Low weight
- Easily mounted on the structures
- Quick response
- Low power consumption
- High efficiency and compactness
- Dual nature (sensing and actuation both)
- Lower prices

But there are several limitations to the use piezoelectric materials. Some of them are:

- **Electrical limitations** – Exposure to strong electric field, having polarity opposite to that of polarizing field will depolarize a piezoelectric material. The degree of depolarization depends on the grade of material, the exposure time, the temperature and the other factors, but field of 200-500V/mm or more typically have a significant depolarizing effect. An alternating current will have a depolarizing effect during each half cycle in which polarity is opposite to that of polarizing effect. Piezoelectric material shows linear relationship in electric field and strain for low field value (max up to 100V/mm) but it shows non linear behavior for large field values and shows hysteresis characteristics. It shows drift from zero state of strain under cyclic electric field, hence it is unable to reproduce strain.
- **Mechanical limitations** – Mechanical stress sufficient to disturb the orientation of the domain in the piezoelectric material can destroy alignment of the dipoles. Like susceptibility to electrical depolarization, the ability to withstand mechanical stress differs among the various grades and brands of piezoelectric materials.
- **Thermal limitations** – If a piezoelectric ceramics material is heated to its Curie point, the domain will become disordered and the material will be depolarized. The

recommended upper operating temperature for a ceramics is usually approximately half-way between 0 degree Celsius and the Curie point. Within the recommended operating temperature range, temperature –associated changes in the orientation of the domain are reversible. On the other hand, these changes can create charge displacement and electric fields. Also sudden temperature fluctuation can generate high voltages, capable of depolarizing ceramic element.

- **Stability** – Most properties of a piezoelectric ceramics element erode gradually, in a logarithmic relationship with time after polarization. Exact rates of aging depend on the composition of the ceramic element and the manufacturing process used to prepare it. Mishandling the element by exceeding its electrical, mechanical, and thermal limitations can accelerate this inherent process.

2.2.1 Classification of Piezoelectric Materials

- Ferroelastic: Materials in which spontaneous polarization is induced by mechanical load.
- Ferroelectrics: Materials in which spontaneous polarization is induced by electric field. Their polarization is changed by reversing the electric field.
- Pyroelectrics: Materials in which the electric field is generated as a result of application of heat and degree of polarization depends on the temperature range.

2.2.2 Piezoelectric constitutive relations

The equations which describe the electromechanical behavior of piezoelectric materials are called piezoelectric constitutive relations. Piezoceramic is considered as the orthotropic materials such as unidirectional laminated composite. The relations are derived by considering several assumptions.

- Piezoelectric material is linear and actuation strain is modeled like thermal strain.
- Total strain in the actuator is the sum of the mechanical strain induced by the stress, the thermal strain due to temperature and the controllable actuation strain due to electric voltage.

The axes are expressed in numeral forms as 1-corresponding x-axis, 2- corresponding y-axis and 3-corresponding z-axis. The z-axis is generally referred as the poling direction in the monolithic-type material. A piezoelectric material produces electric displacement

when it is strained along the poling direction conversely; it produces strain when electric field is applied along the poling direction. Hence, the former property is used as the sensing and latter is used as the actuation.

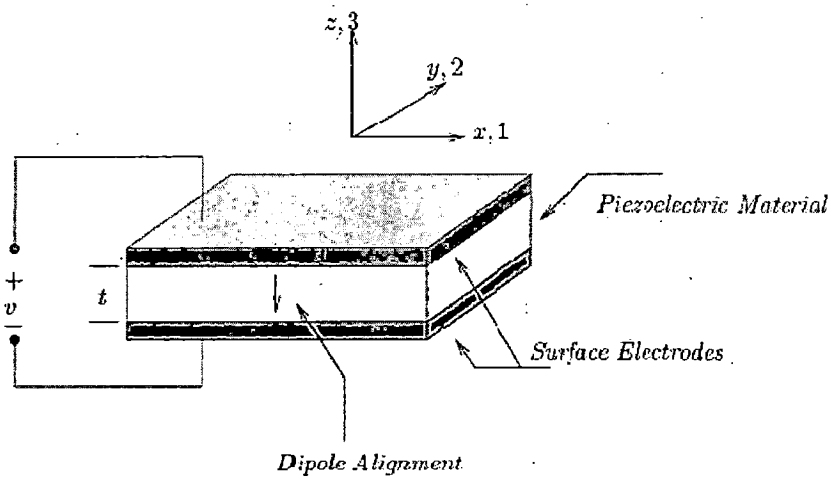

Figure 2.9: Schematic diagram of a piezoelectric transducer [42].

Coupled electromechanical constitutive relations are given as

$$\{\sigma\} = [Q]\{\varepsilon\} - [d]^T\{E\} \tag{2.1}$$

$$\{D\} = [d]\{\varepsilon\} + [s]\{E\} \tag{2.2}$$

Where

$\{\sigma\}$ = stress vector

$\{\varepsilon\}$ = strain vector

$[Q]$ = Elasticity constant matrix

$\{E\}$ = Electric field

$\{D\}$ = Electric displacement

$[d]$ = Piezoelectric constant stress matrix

$[s]$ = Dielectric constant matrix.

If a compressive force is applied in the polarization direction (axis 3), or tensile force is applied in the plane perpendicular to polarization direction (axis 2 or 1), it will result in a voltage that has the same polarity as the original poling direction.

During the manufacture of a Piezoceramic, a large (greater than 1KV/mm) field is applied across the ceramic to create polarization. This is called coercive field during subsequent testing, if a field greater than coercive field, is applied opposite to the polarization direction, the ceramic will lose its piezo electric properties. This phenomenon is called depoling. However, it is possible to repole the material. If an applied electric field is aligned with the initial polarization direction, there is no depoling. Sufficient high voltage in the poling direction can cause arcing or a brittle fracture. Depoling is also possible if high temperature or large stress is applied.

2.2.3 PZT manufacturing processes

PZT are manufactured from their respective oxide / carbonates of Pb, Zr, Ti, rare earths, alkaline earths, transition metals etc. to the specified compositions, well tuned to the end properties, by mixing and solid state reactions. Typical production flowchart is given below:

WEIGHING RAW MATERIALS

⇩

MIXING-BALL-MILL

⇩

OVEN DRY

⇩

SOLID STATE REACTION UPTO 1200^0 C

⇩

MICRO-PULVERISATION T0 A PRE-DETERMINED PARTICLE SIZE RANGE

⇩

FORMING PROCESSES

⇩

SINTERING 1300^0C - QC FOR SINTERABILITY

⇩

GRINDING / LAPPING / SLICING TO THE REQUIRED DIMENSIONS

⇩

FIRED - ON SILVER ELECTRODES

⇩

POLING, HIGH DC FIELDS; TIME-TEMP PROFILE

⇩

TESTING

2.3 Active Vibration Control

Active control methods use external active devices to generate a second set of disturbance of equal amplitude but opposite phase to cancel the targeted unwanted disturbance. Unlike passive control, active control needs an external power supply to its control system. A typical active control system is composed of three basic component; sensors, actuators and controller. Sensors sense the primary unwanted disturbance experienced (structural vibration or acoustic noise) and monitor how well the control system is performing. Based on the sensor inputs and some knowledge of how the plant responds to the actuators, the controller determines the signal that drives the control actuators. The calculated/determined control signal is eventually passed on to the control actuators to generate the second set of anti-disturbance so as to cancel the primary unwanted disturbance.

The development of active control technology is supported by development in the field of physics, control, signal processing and mechanical and electrical engineering. In contrast with passive control, active control works effectively over a wide bandwidth where the working band does not depend on the characteristics of the structure, and is limited only by the bandwidth of the actuators. Furthermore, the actuators are less sensitive to the characteristics of the structure and the vibration sources. Therefore, the same actuators can be used even if the characteristics of the structure or the vibration sources are changed.

More than a decade of intensive research in the area of smart/adaptive structures has demonstrated the viability and potential of this technology. A class of smart structures,

consisting of piezoelectric materials integrated with structural systems, has found widespread use in engineering applications, including active vibration suppression and shape control. Piezoelectric actuators used in adaptive structures are usually thin wafers, which are poled in the thickness direction and bonded to the surfaces of the host structure. The application of an electric field in the thickness direction causes the lateral dimensions of the actuators to increase or decrease, thereby forcing the host structure to deform. These types of actuators, where the electric field is applied parallel to the poling direction to cause normal strains in the piezoelectric material, are known as piezoelectric extension actuators. Piezoelectric extension actuators are usually placed at the extreme thickness positions of a plate-like structure to achieve the most effective actuation [16].

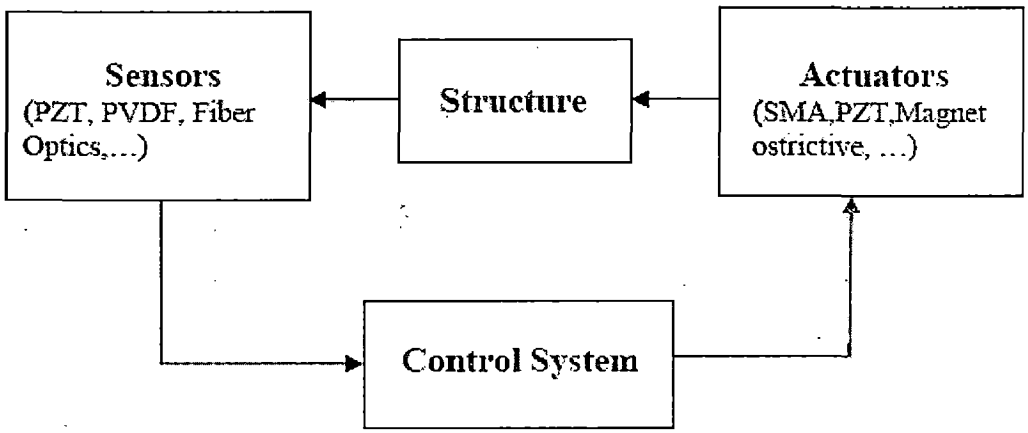

Figure 2.10: An active control system.

Figure2.10 shows a typical active control system. It consists of sensors, which are used to monitor the mechanical response of the structure through changes in displacement, strain or acceleration. Once an adverse or undesirable response of the structure is detected in the sensor, a controller generates the required input to the actuators. The actuators respond to this input and produce a corresponding change in mechanical response of the structure to a more acceptable state.

This chapter presents the literature review regarding active vibration control of structures.

3.1 Smart Materials and Structures

Crawley and Lazarus *et al* (1991) concluded that the induced strain actuation is a common feature of many smart structures whereby actuation strain in a small part of the whole structure can cause induced deformation in the entire structure. Natural mechanism of actuation strain may be thermal expansion, moisture absorption, piezoelectricity, electrostriction, magnetostriction, material phase change etc. One of these mechanisms, piezoelectricity can be easily localized and controlled and hence, is commonly used in smart structures.

Thomson *et al.* (1992) presented an exposition of the embryonic field of smart materials and structures. He discussed different classes of innovative biomimetic materials and their influence on various design practices.

Akella *et al.* (1994) presented the modeling and control issues related to smart structures bonded with piezoelectric sensors and actuators. They applied Hamilton's principle to obtain a linearized equation of motion and then they found natural modes by solving an Eigen value problem.

Brennan *et al.* [1994] presented the use of piezoelectric elements as vibration actuators and sensors on a one dimensional structure. They developed an analytical model to describe how piezoelectric sensors and actuators measure and excite longitudinal and flexural waves on a beam and validated it with simple experiments. They stated the merits of using these elements as error sensors and as a secondary source of active vibration control system and also highlighted some fundamental limitations.

Bronowicki *et al.* [1995] fabricated a member with thin PZT actuator and sensor wafers embedded in a composite layup and then this member was subjected to cyclic loading. They found that the product of PZT modulus and piezoelectric coefficient is a figure of merit for both actuation and sensing.

3.2 Vibration Control

Hwang Woo-Seok *et al.* [1994] presented the vibration control of a laminated composite plate by passive and active control technique. In the passive control technique they investigated the stiffness changes in composite structures due to changes in laminate orientation but in active control technique, negative velocity feedback control with the piezoelectric sensor/actuator was investigated. The effects of passive and active controls are investigated by changing the layer angles of a laminated composite plate or the location and number of the sensor/actuator pairs. Classical lamination theory with induced strain actuation and Hamilton's principle are used to formulate the equation of motion of the system. The system equations are discretized by the finite element method. Finally they have suggested a design strategy for a laminated composite plate with piezoelectric sensor/actuator.

Peng X.Q. *et al.* [1998] developed a finite element model based on third order laminate theory for active position control and vibration control of composite beams with distributed piezoelectric sensor and actuators. They have used direct piezoelectric equation to calculate the total charge created due to the strains on the sensor electrodes. The actuators provide a damping effect on the composite beam by coupling a negative velocity feedback control algorithm in a closed control loop. A modal superposition technique and the Newmark-β method are used in the numerical analysis to compute the dynamic response of the composite beams. Finally, the effect of the number and locations of the sensor/actuators on the control system is investigated.

Hu Yan-Ru *et al* [2002] developed an approach for active vibration control of flexible structures with integrated piezoelectric actuators using control theory. First, dynamic models for a flexible circular plate with integrated piezoelectric actuators and

sensors are derived using the Rayleigh-Ritz method. An active robust controller is designed to suppress vibration of the circular plate. They have discussed the Robustness of the control system of the circular plate for the model parameter uncertainty. This active robot vibration control method is tested via experimental implementation. The experimental results show that the proposed robust active control method is efficient for active vibration suppression.

Karagulle H. ***et al.*** **[2004]** presented the modeling of smart structure with piezoelectric materials using the product ANSYS/Multiphysics. They have realized the integration of control action into the ANSYS solution. First, the procedure is tested on the active vibration control problem with two-degree of freedom system. They have compared the analytical results obtained by the Laplace transformation method and by ANSYS. After that they have studied the smart structure by ANSYS. The input reference value is taken as zero in the closed loop vibration control. The instantaneous value of the strain at the sensor location at a time step is subtracted from zero to find the error signal value. The error value is multiplied by the control gain to calculate the voltage value which is used as the input of the actuator nodes. The process is continued with the selected time step until the steady-state value is approximately reached. The results obtained for the structure are compared with other studies.

Wang S.Y. ***et al*** **[2004]** investigated the dynamic stability of negative-velocity feedback control of piezoelectric composite plates using a finite element model. Lyapunov's energy functional based on the derived general governing equations of motion with active damping is used in order to carry out the stability analysis. The active damping matrix must be positive semi-definite in order to guarantee the dynamic stability. It is found that the imperfect collocation of piezoelectric sensor/actuator pairs is not sufficient for dynamic stability in general and that ignoring the in-plane displacements of the midplane of the composite plate with imperfectly collocated piezoelectric sensor/actuator pairs may cause significant numerical errors, leading to incorrect stability. The numerical results based on a cantilevered piezoelectric composite plate shows that the feedback control system with an imperfectly collocated PZT sensor/actuator pair is unstable. But asymptotic stability can be achieved by either bonding the PZT sensor/actuator pair together or changing the ply

stacking sequence of the composite substrate to be symmetric. This stability analysis is of practical importance for effective design of asymptotically stable control systems as well as for choosing an appropriate finite element model to accurately predict the dynamics of smart piezoelectric composite plates.

Moita Jose M Simoes *et al* [2005] presented a finite element formulation for active control of forced vibrations, including resonance of thin plate/shell laminated structures with integrated piezoelectric layers, acting as sensors and actuators, based on third-order shear deformation theory. The finite element model is a single layer triangular nonconforming plate/shell element with 24 degrees of freedom for the generalized displacements, and one electrical potential degree of freedom for each piezoelectric element layer, which are surface bonded or embedded in the laminate. They used Newmark method to calculate the dynamic response of the laminated structures, forced to vibrate at the first natural frequency. In order to achieve a mechanism of active control of the structure dynamic response, a feedback control algorithm is used, which acts as a coupling in between sensor and active piezoelectric layers.

Sethi Vineet *et al* [2005] presented results of multitude vibration suppression of a smart flexible cantilever beam by using single piezoceramic actuator and a single sensor. Piezoceramic PZT (Lead Zirconate Titanate) patches are surface-bonded on the beam and perform as actuator and sensor. They have employed System identification for the dynamics of the first three modes and model reduction techniques to assist in control system design. They have used the state space model from system identification for state estimation and development of control algorithm. A linear pole placement controller is designed and simulated using the identified model. Experimental results demonstrate the effectiveness of multimodal active vibration of the structure using smart materials.

Fei Juntao *et al* [2006] presented results on active control schemes for vibration suppression of flexible steel cantilever beam with bonded piezoelectric actuators. The PZT patches are surface-bonded near the fixed end of flexible steel cantilever beam. Active vibrator control methods such as strain rate feedback control (SRF) and positive position

feedback control (PPF) are investigated and implemented using xPC Target real time system. Experimental results demonstrate that the SRF control and PPF control achieve effective vibration suppression results of steel cantilever beam.

E. A. Kovalovs *et al* [2007] have used macro-fiber composites (MFC) for vibration reduction of structures. The MFC consist of polyimide films with IDE-electrodes that are glued on the top and the bottom of rectangular piezoceramic fibers. The interdigitated electrodes deliver the electric field required to activate the piezoelectric effect in the fibers and allows invoking the stronger longitudinal piezoelectric effect along the length of the fibers. When this embedded or attached to flexible structures, the MFC actuator provides distributed solid-state deflection and vibration control. The major advantages of the piezoelectric fiber composite actuators are their high performance, flexibility, and durability when compared with the traditional piezoceramic (PZT) actuators. The ability of MFC devices to couple the electrical and mechanical fields is larger than in monolithic PZT. They have experimentally showed that an MFC could be used as actuator to find modal parameters and reduce vibration for structures such as an aluminum beam and metal music plate. Two MFC actuators were attached to the surfaces of test subjects. First MFC actuator used to supply a signal as exciter of vibration and second MFC causes reduction of vibration in the range of resonance frequencies. They have compared experimental results of aluminum beam with MFC actuators with finite element model modeled in ANSYS software. The experimental and numerical results presented in this paper confirm the potential of MFC for use in the vibration control of structures.

3.3 Experimental Work

Crawley *et al.* [1987] presented the analytical and experimental development of piezoelectric actuators as elements of intelligent structures i.e. structures with highly distributed actuators that are either bonded to an elastic substrate or embedded in a laminated composite. These models lead to the ability to predict, a priori, the response of a structural member to a command voltage applied to the piezoelectric patch and give guidance as to the optimal location for the actuator placement. They performed a scaling analysis to demonstrate that the effectiveness of the piezoelectric actuators is independent of

the size of the structure and to evaluate various piezoelectric materials based on their effectiveness in transmitting strain to the structure. They constructed three test specimens of cantilevered beams: an aluminum beam with surface bonded actuators, a glass/epoxy beam with embedded actuators and a graphite epoxy beam with embedded actuators. They used actuators to excite steady state resonant vibrations in the cantilever beams. The response of the specimen compared well with those predicted by the analytical models. Static tensile tests performed on glass/epoxy laminates indicated that the embedded actuators reduce the ultimate strength of the laminated structure by 20%, while not significantly affecting the global elastic modulus of the specimen.

Crawley *et al.* [1991] developed and experimentally verified the induced strain actuation of a plate. They derived equations relating the actuation strain created by induced strain actuators, to the strain induced in the actuator/substrate systems for isotropic and anisotropic plate. They also developed plate strain energy relations. They obtained several exact solutions for simple actuator/substrate system and formulated a general procedure for solving the strain energy equation with Rayleigh-Ritz technique. They verified the accuracy of the basic induced strain actuator/substrate system models by using simple test articles and build cantilever plate test articles.

Han *et al.* [1997] applied active vibration control method both numerically and experimentally in order to reduce the vibration of light weight composite structure. They developed an analytical model of the laminated composite beam with piezoelectric sensors and actuators using classical laminated beam theory and Ritz method. They fabricated and tested smart composite beams and plates with surface bonded piezoelectric sensors and actuators. They designed and implemented a control system using linear quadratic Gaussian control algorithm and known classical control algorithms. They successfully controlled the first and second modes of a cantilever beam and simultaneous bending and twisting modes of a cantilever plate. They concluded that the linear quadratic Gaussian control algorithm shows robustness in noise and control efficiency compared with classical control methods.

Park *et al.* [2002] presented experimental investigations of the vibration testing of an inflated, thin-film torus using smart materials. They show that polyvinylidene fluoride (PVDF) patches and recently developed macro-fiber composite actuators may be used as

sensors and actuators in identifying modal parameters. They suggested that the addition of actuators and PVDF sensors to the torus does not significantly interfere with the suspension modes of a free boundary condition, and can be considered an integral part of the inflated structure. Their results indicate the potential of using smart materials to measure and control the dynamic response of inflated structures.

Lee Y.Y. *et al.* [2003] presented an experimental study for the active vibration control of structures subjected to external excitations using piezoelectric sensors and actuators. They used a simply supported plate and a curved panel as the controlled structures in two experiments. They employed the independent modal space control approach for the controller design. They also incorporated the time domain modal identification technique into the controller for real time update of the system parameter for increasing the adaptability. They tested the adaptive effectiveness of the time domain modal identification technique by fixing an additional mass on the simply supported plate to change its structural properties.

Keir *et al.* [2004] analytically and experimentally investigated the active control of the structure-borne vibration transmission in resonant built up structures. They compared the control performance for both dependent and independent control force arrangements using feed forward active control. They used multiple actuator control forces and multiple error sensors to actively control the frequency response. They also presented the global response of coupled plate structure for active control at discrete resonance frequencies.

Mehrdad *et al.* [2005] presented the fabrication and testing of active composite panels (ACPs) with embedded piezoelectric sensors and actuators. They employed a cross ply type stacking sequence for the ACPs. The Piezoceramic patches were embedded inside the composite laminate. The capacitance of the piezoelectric patches was measured before and after curing for quality control. The manufactured ACPs were trimmed and tested for their functionality. They developed a finite element model to verify the free expansion of the Piezoceramic patches. The experimental results were compared with the finite element model and results showed good agreements. Finally they successfully conducted vibration suppression as well as simultaneous vibration suppression and precision positioning tests

using Hybrid adaptive control on manufactured ACP beams and demonstrated their functionality.

Qiu *et al.* [2006] describe the active vibration control of a plate using self sensing actuator and an adaptive control method. They stated that in a self sensing actuator, the same piezoelectric patch element functions as both sensor and actuator so that the total number of piezoelectric elements required can be reduced. They proposed a method to balance the bridge circuits of self-sensing actuator and confirmed its effectiveness by using an extra piezoelectric sensor. They established a control system including a self-sensing actuator and adaptive controller using a finite impulse response filter and the filtered-X LMS algorithm. They experimentally validated their work and results showed that the bridge circuit was well balanced and the vibration of the plate was successfully reduced at multiple resonance frequencies below 1.2 kHz.

Nagai *et al.* [2007] presented detailed experimental and analytical study of chaotic vibrations of a shallow cylindrical shell panel subjected to gravity and periodic excitation. First, they found the fundamental properties of the shell-panel, linear natural frequencies and characteristics of restoring force of the shell-panel. These results were compared with the relevant analytical results. Then, geometrical parameters of the shell panel were identified. They obtained nonlinear frequency responses of the shell panel by exciting the shell-panel with lateral periodic acceleration. In typical ranges of the exciting frequency, predominant chaotic responses are generated. Chaotic responses are integrated numerically by the Runge–Kutta–Gill method. The chaotic responses, which are obtained by the experiment and the analysis, are inspected with the Fourier spectra, the Poincare projections, the maximum Lyapunov exponents and the Lyapunov dimension. They found that the dominant chaotic responses of the shell-panel are generated from the responses of the sub-harmonic resonance of 12 order and of the ultra-sub-harmonic resonance of 23 order.

Kurpa *et al.* [2007] conducted experiments on an aluminum panel with complex shape of the boundary in order to identify the nonlinear response of the fundamental mode; these experimental results have been compared with numerical results.

Zhang *et al.* [2008] studied active vibration control of a cylindrical shell partially covered by a laminated PVDF actuator and carried out an experiment to actively control the vibration of a clamped–free cylindrical shell using an laminated PVDF actuator (LPA) with different layer numbers. They showed that the control forces of the actuator can be significantly enhanced by increasing the PVDF layer number while keeping the driving voltage unchanged and as a result they showed the modal vibrations of the shell are suppressed quite well under a relatively low control voltage (40 V) with a five-layer LPA whose area is only 21% of that of the shell.

Barrault *et al.* [2008] combined the frequency bandwidth to be controlled, the accuracy of the structural modeling, the robustness of the controller, and the extent to which the disturbance can be quantified to produce a robust, fixed bandwidth controller for which the lower frequency limit for control can be any frequencies larger than 0 Hz. They showed how Subspace Model identification can be used to obtain the system dynamics through experiment. After combining these theories they showed experimentally how to achieve global vibration attenuation for the system.

3.4 Optimal Sensor/Actuator Placement

Obe *et al.* [1985] proposed a scheme for the optimal spatial placement of a limited number of sensors and actuators under a minimum energy requirement for active control of flexible structures. The method was based on the interpretation of the functional relationship between the actuators and the modes of the structural system. They showed that the controllability and the observability of the system with respect to different locations of sensors and actuators can be established. The algorithm presented circumvents prevailing problems encountered in contemporary optimal control applications. In order to support the conclusions, numerical simulation for a prismatic beam subjected to horizontal random wind loads and simply supported square plate modeled as single degree of freedom system were provided.

Tzou *et al.* [1992] studied a new intelligent shell structure composed of a conventional elastic shell, a distributed piezoelectric sensor and actuator and derived system equations of motion coupling sensing and control effects. They concluded that the

distributed sensor is capable of sensing all shell vibration modes and the distributed actuator can control all shell modes.

Hiramoto *et al.* [2000] presented an optimal sensor and actuator placement strategy for active vibration control of flexible structures. They obtained two solutions of generalized algebraic Riccati equations for undamped structure with collocated sensors and actuators. Employing the explicit solution, they obtained a stabilizing controller based on normalized co-prime factorization approach without solving any algebraic Riccati equations numerically. They showed that the amount of computation required in determining the optimal sensor/actuator placement and controller gain increases rapidly for large scale structures. They automatically bounded the closed loop property on the stabilizing norm for all candidates of optimal placement. Hence the optimal sensor/actuator placement problem was formulated to optimize other closed loop properties with less computation required than the model based method. Using the sensitivity formula, they obtained the optimal placement of two pairs of sensors and actuators which minimize the stabilizing norm of closed loop system for a simply supported beam by the quasi-Newton method.

Quek S.T. *at el.* [2003] presented an optimal placement strategy of piezoelectric sensor actuator pairs for vibration control of laminated composite plate. They maximized the active damping effect under a classical control frame work using the finite element approach. They employed classical pattern search method to obtain the local optimum, where the two optimization performance indices based on modal and system controllability were studied. They selected the start point for the pattern search method based on the maxima of integrated normal strains consistent with the size of the collocated piezoelectric patches used. The effectiveness of the strategy was illustrated by numerical simulation using a cantilevered and clamped composite square plate.

Halim Dunant *et al.* [2003] suggested a criterion for the placement of collocated piezoelectric actuator-sensor pairs on a thin flexible plate using modal and spatial controllability measures. The reduction of control spillover effect by adding an extra spatial controllability constraint in the optimization procedure was considered. The spatial controllability is used to find the optimal placement of the collocated sensor-actuator pairs for effective average vibration reduction over the entire structure, while maintaining modal

controllability and observability of the selected vibration modes. They found that the methodology for optimal actuator placement can be used for a collocated system without damaging the observability of the collocated sensors. They experimentally validated the optimal placement done on a simply supported thin plate with a collocated piezoelectric sensor-actuator pair.

Smithmaitrie *et al.* [2004] evaluate the micro-control actions and distributed control effectiveness of segmented actuator patches laminated on hemispherical shells. They developed mathematical models and governing equations of the hemispheric shells laminated with distributed actuator patches, followed by formulations of distributed control forces and micro control actions including circumferential membrane and bending control components. Their analysis indicates that the control forces and membrane/bending components are mode and location dependent. Actuators placed near the free boundary contribute the most significant control actions, and the circumferential membrane control actions dominate the overall control effect.

Wang S. Y. *et al* [2006] presented the problem of topology optimization of collocated piezoelectric sensor/actuator (S/A) pairs for torsional vibration control of a laminated composite plate. Both isotropic and anisotropic PZT S/A pairs are considered and it is highlighted that the torsional vibration can be more effectively damped out by employing the topological optimal design of the S/A pairs than by using the conventional designs. To implement this topology optimization, a genetic algorithm (GA) based on a bit-array representation method is presented and a finite element (FE) simulation model based on the first-order shear theory and an output feedback control law is adopted. Numerical experiments are used to verify the present algorithm and show that the present optimal topology design can achieve significantly better active damping effect than the one using a continuously distributed PZT S/A pair.

Qiu Zhi-cheng *et al* [2007] used piezoelectric ceramics patches as sensors and actuators to suppress the vibration of the smart flexible clamped plate. Firstly, modal equations and piezoelectric control equations of cantilever plate are derived. Secondly, an optimal placement method for the locations of piezoelectric actuators and sensors is

developed based on the degree of observability and controllability indices for the cantilever plate. The bending and torsional modes are decoupled by the proposed method using bandwidth Butterworth filter. Thirdly, an efficient control method by combining positive position feedback and proportional-derivative control is proposed for vibration reduction. The analytical results for modal frequencies, transient responses and control responses are carried out. Finally, an experimental setup of piezoelectric smart plate is designed and built up. The modal frequencies and damping ratios of the plate setup are obtained by identification method. Also, the experimental studies on vibration control of the cantilever plate including bending modes and torsional modes are conducted. The analytical and experimental results demonstrate that the presented control method is feasible, and the optimal placement method is effective.

Yue *et al.* [2008] focuses on analysis of microscopic control actions of segmented actuator patches laminated on the surface of a free paraboloidal membrane shell. They presented governing equations of the membrane shell system and modal control forces of distributed actuator patches. They followed up by conducting the analysis of dominating micro-control actions based on various natural modes, actuator locations and geometrical parameters. Their simulation data reveal significant factors influencing active control behavior of smart free-floating paraboloidal membrane shell systems.

Kumar Ramesh K. *et al* [2008] presented the optimal placement of collocated piezoelectric actuator-sensor pairs on flexible beam using a model-based linear quadratic regulator (LQR) controller. A finite element method based on Euler-Bernoulli beam theory is used. The contributions of piezoelectric sensor and actuator patches to the mass and stiffness of the beam are considered. The LQR performance is taken as the objective for finding the optimal location of sensor-actuator pairs. The problem is formulated as a multi-input, multi-output (MlMO) control model. The discrete optimal senor and actuator location problem is formulated in the framework of a zero-one optimization problem which is solved using genetic algorithms (GAs). Classical control strategies like direct proportional feedback, constant gain negative velocity feedback and the LQR optimal control scheme are applied to study the control effectiveness. They have studied the optimal location of actuator and sensors for different boundary conditions of beams like cantilever, simply supported and

clamped boundary conditions.

AL-Hazmi Mohammed W. *et al* [2008] presented a 3-D finite element analysis for cantilever plate structure excited by patches of piezoelectric actuators. They investigated the influence of actuator location and configuration of piezoelectric actuators attached to the plate structure in order to identify the optimal configuration of the actuators for selective excitation of the mode shapes of the cantilever plate structure. The FEM modeling based on ANSYS package using harmonic analysis is used in this study of cantilever plate structure excited by patch type of piezoelectric actuators. The results clearly indicate that effective active damping of structural vibration of the cantilever plate can be achieved by proper positioning of the piezoelectric actuator patches.

CHAPTER 4 BASIC EQUATIONS AND FORMULATIONS

In this chapter, basic equations and finite element formulation of static and dynamic analysis of cantilever and circular plate with surface mounted PZT patches has been analyzed for its vibration control behavior.

4.1 Cantilever beam

The beam has been modeled as an Euler-Bernoulli beam.

4.1.1 Euler Bernoulli (EB) beam model

Euler Bernoulli (EB) beam is also called the classical beam model which rests upon the following assumptions:

- Planner symmetry: The longitudinal axis is straight and cross section of the beam has longitudinal plane symmetry. The resultant of the force lies on the plane of the cross section. The support conditions are also symmetrical about this plane.
- Cross section variation: The cross section can be either constant or smoothly varying.
- Normality: The Euler Bernoulli beam equation is based on the assumptions that the cross section normal to the neutral axis remains normal to the neutral axis after the deformation or bending. This assumption is true for the large beam length to thickness ratio and small beam deflection. The total beam rotation will be due to the bending stress alone. The rotation θ is about the y axis and it is the slope of the beam as shown in the figure 4.1.

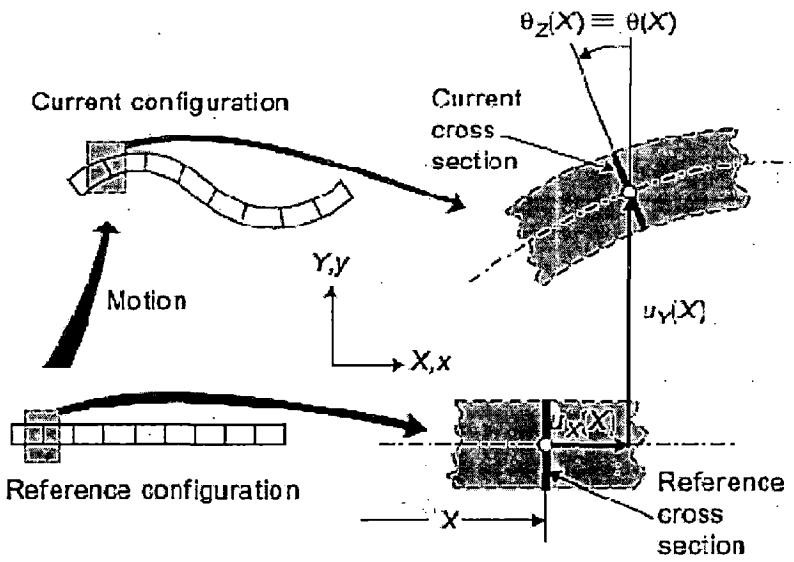

Figure 4.1: Euler Bernoulli beam model.

- Strain energy: The internal strain energy of the member is due to bending deformations and all other contributions such as transverses shear are neglected.
- Material model: The material is assumed to be linear, elastic and isotropic.

Euler Bernoulli Equation is the fundamental equation for beam vibration which may be described as:

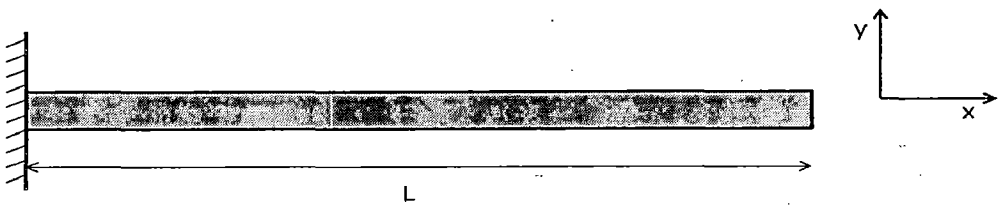

Figure 4.2: A cantilever beam

Let the length of the beam be l, cross sectional area A, density ρ, areal moment of inertia I and Young's Modulus E.

Then the Euler Bernoulli equation is given by:

$$EI\frac{\partial^4 y}{\partial x^4}+\rho A\frac{\partial^2 y}{\partial t^2}=f(x,t)-\frac{\partial m_e(x,t)}{\partial x} \tag{4.1}$$

Where, y represents beam deflection, f the external force intensity and m_e the external moment intensity.

4.1.1 (A) Free vibrations

For free vibrations both f and m_e vanish. This means:

$$EI\frac{d^4y}{dt^4}+\rho A\frac{d^2y}{dt^2}=0 \tag{4.2}$$

Substituting $y(x,t)=p(x)q(t)$

$$\Rightarrow EIq\frac{d^4p}{dx^4}+\rho Ap\frac{d^2q}{dt^2}=0 \tag{4.3}$$

$$\Rightarrow\left(\frac{EI}{\rho A}\right)\frac{1}{p}\frac{d^4p}{dx^4}=-\frac{1}{q}\frac{d^2q}{dt^2}=\omega^2 \tag{4.4}$$

$$c^2=\frac{EI}{\rho A} \tag{4.5}$$

$$\beta^4=\frac{\omega^2}{c^2} \tag{4.6}$$

$$\Rightarrow\frac{d^4p}{dx^4}-\beta^4p=0 \tag{4.7}$$

$$\frac{d^2q}{dt^2}+\omega^2q=0 \tag{4.8}$$

Thus we get

$$\begin{aligned}p(x)&=C_1\cos\beta x+C_2\sin\beta x+C_3\cosh\beta x+C_4\sinh\beta x\\ q(t)&=A_1\cos\omega t+A_2\ \sin\omega t\end{aligned} \tag{4.9}$$

The boundary conditions are

$$p_i(0)=0,\ p_i'(0)=0,\ p_i''(L)=0,\ p_i'''(L)=0$$

$$\Rightarrow p_i(x)=\frac{1}{\sqrt{\rho AL}}\left[(\cos\beta_i x-\cosh\beta_i x)+\left(\frac{\sin\beta_i L-\sinh\beta_i L}{\cos\beta_i L+\cosh\beta_i L}\right)(\sin\beta_i x-\sinh\beta_i x)\right] \tag{4.10}$$

Where,

$$1+\cos(\beta_i l)\cosh(\beta_i l)=0$$

The modes satisfy the orthogonality criterion and are normalized.

4.1.1 (B) Forced vibrations

For forced vibrations, we have

$$EI\frac{\partial^4 y}{\partial x^4}+\rho A\frac{\partial^2 y}{\partial t^2}=f(x,t)-\frac{\partial m_e(x,t)}{\partial x} \tag{4.11}$$

$$y(x,t)=\sum_{i=1}^{\infty}p_i(x)q_i(t)$$

$$\Rightarrow \frac{d^4 p_i}{dx^4}-\beta_i^4 p_i=0 \tag{4.12}$$

$$\Rightarrow EI\frac{\partial^4\sum_{i=1}^{\infty}p_i(x)q_i(t)}{\partial x^4}+\rho A\frac{\partial^2\sum_{i=1}^{\infty}p_i(x)q_i(t)}{\partial t^2}=f(x,t)-\frac{\partial m_e(x,t)}{\partial x} \tag{4.13}$$

$$\Rightarrow EI\sum_{i=1}^{\infty}(\beta_i^4)p_i q_i+\rho A\sum_{i=1}^{\infty}p_i\frac{d^2 q_i}{dt^2}=f(x,t)-\frac{\partial m_e(x,t)}{\partial x} \tag{4.14}$$

$$\Rightarrow \frac{\beta_i^4 EI}{\rho A}q_i+\frac{d^2 q_i}{dt^2}=\int_0^L p_i(x)\left(f(x,t)-\frac{\partial m_e(x,t)}{\partial x}\right)dx \tag{4.15}$$

$$\Rightarrow \omega_i^2 q_i+\frac{d^2 q_i}{dt^2}=\int_0^L p_i(x)\left(f(x,t)-\frac{\partial m_e(x,t)}{\partial x}\right)dx \tag{4.16}$$

4.1.2 Theoretical Modelling of Piezo Patches

The piezo patches used in this experiment are made of Lead Zirconate Titanate(PZT). When a voltage V is applied across the thickness of these patches, a strain ε_p is created on the patches perpendicular to the direction of the app lectric field.

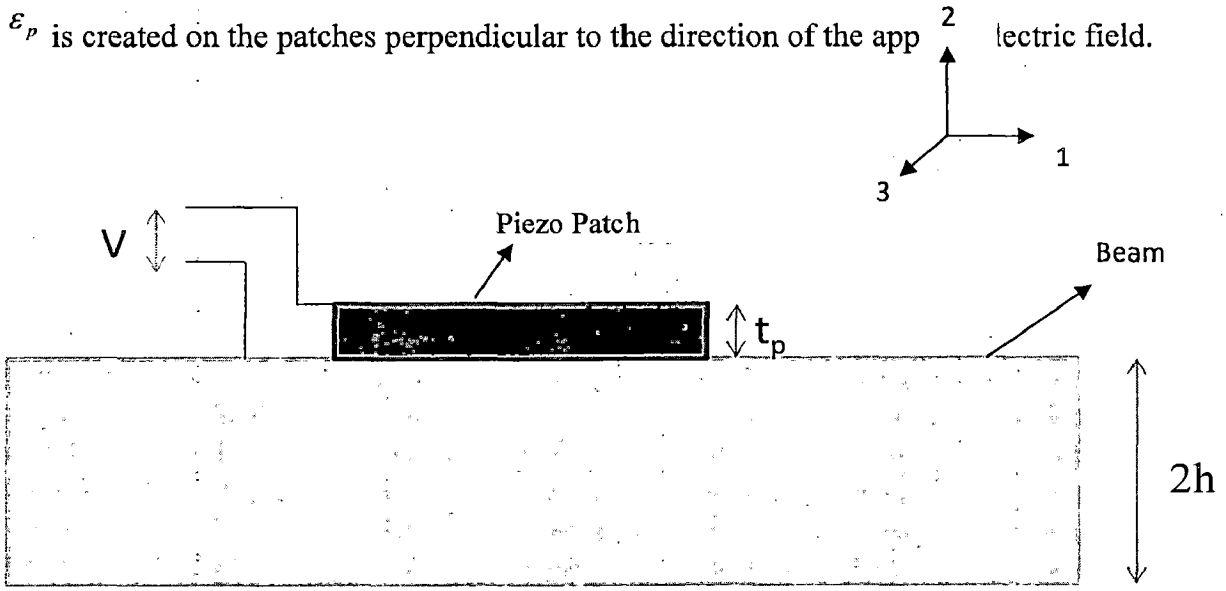

Figure 4.3: Piezo patch action

If the patch is unconstrained i.e. not bonded to any surface the strain is given by-

$$\varepsilon_p = \frac{d_{31}V}{t_p} \tag{4.17}$$

If the patch is bonded to the beam as shown in the figure, the situation is different. Let the z direction be parallel to direction 3 as indicated in the figure and the origin of the xyz coordinate system be in the centre of the beam. Then-

Let the strain distribution in the beam and the patch be given by-

$$\varepsilon(z) = \varepsilon_o + Cz \tag{4.18}$$

Where, ε_o and C_z are constants

Let $\sigma_p(z)$ and $\sigma_b(z)$ be the stress distribution in the piezo patch and the beam respectively. Then we have-

$$\sigma_b(z) = E_b(\varepsilon_o + Cz)$$
$$\sigma_p(z) = E_p(\varepsilon_o + Cz - \varepsilon_p) \tag{4.19}$$

Then for equilibrium the net force and net moment should be zero. This implies-

$$\int_{-h}^{h} \sigma_b(z)dz + \int_{h}^{h+t_p} \sigma_p(z)dz = 0$$
$$\int_{-h}^{h} \sigma_b(z)zdz + \int_{h}^{h+t_p} \sigma_p(z)zdz = 0 \tag{4.20}$$

From this it can be shown that the moment M_e exerted by the patch equals-

$$M_e = E_b I_b C = E_b I_b k^f d_{31} \frac{V}{t_p} = C_o d_{31} \frac{V}{t_p} \tag{4.21}$$

Where

$$k^f = \frac{12E_bE_pt_ph(2h+t_p)}{16E_b^2h^4 + E_bE_p(32h^3t_p + 24h^2t_p^2 + 8ht_p^3) + E_p^2t_p^4}$$

4.2 Circular plate

4.2.1 Classical Plate Theory

A plate is a structural element with plan form dimensions that are large compared to its thickness and is subjected to loads that cause bending deformation in addition to stretching. Plate theories are developed by assuming the form of the displacement or stress field as a linear combination of unknown functions and the thickness coordinate.

$$\varphi_i(x,y,z,t) = \sum_{i=0}^{N} (z)^j \varphi_i^j(x,y,t) \tag{4.22}$$

where φi is the i th component of displacement or stress, (x, y) are the in-plane coordinate, z is the thickness coordinate, t denotes the time, and φ^j are the functions to be determined [40].

The classical plate theory is one in which displacement field is selected so as to satisfy the *Kirchhoff hypothesis*. The *Kirchhoff hypothesis* has the following three assumptions [35].

(1) Straight lines perpendicular to the mid-surface (i.e., transverse normal) before deformation remain straight after deformation.

(2) The transverse normal do not experience elongation (i.e., they are in-extensible).

(3) The transverse normal rotates such that they remain perpendicular to the mid-surface after deformation.

4.2.2 Modeling of Circular Plate with Piezoelectric patches

The structure under consideration consists of a thin circular plate with piezoelectric patches bonded on the surface of it. The plate is clamped around the inner boundary and free at the outside edge. The free patches generate strains in response to an applied voltage. When the plate is bonded to an underlying structure, these strains lead to the generation of in-plane forces and / or bending moments. The circular plate is also assumed to be made of linearly elastic, homogeneous and isotropic material. For wave propagation in this structure, the displacement field is according to Classical Plate Theory (CPT) is given as [35].

$$u_r(r,\theta,z,t) = u_o(r,\theta,t) - z\frac{\partial w_o}{\partial r} \tag{4.23}$$

$$u_\theta(r,\theta,z,t) = v_o(r,\theta,t) - z(\frac{1}{r}\frac{\partial w_o}{\partial \theta}) \tag{4.24}$$

$$u_z(r,\theta,z,t) = w_o(r,\theta,t) \tag{4.25}$$

where r-coordinate is taken radially outward from the centre of the plate, z-coordinate along the thickness (or height) of the plate and θ coordinate is taken along the circumference of the plate. The displacements (u_r,u_θ,u_z) are along the coordinate (r,θ,z) and functions of r,θ and z coordinates.

(u_o,v_o,w_o) are the radial, angular and transverse displacements respectively of a point on the midplane (i.e., $z = 0$) of the plate.

The nonlinear strains are given as (accounting only Von Karman non linearity):

$$\epsilon_{rr}=\frac{\partial u_r}{\partial r}+\frac{1}{2}\left(\frac{\partial u_z}{\partial r}\right)^2 \quad (4.26)$$

$$\epsilon_{\theta\theta}=\frac{u_r}{r}+\frac{1}{r}\frac{\partial u_\theta}{\partial \theta}+\frac{1}{2}\left(\frac{1}{r}\frac{\partial u_z}{\partial \theta}\right)^2 \quad (4.27)$$

$$\epsilon_{zz}=\frac{\partial u_z}{\partial z} \quad (4.28)$$

$$\epsilon_{r\theta}=\frac{1}{2}\left(\frac{1}{r}\frac{\partial u_r}{\partial \theta}+\frac{\partial u_\theta}{\partial r}-\frac{u_\theta}{r}\right) \quad (4.29)$$

$$\epsilon_{z\theta}=\frac{1}{2}\left(\frac{\partial u_\theta}{\partial z}+\frac{1}{r}\frac{\partial u_r}{\partial \theta}\right) \quad (4.30)$$

$$\epsilon_{rz}=\frac{1}{2}\left(\frac{\partial u_r}{\partial z}+\frac{\partial u_z}{\partial r}\right)+\frac{1}{2}\frac{\partial u_z}{\partial r}\frac{\partial u_r}{\partial z} \quad (4.31)$$

Moment-displacement relations are given as:

$$M_{rr}=-D\left[\frac{\partial^2 w_o}{\partial r^2}+V\left(\frac{1}{r}\frac{\partial w_o}{\partial r}+\frac{1}{r^2}\frac{\partial^2 w_o}{\partial \theta^2}\right)\right] \quad (4.32)$$

$$M_{\theta\theta}=-D\left[V\frac{\partial^2 w_o}{\partial r^2}+\frac{1}{r}\frac{\partial w_o}{\partial r}+\frac{1}{r^2}\frac{\partial^2 w_o}{\partial \theta^2}\right] \quad (4.33)$$

$$M_{r\theta}=-(1-V)D\left[\frac{1}{r}\frac{\partial^2 w_o}{\partial r\partial \theta}-\frac{1}{r^2}\frac{\partial w_o}{\partial \theta}\right] \quad (4.34)$$

Shear force displacement are given as:

$$Q_r=-D\frac{1}{r}\frac{\partial(\nabla^2 w_o)}{\partial r} \quad (4.35)$$

$$Q_\theta=-D\frac{1}{r}\frac{\partial(\nabla^2 w_o)}{\partial \theta} \quad (4.36)$$

Where,

$$\nabla^2=\frac{1}{r}\frac{\partial\left(r\frac{\partial}{\partial r}\right)}{\partial r}+\frac{1}{r^2}\frac{\partial^2}{\partial \theta^2}$$

Force resultants are given as:

$$N_{rr}=\int_{-h/2}^{h/2}\sigma_{rr}\,dz \quad (4.37)$$

$$N_{\theta\theta}=\int_{-\frac{h}{2}}^{\frac{h}{2}}\sigma_{\theta\theta}\,dz \quad (4.38)$$

$$N_{r\theta}=\int_{-h/2}^{h/2}\sigma_{r\theta}\,dz \quad (4.39)$$

The poling direction of the piezoelectric material is assumed to be in the z- direction. When an external electric potential is applied across the piezoelectric layer, a differential strain is induced that results in the bending of the plate. The strain in the plate and the piezoelectric patch with respect to the radial and tangential directions and the shear components are according to equations (4.26), (4.27), and (4.29). The piezoelectric ceramics equations are taken from the equations (4.59) and (4.60). For plate stress tensor equation are given as

$$\{\sigma\}=[C]\{\epsilon\} \tag{4.40}$$

Where, [C] is the elastic stiffness matrix of the plate.

In order to satisfy the assumptions, an electric field E is applied along the z-direction. (ie. $E_1 = E_2 = 0$ and $E_3 = E(r,t)$) and thus the following conditions must be satisfied. $d_{32} = d_{31}$, $d_{36} = 0$ and $d_{24} = d_{15}$ also for piezoelectric material, $e_{32}=e_{31}$, $e_{36}=0$. The relationship in between electric field E and the applied voltage is given by

$$\{E\}= \{L^T_\phi\}\, \phi \tag{4.41}$$

Where,

$$[L^T_\phi] = \left\{-\frac{\partial}{\partial x}, -\frac{\partial}{\partial y}, -\frac{\partial}{\partial z}\right\}$$

Hence, when a constant voltage is applied to the network along the Z-direction, the electric field generated is $\{0, 0, d\phi/dz\}^T$. The electric charge is obtained from electrical displacement by following relation

$$[Q] = \int_s^z \{D\}\, ds \tag{4.42}$$

where, $\{Q\}^T = [Q_1, Q_2, Q_3]$ and S denotes the surface area of the electrode.

The radial stresses in the Piezo-layers are assumed to be uniformly distributed in the direction perpendicular to the plate because of the plate's small thickness. The equations of each piezoelectric layer have the following form.

$$\sigma_r = \frac{E_p}{1-V_p^2}\left\{\frac{\partial u_r}{\partial r} + V_p\left(\frac{u_r}{r} + \frac{1}{r}\frac{\partial u_\theta}{\partial \theta}\right)\right\} - \frac{V d_{3r} E_p}{h_p(1-V_p)} \tag{4.43}$$

$$\sigma_\theta = \frac{E_p}{1-V_p^2}\left(\frac{u_r}{r} + \frac{1}{r}\frac{\partial u_\theta}{\partial \theta} + V_p\frac{\partial u_r}{\partial r}\right) - \frac{V d_{3\theta} E_p}{h_p(1-V_p)} \tag{4.44}$$

$$D_3 = d_{3r}\frac{\partial u_r}{\partial r} + d_{3\theta}\frac{u_r}{r} - \epsilon_{33}\frac{V}{h_p} \tag{4.45}$$

where, σ_r, σ_θ and τ are respectively, radial stress, circumferential stress, and shear stress on the interface surface, d_{3r} and $d_{3\theta}$ are transverse piezoelectric constants in the radial and circumferential directions respectively. V is the voltage acting in the direction perpendicular to plate. E_p and V_p are the modulus and Poisson ratio of the actuator. D_3 is the electrical displacement and ϵ_{33} is the permittivity coefficient [65].

The constitutive equation of the plate

$$\sigma_r = \frac{E}{1-V^2}\left[\frac{\partial u_r}{\partial r} + V\left(\frac{u_r}{r} + \frac{1}{r}\frac{\partial u_\theta}{\partial \theta}\right)\right] \tag{4.46}$$

$$\sigma_\theta = \frac{E}{1-V^2}\left(\frac{u_r}{r} + \frac{1}{r}\frac{\partial u_\theta}{\partial \theta} + V\frac{\partial u_r}{\partial r}\right) \tag{4.47}$$

$$\tau_{r\theta} = \frac{E}{2(1+V)}\left(\frac{\partial u_\theta}{\partial r} + \frac{1}{r}\frac{\partial u_r}{\partial \theta} - \frac{u_\theta}{r}\right. \tag{4.48}$$

where, E and V are the modulus and Poisson ratio of the material of the plate. For the radial actuator motion, the dynamics equation is expressed as

$$\left(r\frac{\partial \sigma_r}{\partial r} + \sigma_r - \sigma_\theta\right)h_p - \tau r = \rho_p h_p r\frac{\partial^2 u_r}{\partial r^2} \tag{4.49}$$

The balance of the moment is expressed as:

$$\frac{\partial(rM_r)}{\partial r} - M_\theta - rT + hr\tau = 0 \tag{4.50}$$

Using Hooke's law the moment due to the plate transverse displacement is given as:

$$M_r = -D\left(\frac{\partial^2 w}{\partial r^2} + V\frac{\partial w}{r\partial r}\right) \tag{4.51}$$

$$M_\theta = -D\left(\frac{\partial w}{r\partial r} + V\frac{\partial^2 w}{r\partial^2 r}\right) \tag{4.52}$$

$$D = \frac{Eh^3}{12(1-V^2)} \tag{4.53}$$

where, T is the shear force, M_r and M_θ are internal plate moments, D is the plate cylindrical stiffness, h_p is the thickness of the actuator, ρ_p is the modified density of the actuator and t is the time. Differentiating equation (4.50) with respect to r,

$$r\frac{\partial^2 M_r}{\partial r^2} + 2\frac{\partial M_r}{\partial r} - \frac{\partial M_\theta}{\partial r} - \frac{\partial T_r}{\partial r} + h\frac{\partial(r\tau)}{\partial r} = 0 \tag{4.54}$$

The equation of the transverse plate motion is

$$\frac{\partial(T_r)}{\partial r} = \rho hr\frac{\partial^2 w}{\partial r^2} \tag{4.55}$$

where, ρ is the density for combined structures given by $\rho = \rho_1 + n\,\rho_p\,\chi_i(r,\Theta)$ in which , ρ_1, ρ_p and n are the density coefficient for the plate, the patches and the number of piezoelectric patches respectively. $\chi_i(r,\Theta)$ is the characteristics function which has a value of 1 in the region covered by the i th and 0 elsewhere. Taking into account a perfect bonding the plate transverse displacement is related to the radial actuator displacement by

$$u_r = -\frac{h}{2}\frac{\partial w}{\partial r} \tag{4.56}$$

Substituting equation (4.55) into equation (4.54) differentiating equation (4.49) with respect to r, and replacing the term $\partial(r\tau)/\partial r$ finally, the equation for modeling the transverse motion is as follow

$$\nabla^4 w + \rho\frac{h}{D_p+D}\frac{\partial^2 w}{\partial t^2} - \frac{h^2 h_p \rho_p}{2(D_p+D)}\nabla^2\frac{\partial^2 w}{\partial t^2} = \frac{p}{D_p+D} \tag{4.57}$$

$$D_p = n\frac{E_p h_p h^2}{2(1-V_p^2)}\aleph_i(r,\theta) \tag{4.58}$$

where,

$$\nabla^4 = \frac{1}{r}\frac{\partial}{\partial r}\left(r\frac{\partial}{\partial r}\frac{1}{r}\left\{\frac{\partial}{\partial r}\left(r\frac{\partial}{\partial r}\right)\right\}\right)$$

is the bi-harmonic operator in the polar coordinates r and Θ, n is the number of actuators and P is the external surface force. The displacement in the transverse z- direction w of the circular plate integrated with piezo-ceramic actuators is governed by equation (4.57). To obtain the natural frequencies and mode shapes all external mechanical and electric excitations are assumed to be zero.

4.3 Constitutive Equations of Piezoelectric Materials

The linear piezoelectric constitutive equations coupling the elastic field and the electric field can be expressed as the direct and the converse piezoelectric equations, respectively. It is assumed that thermal effect is not considered in the analysis. The piezoelectric sensor equations can be derived from the direct piezoelectric equation [40].

$$\{\sigma\} = [C_p](\{\in\} - [d^T]\{E\}) \tag{4.59}$$

$$\{D_e\} = [e]\{\in\} + [\in^s]\{E\} = \{\sigma\}[d] + [\in^\sigma]\{E\} \tag{4.60}$$

where,

σ= stress vector

Cp = electric stiffness matrix of piezoelectric ceramic

ε =strain vector

E=electric field vector

e=piezoelectric constant (piezoelectric stress/charge tensor)

De =electric displacement vector

ε^s =piezoelectric permittivity| constant under constant strain condition

ε^σ =piezoelectric permittivity constant under constant stress condition

$$[e] = [d][C_p] \tag{4.61}$$

$$[\in^s] = [\in^\sigma] - [d][C_p][d]^T \tag{4.62}$$

The superscript "T" denotes the transpose of a vector or matrix.

4.4 Sensor and Actuator Voltages

We assume that the addition of the piezo patches do not affect significantly the maximum bending stresses in the beam. Then the strain ε felt by the piezo patch would be the maximum value of the bending strain at the surface of the beam. Assume that the location of this strain is midway between s_{11} and s_{12} which we shall denote by l_c

$$l_c = \frac{s_{11} + s_{12}}{2} \tag{4.63}$$

$$\Rightarrow \varepsilon = -h\left(\frac{\partial^2 y}{\partial x^2}\right)_{x=l_c} \tag{4.64}$$

By the constitutive relation we have-

$$V_s(t) = \left\{ -\frac{t_p h}{d_{31}} \left(\frac{\partial^2 y}{\partial x^2} \right)_{x=l_e} \right\} (5U) \tag{4.65}$$

Where 5U represents the gain in the sensor voltage- 5 being the gain chosen by us on the instrument and U is the unknown gain said to occur within the instrument.

4.5 The Control Law

The block diagram of the vibration control system is shown in the figure 4.5. It is single input single output feedback control system. The feedback signal is generated by the piezo sensor. The signal is then amplified with gain and applied to the piezo actuator.

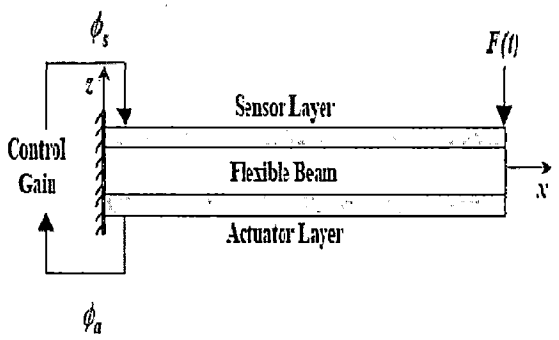

Figure 4.5: A cantilever beam with distributed actuator and sensor.

Depending upon the type of the signal conditioning, the vibration control can be realized by proportional control method. In proportional control method the feedback voltage $\Phi_a(t)$ is obtained by multiplying sensing voltage $\Phi_s(t)$ with gain G, therefore the control equation is written in given form.

$$\Phi_a(t) = G\Phi_s(t) \tag{4.67}$$

In the proportional control method, the actuation action is function of position quantities and gain value for the vibration suppression is chosen arbitrarily.

CHAPTER 5 EXPERIMENTATION

The experimental setup fabricated for the present work is described in this chapter. Detailed specification of devices used in the experimentation is given. This chapter also includes the procedure and method used in experimentation.

5.1 Experimentation

5.1.1 Objectives

(1) To monitor real time vibration of cantilever beam and circular plate.

(2) To record the signal file and to find the response of the beam using sensor voltage.

(3) To apply active vibration using closed loop proportional control method.

5.1.2 Equipments

Following equipments are used in the experimental work:

(1) Function Generator.

(2) Piezoelectric sensors and piezoelectric actuators (PZT patches).

(3) Aluminium cantilever beam and axially clamped circular plate.

(4) Vibration control unit (Piezo sensing and actuation system).

(5) Band pass filter.

(6) USB based Data acquisition card (NI USB 6009).

(7) Computer with LAB View software installed.

(8) Connections BNC connector cables.

(9) CRO

(10)Vibration Generator

(11) Power supply 240V, 50 Hz.

Specifications of all equipments are given in the following tables:

Table 5.1 (a) Material properties of the straight beam:

Property name	
Material	Aluminium
Dimension (mm)	263 X 29 X 1.5
Young's Modulus (N/m^2)	72E09
Density (Kg/m^3)	2800

Table 5.1 (b) Material properties of the circular plate:

Properties	Aluminium circular plate	Unit
Young's Modulus	72E09	Pa
Dimension	Outer radius = 300, Inner radius = 90, Thickness = 0.5	mm
Poisson ratio	0.3	
Density	2800	Kg/m^3

Piezo sensing system:

It consists of high quality charge to voltage converting signal-conditioning amplifier with variable gain, individual input/output connectors to cater for 4 channels displacement and velocity conditioner. The signal conditioners are biased with built in DC power supply.

Piezo actuation system:

It consists of a preamplifier circuit given as input and a power amplifier circuit. The output of the power amplifier is given to a step up transformer to boost the input Voltage of 0-5 Volts to 240 V RMS.

Table 5.2(a) Specifications of the Piezo sensing unit supplied by Spranktronics Inc

Sensor	Piezo electric crystal
Output	Sine/random
No of channels	4
Frequency range	10- 20000 Hz
Maximum input voltage	10 volt (RMS)
Maximum output voltage	200 volt (RMS)
Input / output connection	PT 10 terminals / BNC connectors
Input power	230 V, 50 Hz AC

Table 5.2(b) Specifications of the Piezo actuator unit supplied by Spranktronics Inc

Actuator	Piezo electric crystal
Output	Sine/random
No of channels	4
Frequency range	10- 20000 Hz
Maximum output voltage	200 volt (RMS) (adjustable gain)
Input / output connection	PT 10 terminals / BNC connectors
Input power	230 V, 50 Hz AC

Table 5.3 Properties of the piezoelectric sensor and actuator (PZT patches) by Sparkler Ceramics Pvt. Ltd:

Property name	
Material	Lead zirconate titanate.
Dimension (mm)	25 X 25 X 0.5
Young's Modulus (N/m^2)	63E09
Density (Kg/m^3)	7600
Dielectric constant (d_{31}) (m/V)	254e-12
Stress constant (g_{31})(Vm/N)	9E-3

Table 5.4 USB based Data acquisition card (NI USB 6009) by National Instruments Inc:

Property name	
Analog input	8 single ended, 4 differential software selectable
Max sampling rate	48 KS/sec
Input range	+/- 10 volt for single ended
Input resolution	13 bits
Analog output	2
Maximum update rate	150 Hz, software timed
Output range	0-5 Volt

5.2 Experimental Setup

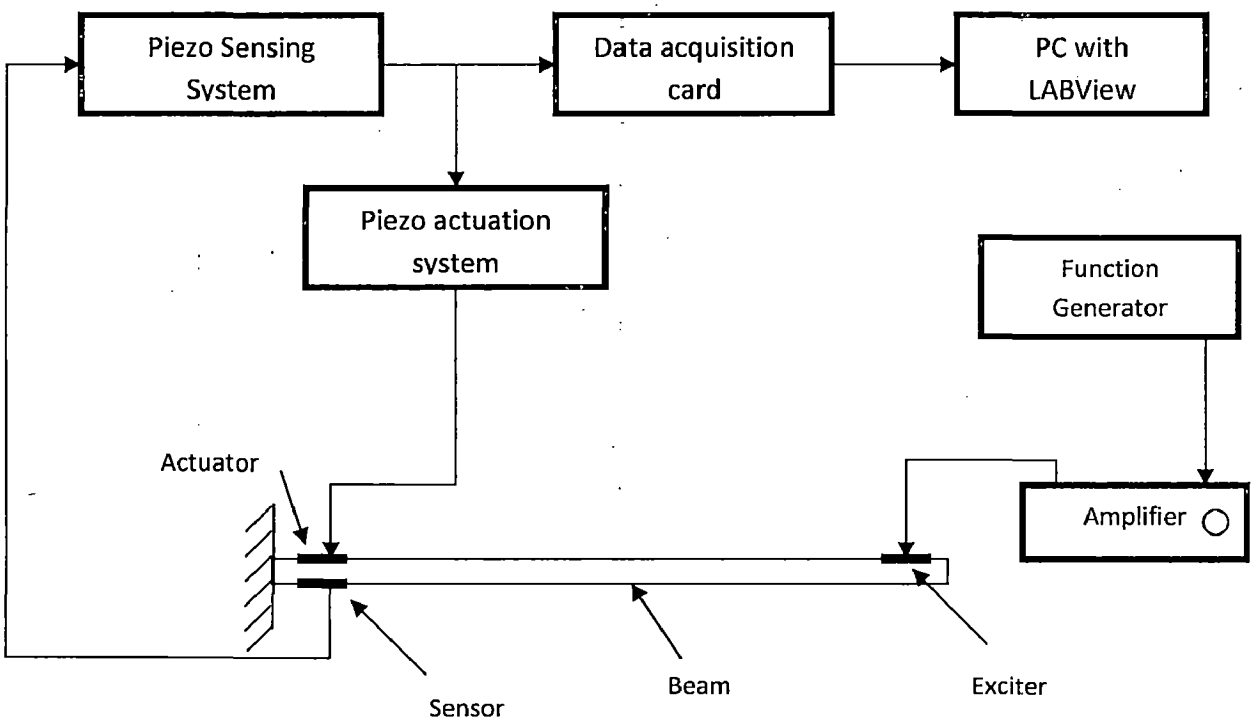

Figure 5.1: Block Diagram of experimental setup for proportional feedback control

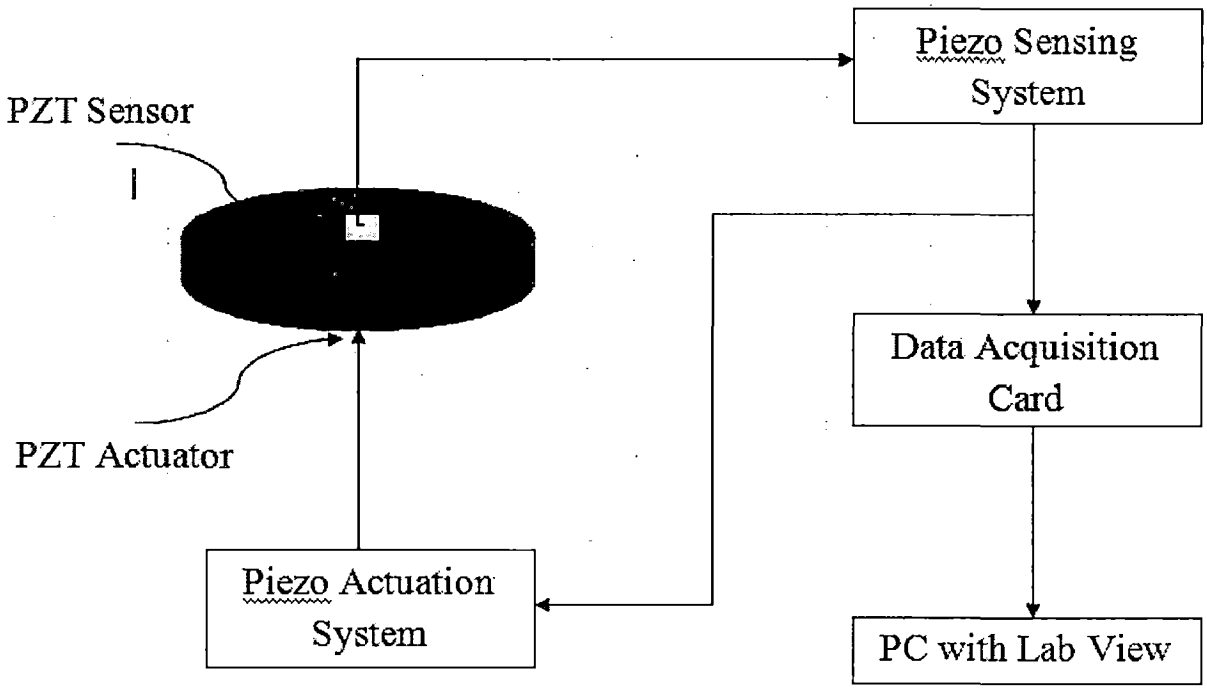

Figure 5.2: Block Diagram of experimental setup for proportional feedback control(circular plate)

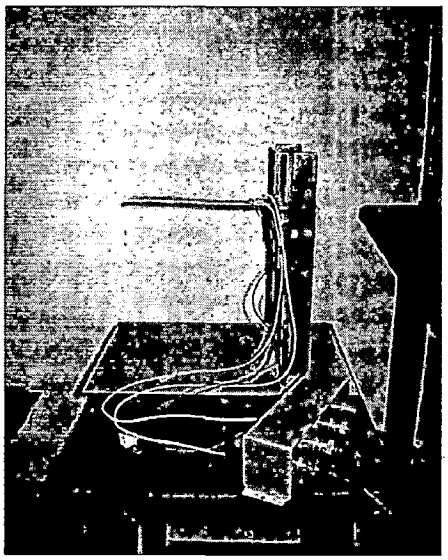

Figure 5.3: Cantilever beam

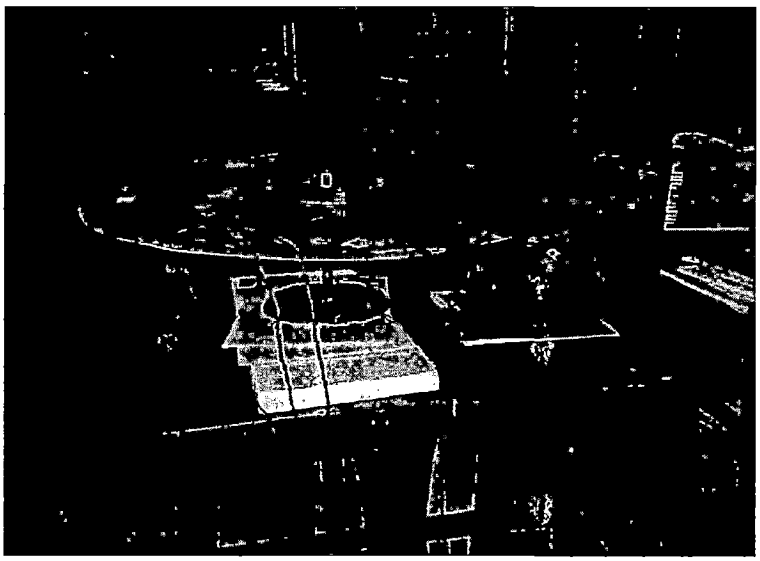

Figure 5.4: Circular plate

Figure 5.5: Experimental Setup of the Active vibration control system

Figures 5.1 and 5.2 show the schematic block diagram of the active vibration control. Figure 5.5 shows the experimental setup of the active vibration control system.

It is seen from the above diagram that PZT patch, piezo sensing and actuation and NI card forms a closed control loop. Functions of each of the above components are explained in the following sub section.

5.2.1 Piezoelectric material (PZT patch)

Smart material used in the experiment is PZT patch made by the Sparkler Ceramics Pvt Ltd with detail specification given in the table 5.3. Two PZT patches are used for the vibration suppression of the beam and one is used for providing the excitation to the beam. One PZT is mounted near the root of the beam and second PZT is mounted at the same location but on the other side of the beam in a symmetric position. One PZT patch acts as sensor and other acts as the actuator. Also one pair of PZT Patches is mounted near the free end in the same manner for better vibration suppression. Before PZT patch is bonded to the Aluminum beam, terminals are soldered by right polling direction as indicated on the both

surface of the PZT. Patch is bonded to the structure using good epoxy as shown in the figure 5.3 or figure 5.4. When the beam is excited with signal generator, the vibration of beam starts and the sensor when deformed mechanically develops the voltage across it terminals.

For the axially clamped circular plate, one PZT is mounted near the clamped end and other PZT is mounted at the same location but on the other side of the circular plate in a symmetric fashion. One PZT patch acts as sensor and other acts as the actuator. Also one pair of PZT Patches is mounted near the free end in the same manner for better vibration suppression. Patch is bonded to the structure using epoxy as shown in the Figure 5.4. When the axially clamped circular plate is excited by the function generator, it starts vibrating and the sensor when deformed mechanically develops a voltage across it terminals.

5.2.2 USB based data acquisition

As shown in the figure 5.6, data acquisition system is a National Instrument Inc, make card. This card may be used for measuring and recording of various parameters like displacement, voltage, velocity, acceleration, strain, temperature etc. in a machine, equipments or any other mechanical components. PC based DAQ normally finds application in storing real time signal. It is able to store the signal parameter so that later on it can be easily used for further analysis. Various internal devices are used for signal measurement and conversion. One of the most useful devices is the analog to the digital and digital to analog converter. Multiplexer is used to combine several input signals into a vector from for the I/O port. Counters and timers are used to control the signal time and also keep the data in the buffer for the required amount of time. Counter clock runs with CPU clock and is used to synchronize all elements.

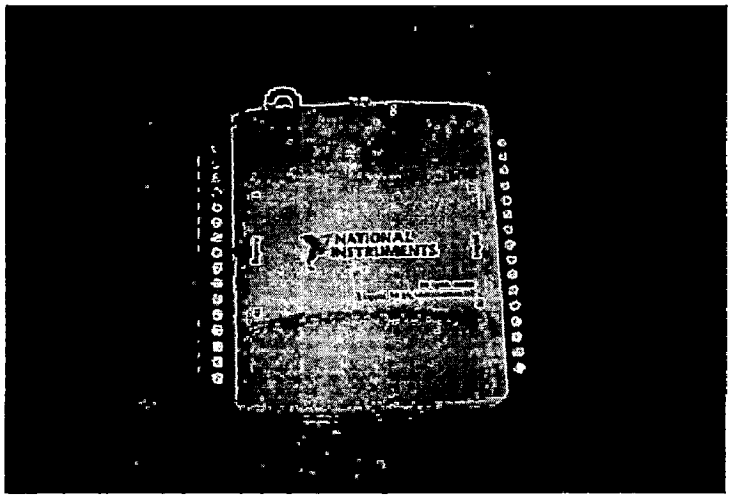

Figure 5.6: NI USB 6009 DAQ Card

In this experimentation, National instrument make USB based DAQ is used. Specimen is excited at tip by providing a known signal to the PZT patch with the help of a function generator and PZT sensor bonded at root of the beam/circular plate sends the sensed signal. This voltage is amplified by the piezo sensing system and is given to the NI card and piezo actuator system. It is able to sense the voltage generated by the PZT sensor mounted on the beam surface. PZT sensor is connected to the DAQ card through signal sensing device. The sensed voltage is scanned and stored in the computer using LABView software. The file can be used for further post processing.

The input port of the N.I card is adjustable. It is adjusted with the help of DAQ assistance in LAB view. Through DAQ assistance, connection to the DAQ card can be identified. The connection is shown in Figure 5.7.

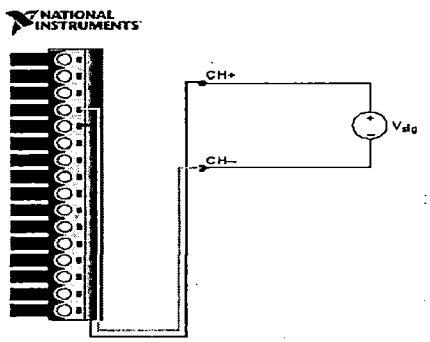

Figure 5.7: Connection of DAQ Card.

5.2.3 Piezo sensing and actuation system

Piezo sensing and actuation system shown in figure 5.8 was used in the experiment for sensing the strain generated in the PZT patch and for amplifying the signal so that it can be used for further processing. This system has four channel sensing and four channel actuation capability. Output of the PZT sensor is connected to this system using BNC cable and output of this sensing device is connected to the NI card and also connected to the actuation system. Piezo actuation system is a voltage amplifier which amplifies the voltage sensed by the sensing system so that it can actuate the PZT for vibration suppression.

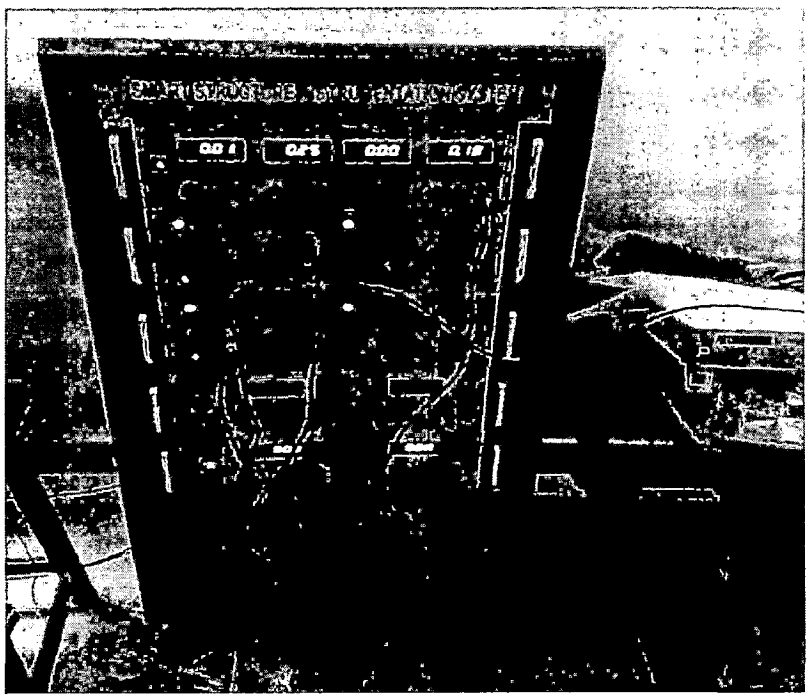

Figure 5.8: Piezo sensing and actuation system

This system has the capability that is operate in both in and out of phase of the signal. First the signal is inverted and amplified by the system, then it is supplied the PZT actuator. If the sensed signal is in phase then output signal can be made out of phase for the suppression of the vibration of the structure. The output gain may be adjusted by the knob on the actuation and sensing system. The vibration control can be made more effective by increasing the gain value of the piezo actuation system.

5.2.4 Computer with LabVIEW software

DAQ card is connected to the computer using USB data cable with USB port of the PC. LabVIEW programs are called virtual instruments, or VIs, because their appearance and operation imitate physical instruments, such as oscilloscopes and multimeters. LabVIEW contains a comprehensive set of tools for acquiring, analyzing, displaying, and storing data, as well as tools in the troubleshooting code. LabVIEW can be used to build a user interface, or front panel, with controls and indicators. Controls are in form of knobs, push buttons, dials, and other input mechanisms. Indicators are graphs, LEDs, and other output displays. After building the user interface, a add code may be added using VIs and structures to control the front panel objects. The block diagram contains this code.

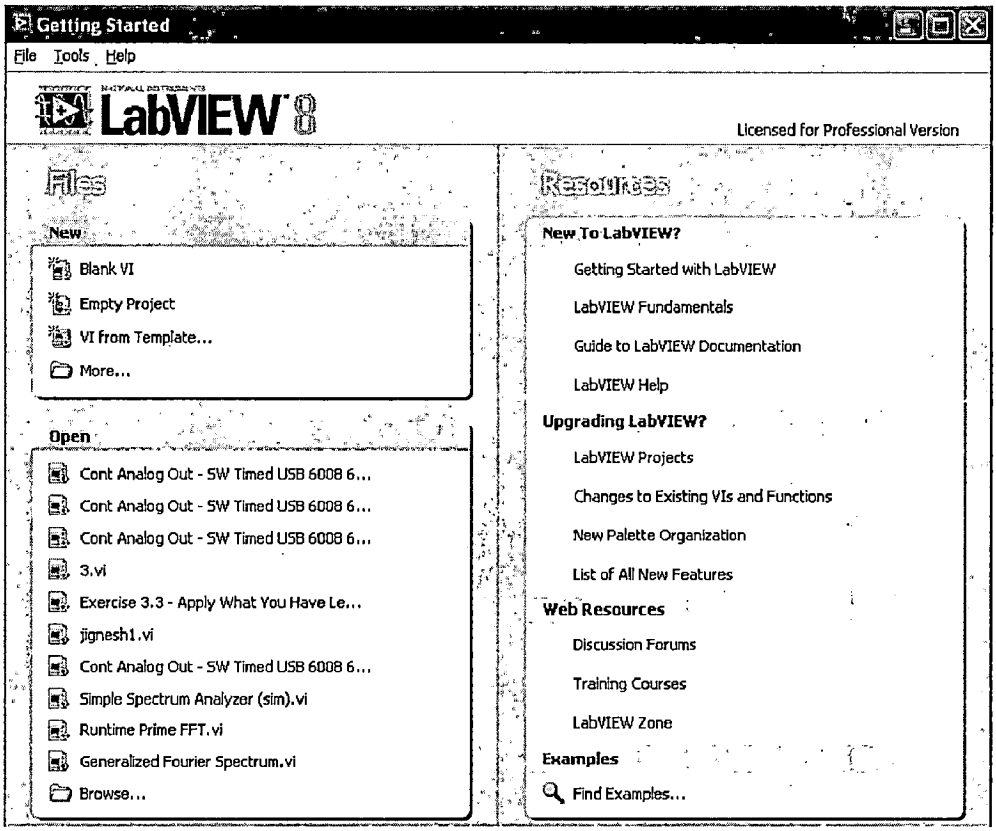

Figure 5.9: LabVIEW main screen.

The front main screen of the LabVIEW is shown in the figure 5.9. One VI is developed in the software that scans the data from the NI DAQ card. The data can be seen in the real time mode and through FFT it is possible to plot the frequency plot of the time base

data. Figure 5.10 and 5.11 show the block diagram of the program and front panel of the VI. In the block diagram, the voltage signal is scanned using the DAQ assistant block and various parameter can be setup as shown in the figure 5.12. It is also possible to change the sampling rate and frequency rate.

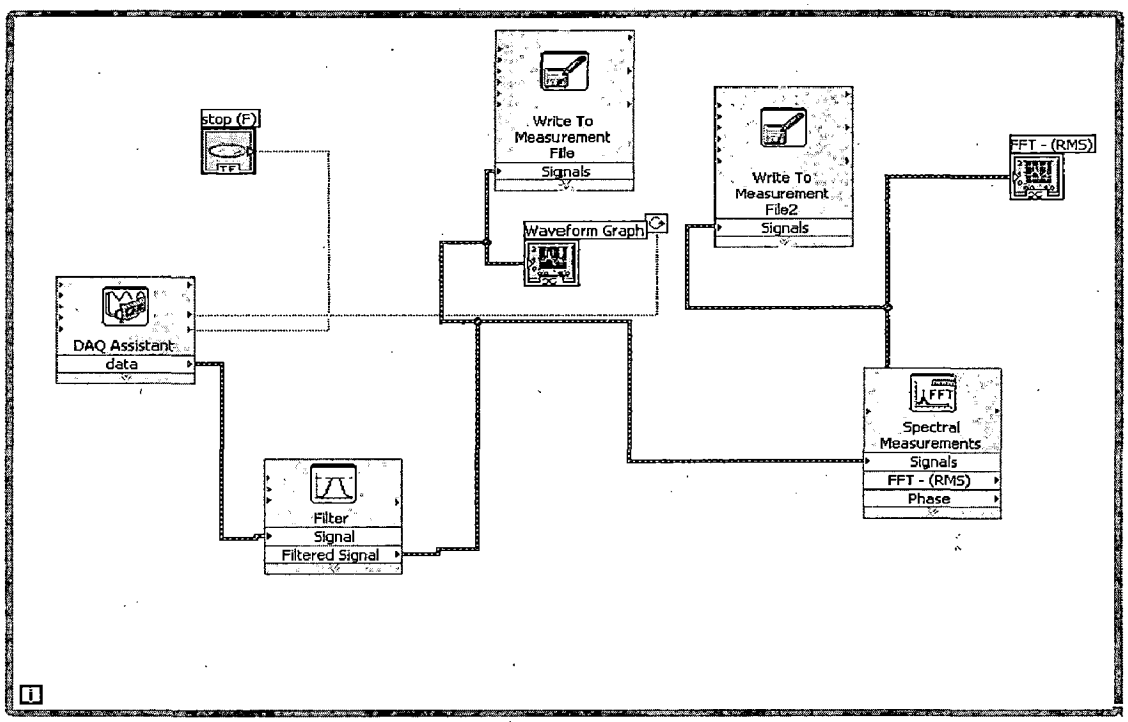

Figure 5.10: Block diagram of proportional feedback control system the LABVIEW VI program

As shown in the block diagram, the wire is connected to graph indicator block where it is possible to see the real time signal of the sensor from the PZT. Band pass filter block is fixed between the graph indicator and DAQ assistant and between the FFT block and DAQ assistant so that it removes the high frequency component from the signal. FFT block is used here for finding the natural frequency of the signal so that it can be compared to the modal frequency and the theoretical frequency. Both time domain file and FFT file can be stored on the hard disc of the PC using file to measurement block as shown in the block diagram. Front panel of the VI shows only two graphs, one for the time domain signal and other for the frequency domain signal.

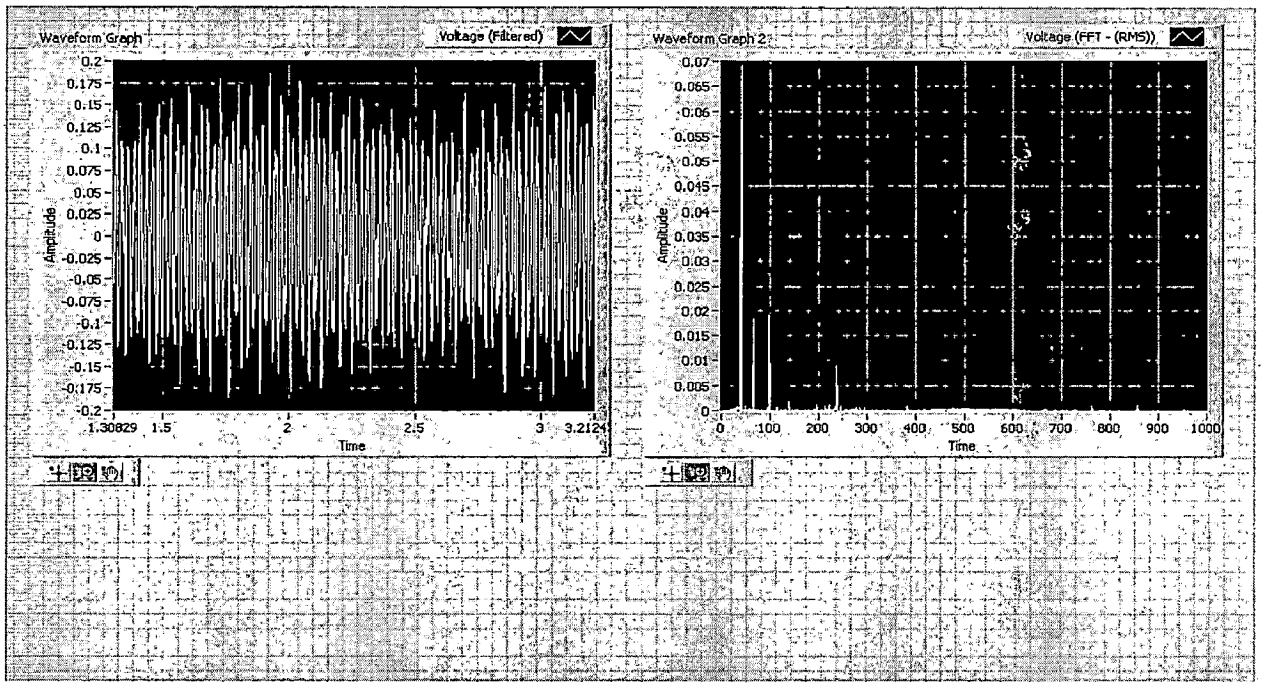

Figure 4.11: Front panel of the LABVIEW VI program

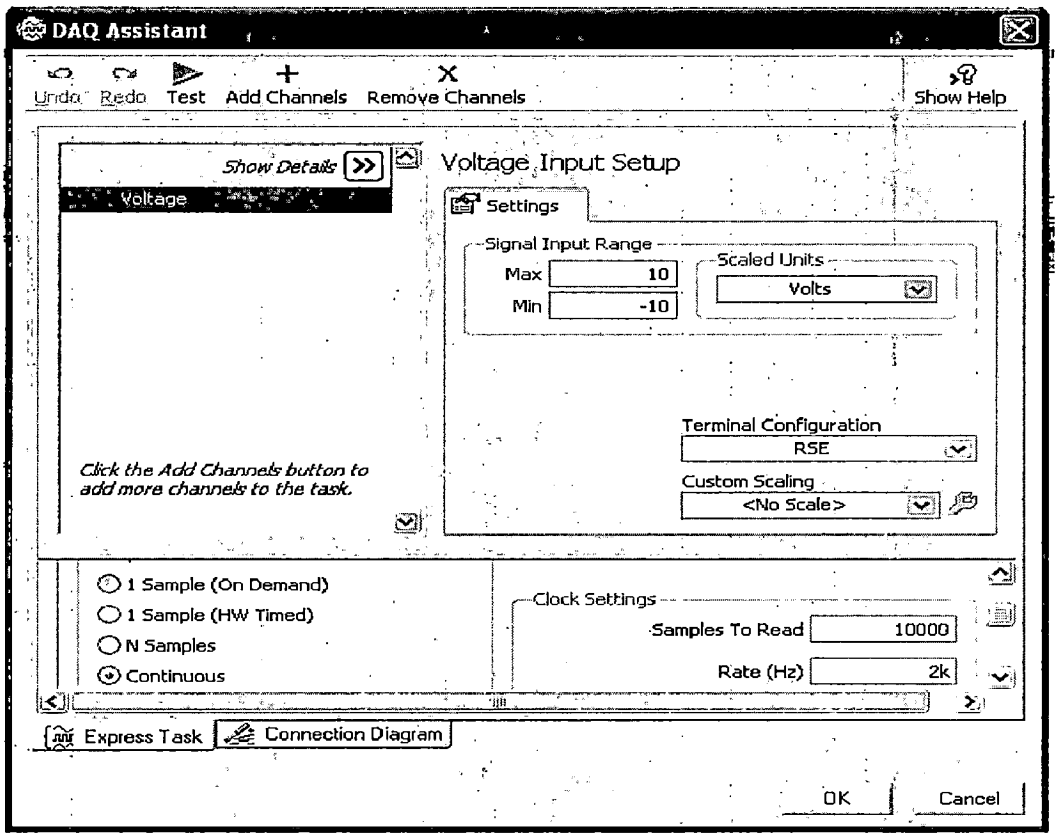

Figure 5.12: DAQ assistant parameter dialogue box

5.3 Procedure

The proportional control method has been used for the vibration suppression Therefore the output of the sensor is given to the input of the actuation system directly. For performing the experiment, the beam/ circular plate is excited using function generator. Sensed voltage is recorded in the PC without and with gain applied to the actuation system. It implies that the data are stored without control action and with control action. Both data are then normalized with the sensor voltage. These normalized data are compared with each other on the same scale with different excitation voltage and frequency and also compared for vibration control with single and multi patches.

Following procedures are adopted during the experiment.

(1) Aluminum beam with patch bonded on to the surface is placed properly in the clamping structures.

(2) PZT patches are wired to the piezo sensing and actuation system properly.

(3) DAQ NI card is connected to the PC using USB cable. The output of the sensing system is connected to the proper analog input port of the NI card and input of the actuation system.

(4) BNC and coaxial wire connection is mostly used for the interconnection of all the devices to avoid shorting of wires and to reduce the noise level.

(5) Keeping the phase IN/OUT switch in PHASE position.

(6) Keeping the voltage adjusting switch below 50V.

(7) Slowly increasing the actuation voltage till the Piezo sensing voltage is reached.

6.1 Validation of Results obtained

The properties of the Aluminum structures and PZT patch used in the experimental setup are given in the table 6.1(a) and table 6.2(a). Two PZT patches are bonded on the top and bottom surface of the structures in a symmetrical manner. Structures are excited by a function generator and the sensor reading is recorded in the computer using the NI make data acquisition card. The sensor reading is taken for various amplitudes and frequencies and the plot is compared with and without the proportional control strategies. Here the sensor data is normalized for comparing the response with and without the control.

Table 6.1(b) and 6.2(b) show the comparison of the natural frequency of the structures. It has been observed that the experimental results of the present work compares very well with the theoretical results.

Table 6.1(a) Properties of the aluminum beam and PZT

Property name	Aluminum beam	PZT (Sparkler Inc.)
Dimension (mm x mm x mm)	263 X 29 X 1.5	25 X 25 X 0.5
Young's modulus (N/m^2)	72E09	63E09
Density (Kg/m^3)	2800	7600
Stress constant (g_{31}) (Vm/N)	-	9E-3

Table 6.1(b) Comparison of Natural frequency of beam.

Mode	Theoretical	Experimental	Percentage error
1	26.85	25.75	4.09
2	55.65	53.25	4.31
3	125.26	123.30	1.56
4	165.55	162.35	1.92
5	190.3	187.15	1.65

Table 6.2(a) Material properties of the circular plate and PZT:

Properties	Aluminium circular plate	PZT (Sparkler Inc.)
Young's Modulus (N/m^2)	72E09	63E09
Dimension(mm x mm x mm)	Outer radius = 300, Inner radius = 90, Thickness = 0.5	25 X 25 X 0.5
Poisson ratio	0.3	
Density (Kg/m^3)	2800	7600

Table 6.2(b) Comparison of Natural frequency of beam.

Mode	Theoretical	Experimental	Percentage error
1	28.80	27.65	3.99
2	68.75	66.25	3.63
3	135.25	133.30	1.44
4	170.35	167.35	1.76
5	210.40	206.45	1.87

6.2 Experimental results

In this section, the response of structures is obtained from experiment for the proportional feedback control for different excitation voltage and frequency. Vibration control achieved with single and multi patches are also compared. The properties of the structures and PZT patch used in the experimental setup given in the table 5.1(a), 5.1(b) and 5.3. Two PZT patches are bonded on the top and bottom surface of the structures near the fixed end and two PZT patches are bonded at other location near the free end in a symmetrical manner. The structures are excited by an impulse force at the free end near the centre line of the structures. The sensor reading is recorded in the computer using the NI make data acquisition card. The sensor reading is taken during each impulse and the plot is

compared with and without the proportional control strategies. The results with single patches and multi patches configuration were obtained in same manner. Here the sensor data is normalized for comparing the response with and without the control.

6.2.1 Cantilever beam

Experimentation was done on the cantilever beam by exciting it at the tip using a function generator. Readings were taken for a number of natural frequencies of the beam, as well as for some frequencies above and below the natural frequency. For a given frequency, voltage of exciting current was varied in increments of 0.1 V. The range of the wave function was used as an indicator to measure the amount of controlling action achieved.

A sample of the readings thus obtained is shown below. The frequency of excitation is 20 Hz (second natural frequency of beam is 26 Hz), and the applied voltage is 0.5 V. The uncontrolled and controlled voltages detected by the sensor are:

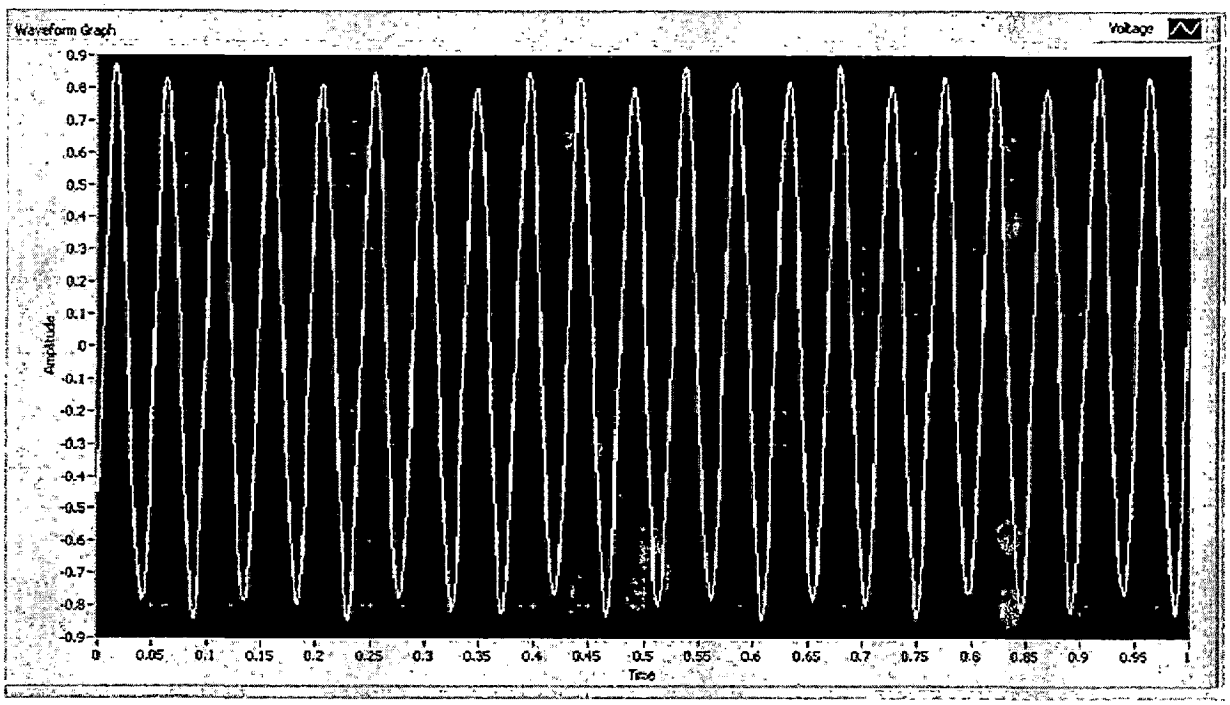

Figure 6.1: Amplitude uncontrolled, excitation by function generator

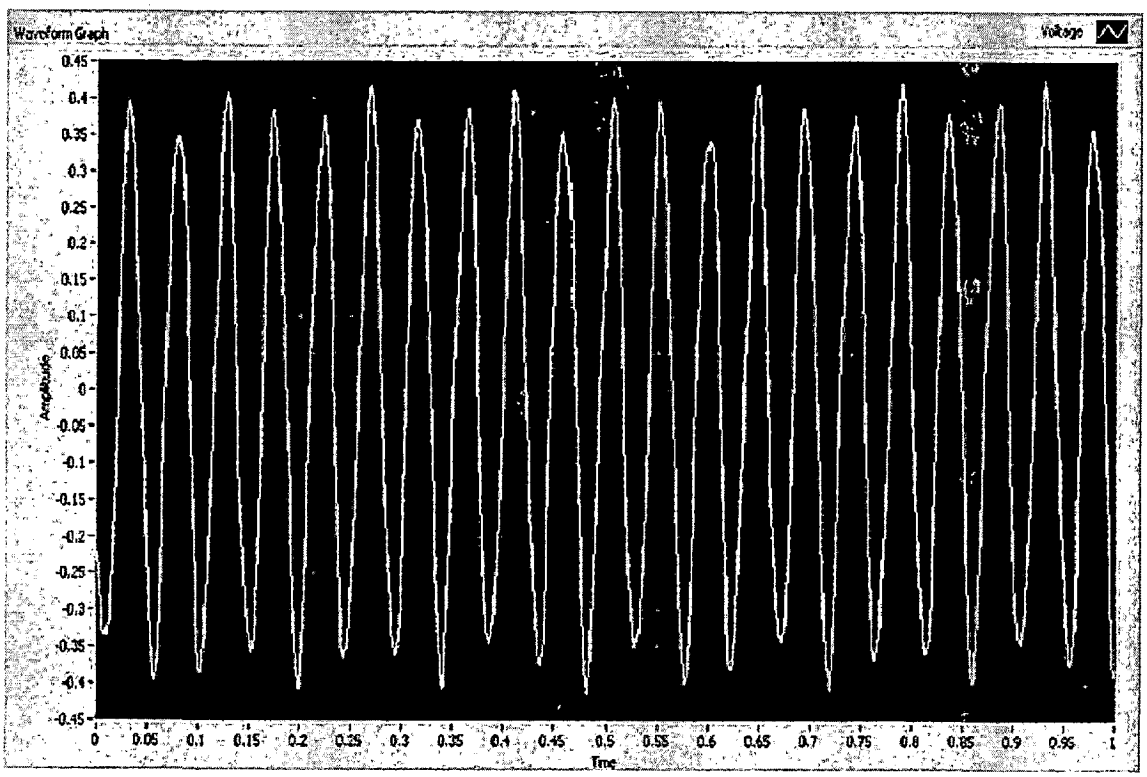

Figure 6.2: Amplitude controlled, excitation by function generator

In the above figures, in case of uncontrolled vibrations, it can be seen that the range of the waveform is approximately 1.65 volts. But after proportional feedback control method is applied, the same range reduces to about 0.81 volts. Hence, we observe a vibration reduction of nearly 51%.

As the frequency reaches the natural frequency, the magnitude of the vibrations increases, but the nature of the waveform still remains sinusoidal.

In a similar manner, % control was found out for a number of frequencies for the beam at increments of 0.1 volt. The readings are summarized in the following table:

Frequency	Voltage (V)	Range(Uncontrolled)	Range(controlled)	Actuation Voltage	%Control
20	0.5	1.65	0.81	36	50.9
	0.6	1.92	0.94	41	51.04
	0.7	2.2	1.04	47	52.73
	0.8	2.58	1.2	54	53.49
	0.9	2.9	1.37	60	52.76
	1	3.16	1.54	65	51.27
26	0.5	3.5	1.6	67	54.28
	0.6	4.2	1.89	78	55
	0.7	5	2.2	87	56.2
	0.8	5.55	2.5	96	54.54
	0.9	6.1	2.8	103	54.1
	1	7.1	3.2	112	54.92
32	0.5	3.5	1.6	70	54.29
	0.6	4.2	1.92	79	54.29
	0.7	5.3	2.4	96	54.72
	0.8	6.5	2.7	107	55.37
	0.9	7.3	3.4	119	53.42
	1	8.2	3.75	128	54.2

Table 6.1 Experimental readings for cantilever beam with single pair PZT patches configuration.

As can be seen, the controlling action remains in the vicinity of 50%. This is consistent with theoretical models, which predict the controlling action to be a little more than 50% for proportional control method. Thus, this establishes the correctness of the theoretical analysis.

Based on the above readings, plots were obtained for the % controlling action versus the voltage applied for a given frequency. A rough pattern was observed in sense that as the frequency approached the natural frequency, the % controlling action increased slightly, and then showed a decreasing trend again as frequency was increased beyond the natural frequency. This trend can be clearly seen from the following plot:

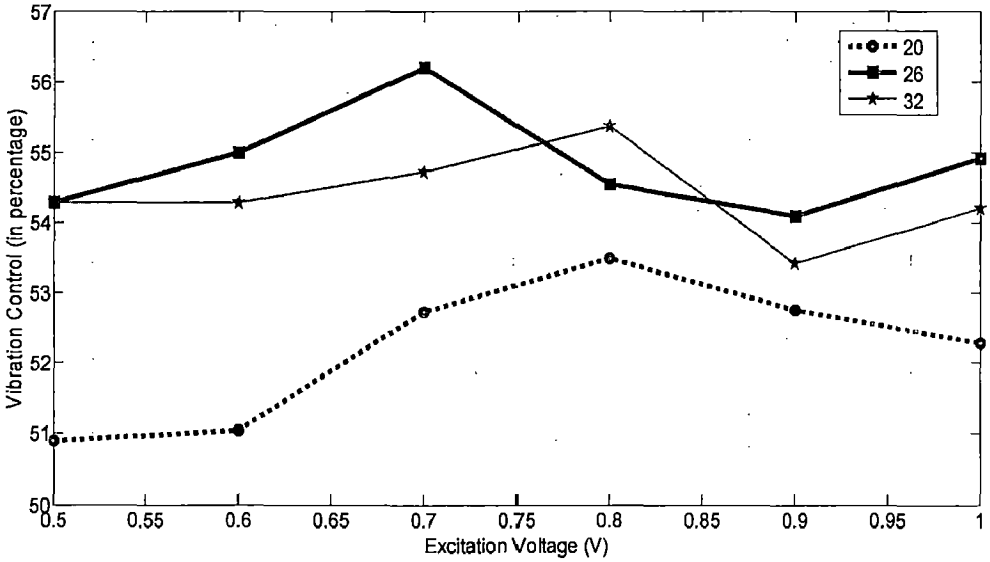

Figure 6.3: Plot for controlling action versus voltage for cantilever beam with different excitation frequencies.

After experimenting with the single patches configuration, one extra pair of PZT patches (sensor and actuator) was mounted near the midpoint of the beam, ie, 144mm from fixed end. Sensor reading was taken without and with control gain. A sample of the readings thus obtained is shown below. The frequency of excitation is 20 Hz and the applied voltage is 0.5 V. The uncontrolled response is shown in figure 6.1 and controlled response in figure 6.4.

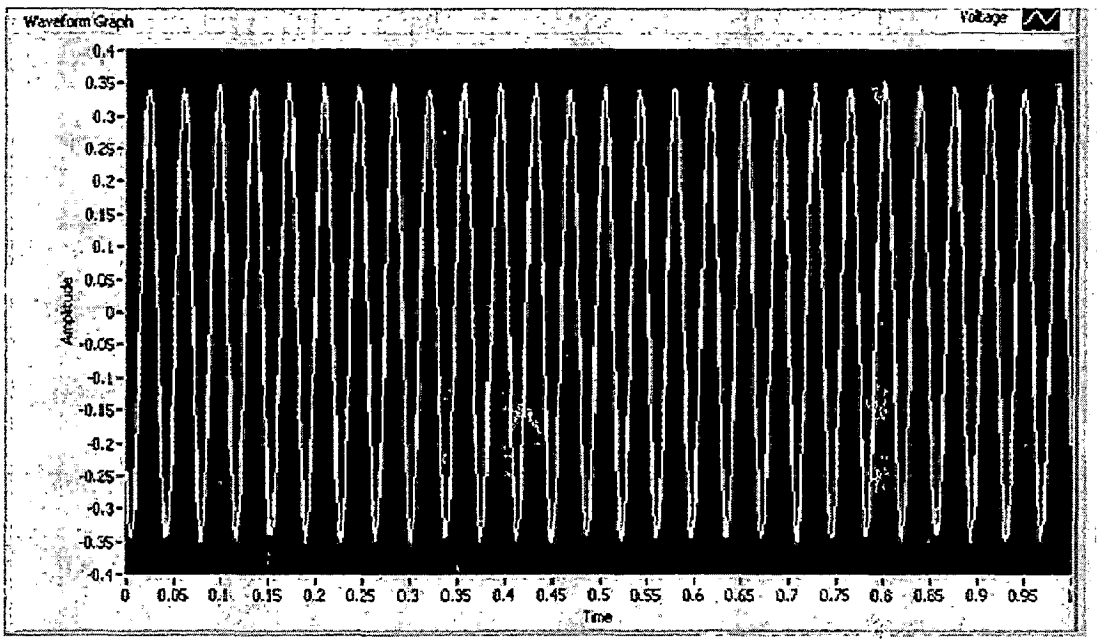

Figure 6.4: Amplitude controlled, excitation by function generator

In the above figures, in case of uncontrolled vibrations, it can be seen that the range of the waveform is approximately 1.65 volts. But after proportional feedback control method with two PZT patches configuration is applied, the same range reduces to about 0.7 volts. Hence, we observe a control of nearly 57.57%.

In a similar manner, % control was found out for a number of frequencies for the beam at increments of 0.1 volt. The readings are summarized in the following table:

Frequency	Voltage (V)	Range(Uncontrolled)	Range(controlled)	Actuation Voltage	%Control
20	0.5	1.65	0.7	24	57.57
	0.6	1.92	0.78	28	59.37
	0.7	2.2	0.89	33	59.54
	0.8	2.58	1.1	39	57.36
	0.9	2.9	1.25	45	56.89
	1	3.16	1.42	49	55
26	0.5	3.5	1.44	52	58.85
	0.6	4.2	1.72	59	59.04
	0.7	5	2	65	60
	0.8	5.55	2.25	73	59.45
	0.9	6.1	2.5	80	59.01
	1	7.1	2.9	87	59.15
32	0.5	3.5	1.4	54	59.14
	0.6	4.2	1.7	62	59.52
	0.7	5.3	2.2	74	58.49
	0.8	6.5	2.75	83	57.69
	0.9	7.3	3.1	92	57.53
	1	8.2	3.51	104	57.19

Table 6.2 Experimental readings for cantilever beam with two pair PZT patches configuration.

As can be seen, the controlling action of beam response with two pair PZT patches configuration is better than with single pair PZT patches configuration. It's has 5-7% better control of vibration of cantilever beam.

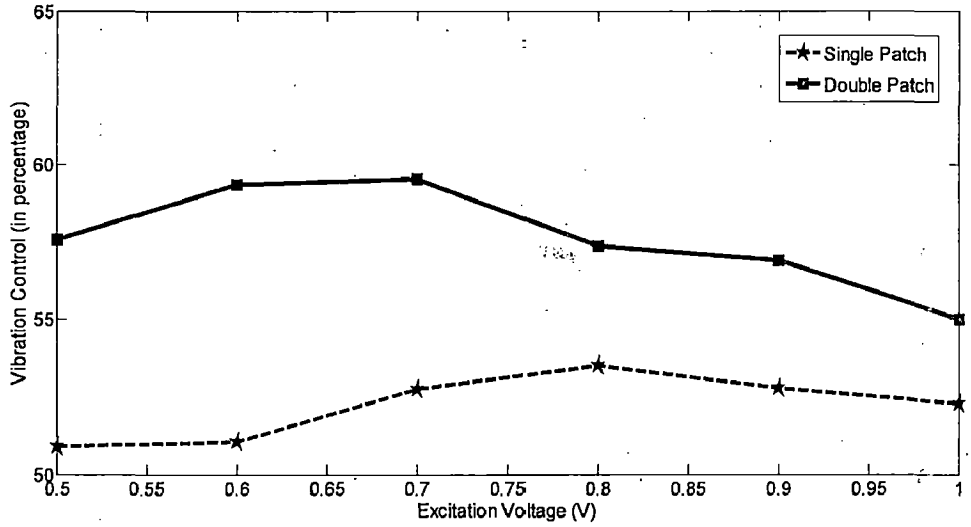

Figure 6.5: Plot for controlling action versus voltage for single and double PZT patches configuration.

6.2.2 Axially clamped circular plate

Again, in this case also, readings were taken for the % controlling action at different frequencies of excitation, for increments of excitation voltage by 0.2 Volt. However, this case is fundamentally different from that of cantilever beam in two aspects:

a) An additional parameter 'ø' is introduced, where 'ø' is the angular separation between the point at which exciting force is applied and the point where sensor and actuator are placed.

b) Due to complex mode shapes for circular plate, the voltage waveform detected by sensor patch may not be perfectly sinusoidal always. Hence, the range of the waveform can no longer be used as a reliable measure for calculating the % control achieved. Instead, the reduction in RMS value of the sensor voltage is used to indicate the amount of control observed.

An interesting observation in case of circular plate was that resonance was spread over a frequency range instead of being concentrated at a single frequency. Further, this range was found to vary with the angular distance between the point of excitation and the sensor/actuator. This was probably because of the non symmetric shapes at different modes, leading to different kinds of excitations at different frequencies.

Hence, we obtained a set of readings at increments of 30 degree angles. The readings are summed up in a tabular form. The following pictures show a sample of such readings for which the angle between point of excitation and sensor is 0 degrees, applied voltage is 0.6 volts and the frequency of excitation is 24 Hz.

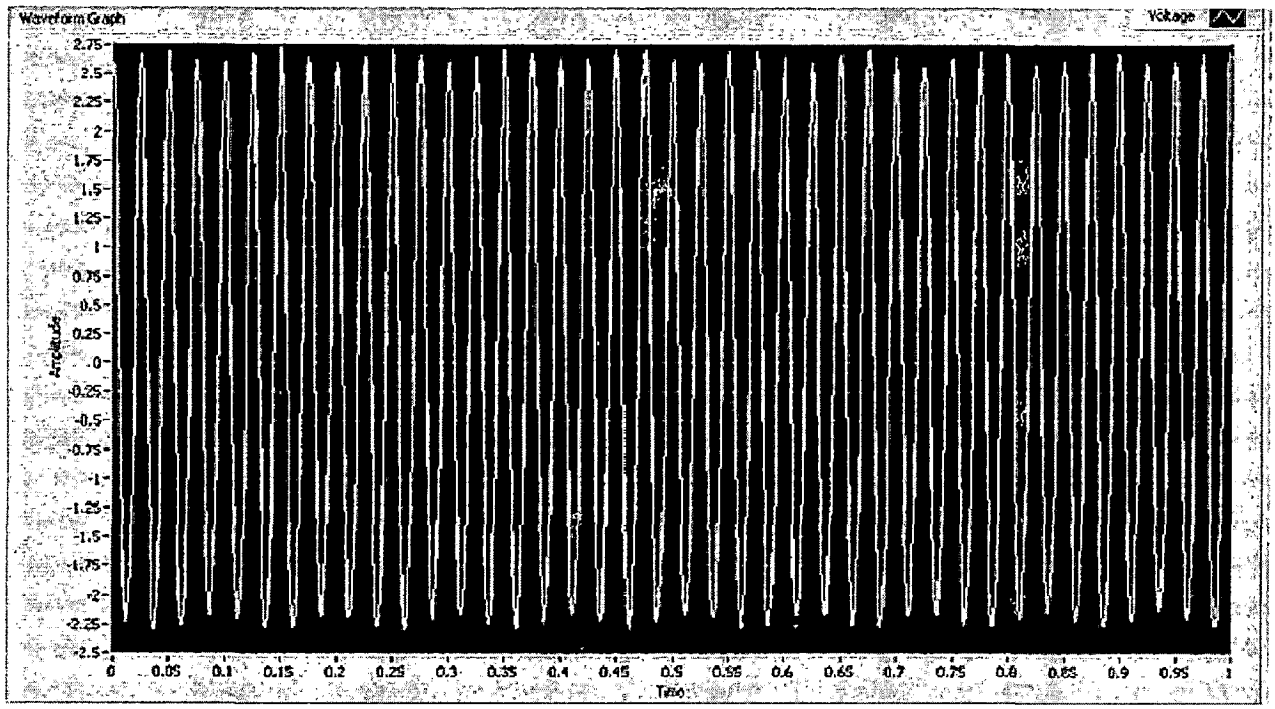

Figure 6.6: Amplitude uncontrolled, excitation by function generator (Circular plate)

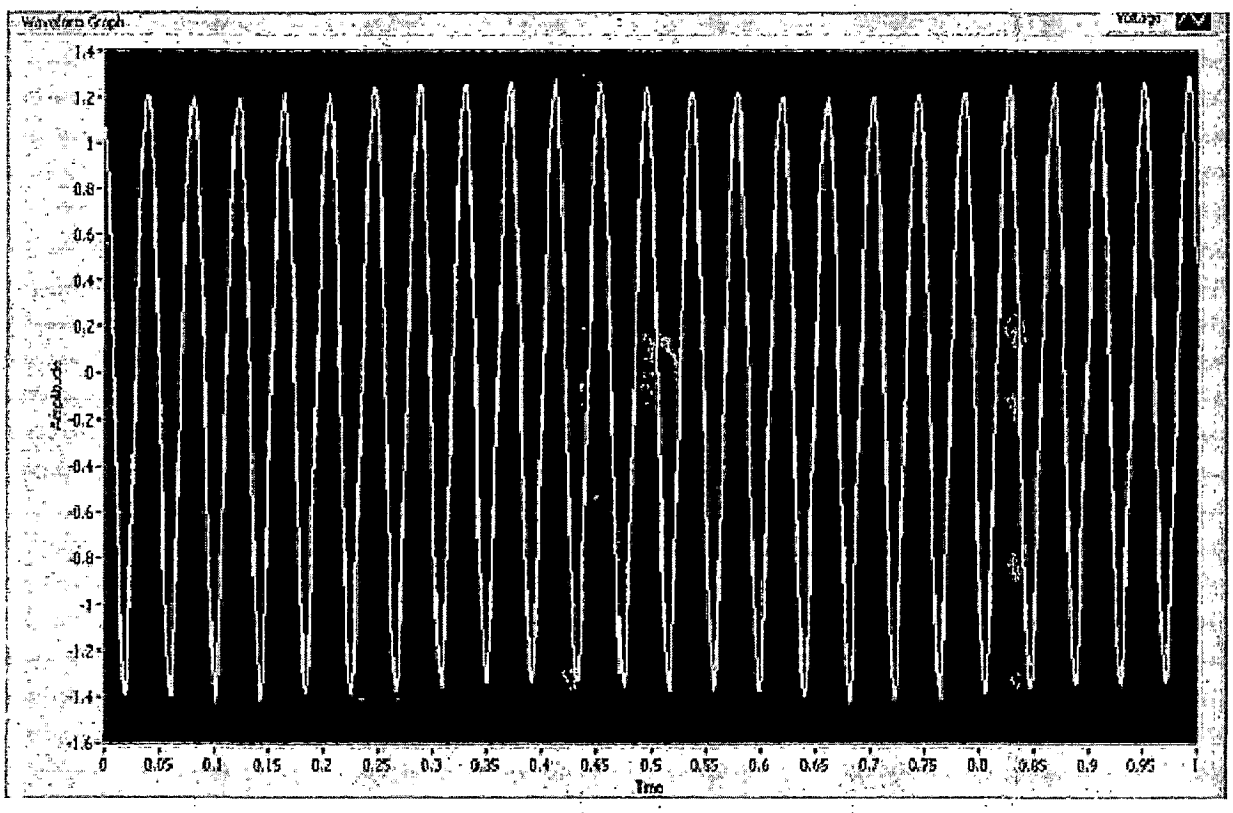

Figure 6.7: Amplitude controlled, excitation by function generator (Circular plate)

In the above figures, in case of uncontrolled vibrations, it can be seen that the range of the waveform is approximately 5.0 volts. But after proportional feedback control method is applied, the same range reduces to about 2.6 volts. Hence, we observe a control of nearly 48%.

Even though it may be expected that due to sheer size, the controlling action for circular plate will be significantly lesser than cantilever beam, the reason we are seeing similar actions here is that the thickness of the circular plate is much lesser than the cantilever beam. Hence, due to size effect, the controlling action gets magnified.

Readings similar to the ones shown above were obtained and tabulated. Following is a sample table for such readings:

Frequency(Hz)	Voltage (V)	Range(Uncontrolled)	Range(Controlled)	%Control
24	0.6	5	2.6	48
	0.8	6.4	3.24	49.37
	1	8.5	4.1	51.76
	1.2	10.5	5.3	49.52
	1.4	12.2	6.2	49.18
28	0.6	8.5	4.25	50
	0.8	11.3	5.6	50.44
	1	14.4	7	51.38
	1.2	17.2	8.65	49.7
	1.4	19.6	9.85	49.74
40	0.6	7	3.6	48.57
	0.8	10.2	5	50.98
	1	13.2	6.6	50
	1.2	15.8	8	49.36
	1.4	18.4	9.3	49.45

Table 6.3 Experimental readings for circular plate at a particular angle (0 degrees) with single pair PZT patches configuration.

Based on the above readings, plots were obtained for the % controlling action versus the voltage applied for a given frequency. A rough pattern was observed in the sense that as the frequency approached the natural frequency, the % controlling action increased slightly, and then showed a decreasing trend again as frequency was increased beyond the natural frequency. This trend can be clearly seen in the figure 6.8. It was noted that at some frequencies, lot of noise was emitted at resonance while at some other frequencies, resonance occurred without noise emission. It was further noted that at those frequencies at which noise is emitted, controlling action reduces significantly.

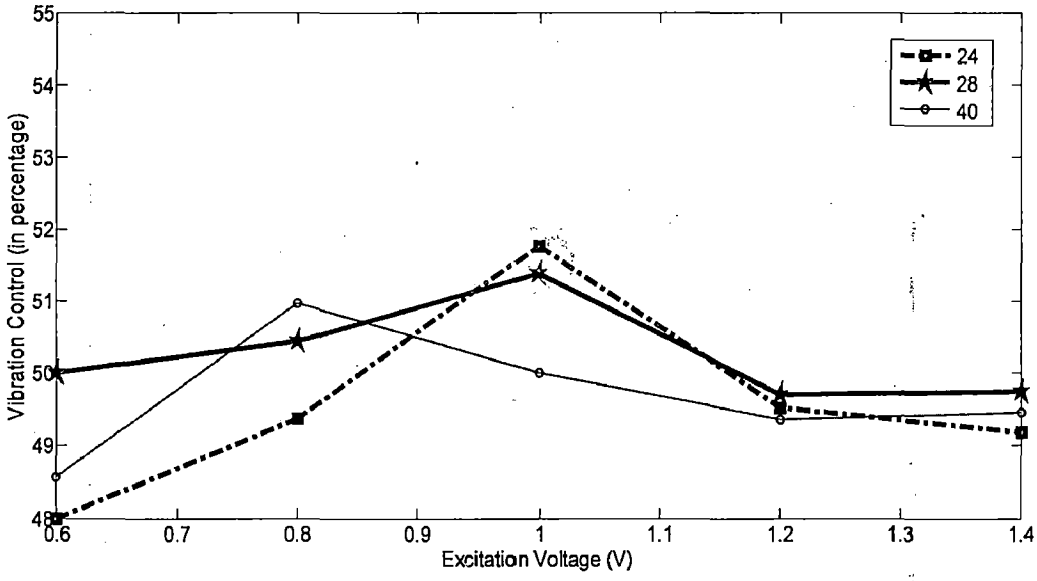

Figure 6.8: Plot for controlling action versus voltage for circular plate with different excitation frequencies.

After experimenting with the single patches configuration, one extra pair PZT patches (sensor and actuator) was mounted near the free end of the circular plate (at 230 mm radius). Sensor reading was taken without and with control strategies. A sample of the readings thus obtained is shown below. The frequency of excitation is 24 Hz and the applied voltage is 0.6 V. The uncontrolled response is shown figure 6.5 and controlled response in figure 6.9,

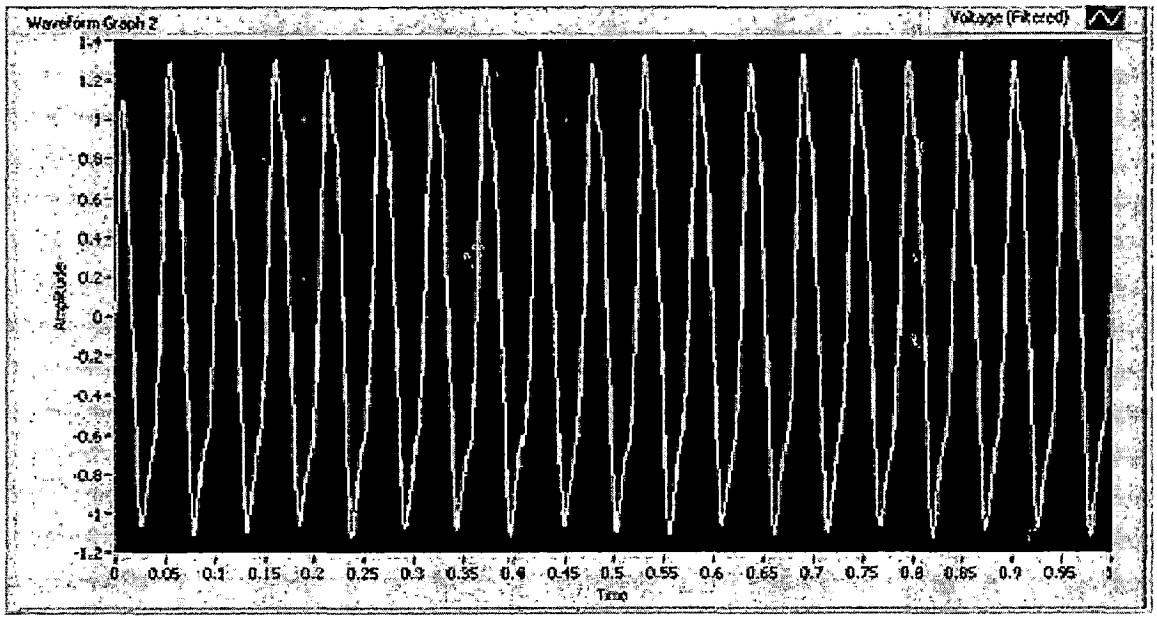

Figure 6.9: Amplitude controlled, excitation by function generator (Circular plate)

In the above figures, in case of uncontrolled vibrations, it can be seen that the range of the waveform is approximately 5.0 volts. But after proportional feedback control method with two PZT patches configuration is applied, the same range reduces to about 2.4 volts. Hence, we observe a control of nearly 52%.

In a similar manner, % control was found out for a number of frequencies for the circular plate at increments of 0.2 volt. The readings are summarized in the following table:

Frequency(Hz)	Voltage(V)	Range(Uncontrolled)	Range(Controlled)	%Control
24	0.6	5	2.4	52
	0.8	6.4	2.95	53.9
	1	8.5	3.8	55.29
	1.2	10.5	4.9	53.34
	1.4	12.2	5.65	53.68
28	0.6	8.5	3.95	53.52
	0.8	11.3	5.15	54.42
	1	14.4	6.45	55.2
	1.2	17.2	7.9	54.06
	1.4	19.6	9.1	53.57
40	0.6	7	3.35	52.14
	0.8	10.2	4.65	54.41
	1	13.2	6.05	54.16
	1.2	15.8	7.4	53.16
	1.4	18.4	8.8	52.17

Table 6.4 Experimental readings for circular plate at a particular angle (0 degrees) with two pair PZT patches configuration.

We can see that, the controlling action of vibration response of circular plate with two pair PZT patches configuration is better than with single pair PZT patches configuration. It's has 4-6% better control of vibration of circular plate than single patches configuration.

Also the reading of vibration response of circular plate with 30 degree angle between the point of excitation and sensor /actuator pair were taken. The following figures show a sample of such readings, applied voltage is 0.6 volts and the frequency of excitation is 24 Hz.

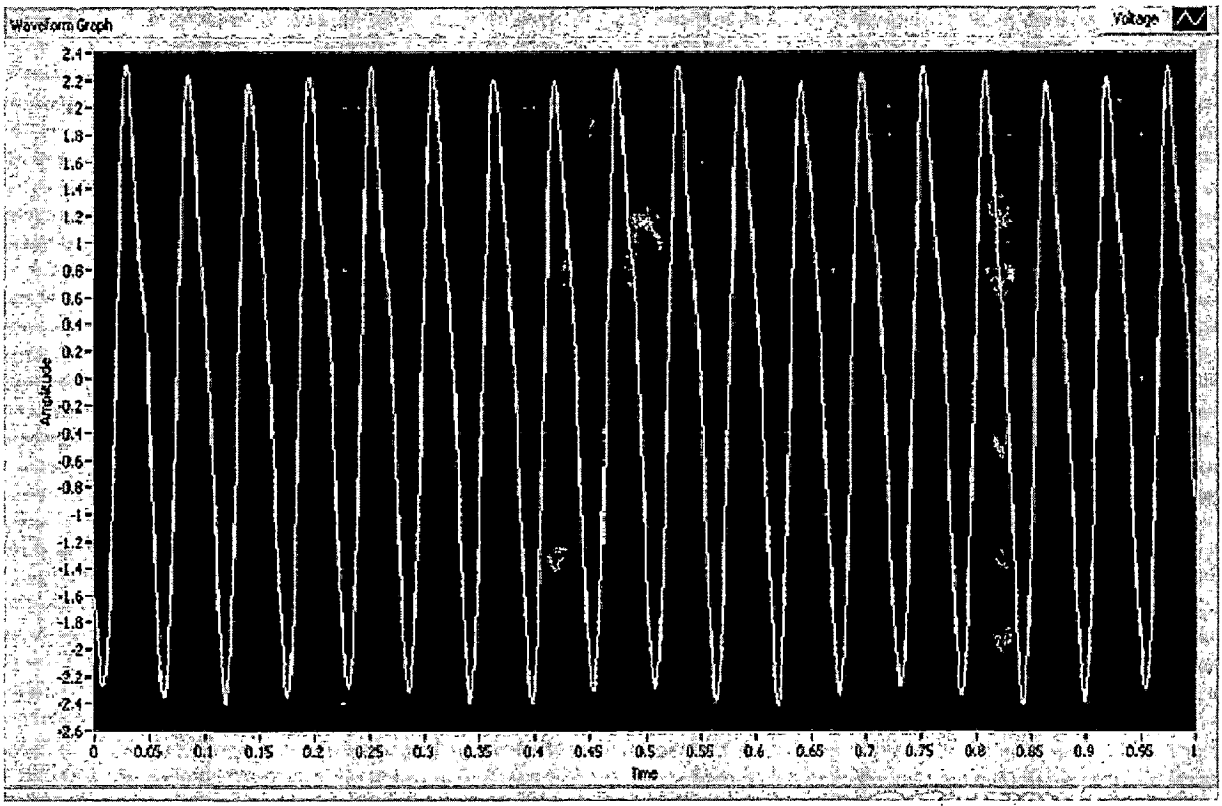

Figure 6.8: Amplitude uncontrolled, excitation by function generator

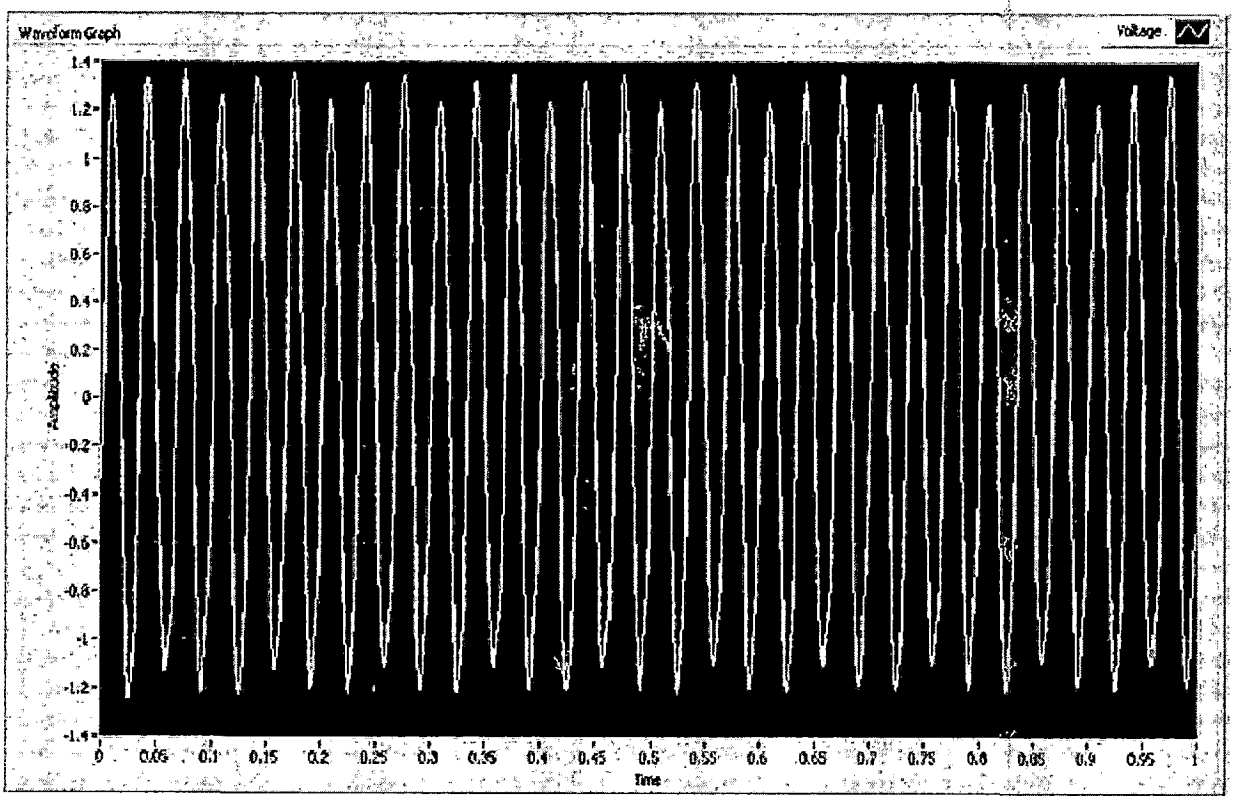

Figure 6.9: Amplitude controlled, excitation by function generator

In the above figures, in case of uncontrolled vibrations, it can be seen that the range of the waveform is approximately 4.7 volts. But after proportional feedback control method is applied, the same range reduces to about 2.55 volts. Hence, we observe a control of nearly 46%.

Readings similar to the ones shown above were obtained and tabulated. Following is a sample table for such readings:

Frequency(Hz)	Voltage(V)	Range(Uncontrolled)	Range(Controlled)	%control
24	0.6	4.7	2.55	45.74
	0.8	6.2	3.3	46.77
	1	8	4	50
	1.2	10	5.1	49
	1.4	11.8	6.1	48.3
28	0.6	7	3.7	47.14
	0.8	9.7	5	48.45
	1	12.5	6.25	50
	1.2	15.8	8.1	48.73
	1.4	18.4	9.4	48.91
34	0.6	6.2	3.45	44.35
	0.8	8.1	4.35	46.29
	1	10.9	5.6	48.62
	1.2	13.5	6.84	49.33
	1.4	15.9	8.25	48.1

Table 6.5 Experimental readings for circular plate at angle (30 degrees) with single pair PZT patches configuration.

Similarly, the controlling action of vibration responses of circular plate with two PZT patches at the 30 degrees angle between point of excitation and sensor /actuator pair are shown as following figures and table,

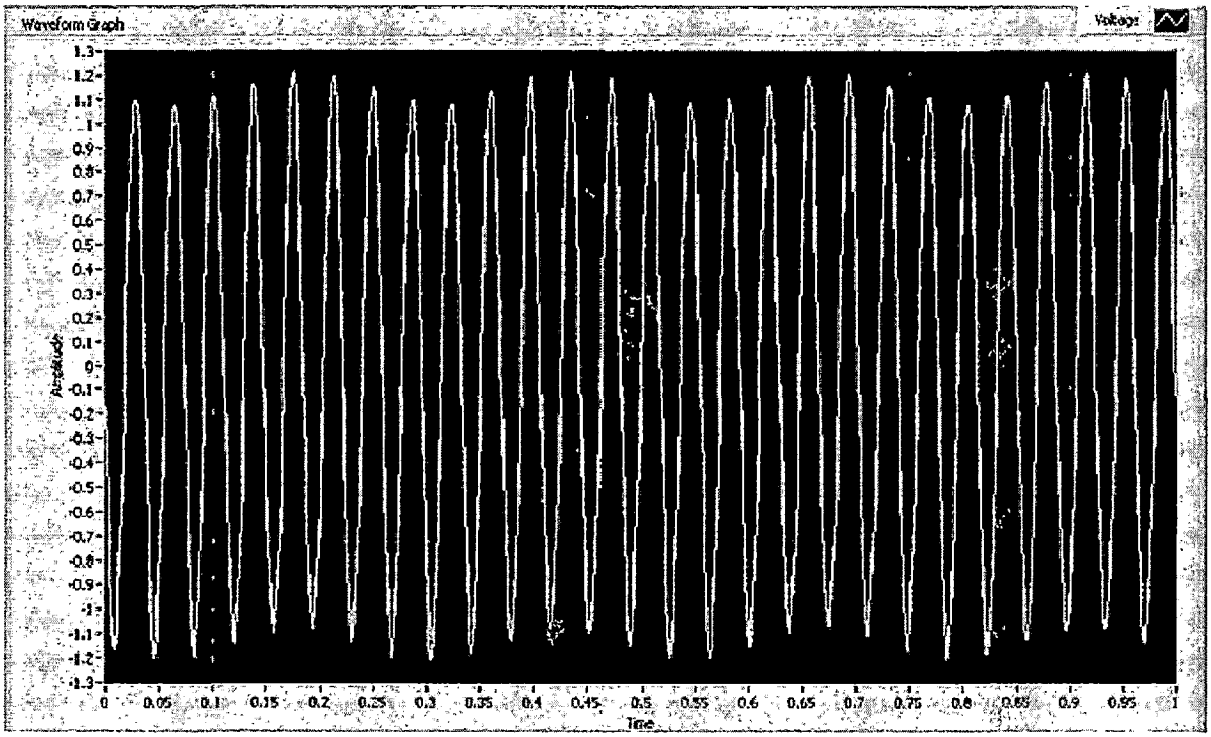

Figure 6.10: Amplitude controlled, excitation by function generator

Here, in case of uncontrolled vibrations (figure6.8), it can be seen that the range of the waveform is approximately 4.7 volts. But after proportional feedback control method is applied, the same range reduces to about 2.38 volts (figure 6.10). Hence, we observe a control of nearly 50%.

In a similar manner, % control was found out for a number of frequencies for the circular plate at increments of 0.2 volt. The readings are summarized in the following table:

Frequency (Hz)	Voltage (V)	Range (Uncontrolled)	Range (Controlled)	%Control
24	0.6	4.7	2.38	49.36
	0.8	6.2	3.1	50
	1	8	3.75	53.12
	1.2	10	4.75	52.25
	1.4	11.8	5.55	52.96
28	0.6	7	3.4	51.42
	0.8	9.7	4.55	53.09
	1	12.5	5.7	54.4
	1.2	15.8	7.45	52.84
	1.4	18.4	8.65	52.98
34	0.6	6.2	3.2	48.38
	0.8	8.1	4.05	50
	1	10.9	5.2	52.29
	1.2	13.5	6.3	53.34
	1.4	15.9	7.6	52.2

Table 6.6 Experimental readings for circular plate at angle (30 degrees) with two pair PZT patches configuration.

Similarly, the angle between point of excitation and sensor /actuator pair is now increased to 60 degrees. Vibration response of circular plate without and with proportional feedback control strategies is obtained. The following figures show a sample of such readings, applied voltage is 0.6 volts and the frequency of excitation is 29 Hz.

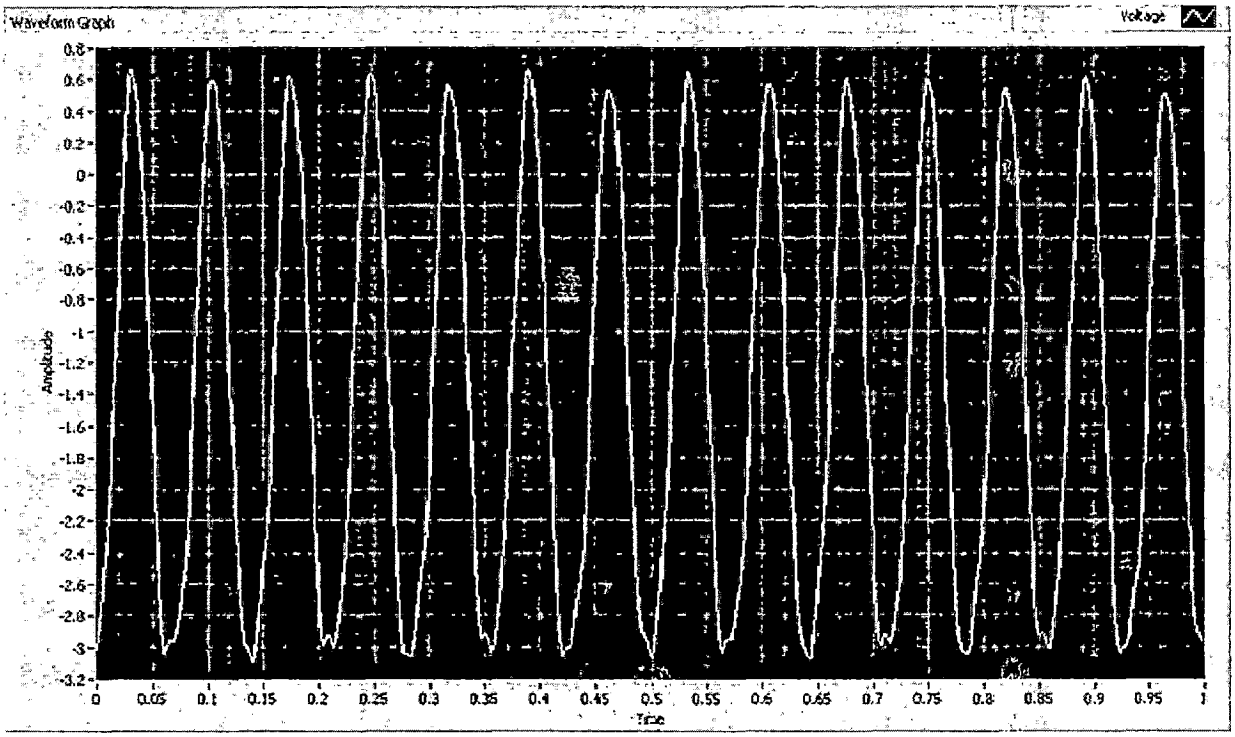

Figure 6.11: Amplitude uncontrolled, excitation by function generator

Figure 6.12: Amplitude controlled, excitation by function generator

In case of uncontrolled vibrations (figure 6.11), it can be seen that the range of the waveform is approximately 3.65 volts. But after proportional feedback control is applied, the same range reduces to about 2.25 volts. Hence, we observe a control of nearly 39%.

Readings similar to the ones shown above were obtained and tabulated. Following is a sample table for such readings:

Frequency (Hz)	Voltage (V)	Range (Uncontrolled)	Range (Controlled)	%Control
29	0.6	3.65	2.25	38.35
	0.8	4.9	2.95	39.79
	1	6.35	3.7	41.73
	1.2	7.5	4.45	40.66
	1.4	8.8	5.35	39.27
34	0.6	5.4	3.25	39.81
	0.8	7.2	4.2	41.66
	1	9.2	5.25	42.93
	1.2	11	6.4	41.81
	1.4	13	7.54	42
39	0.6	4.5	2.8	37.77
	0.8	5.75	3.5	39.13
	1	7.4	4.35	41.21
	1.2	9	5.35	40.55
	1.4	10.6	6.35	40.09

Table 6.7 Experimental readings for circular plate at angle (60 degrees) with single pair PZT patches configuration.

It can be seen from the above tables that, as the angle between points of excitation and sensor /actuator pair are increased, the vibration control of circular plate decreases. It can be seen from figure 6.13 given below for 28Hz excitation frequency,

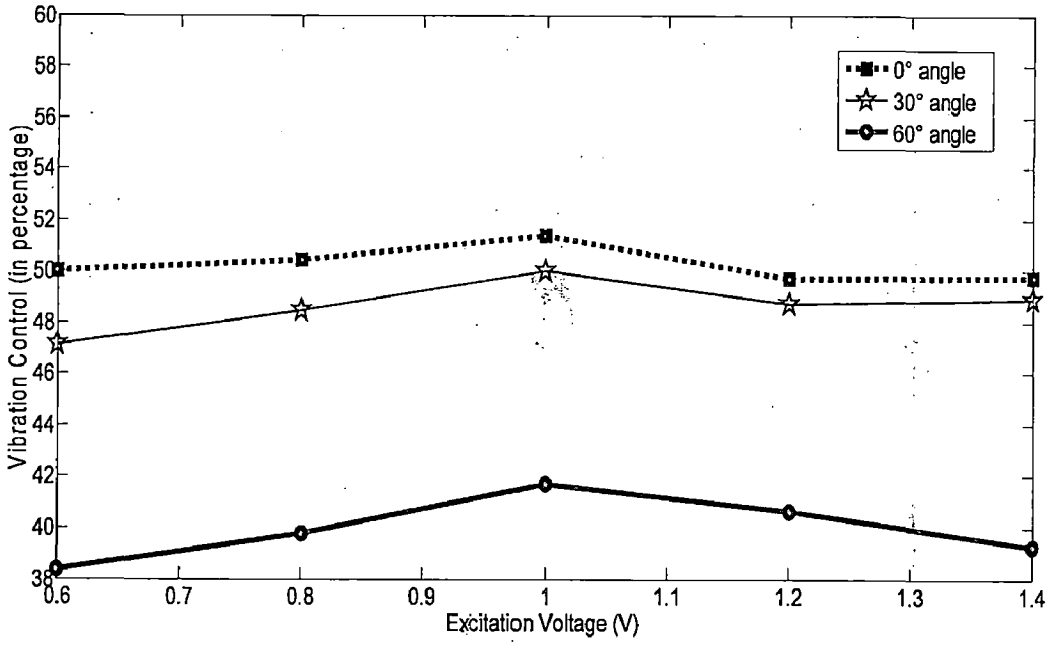

Figure 6.13: Plot for controlling action versus voltage for circular plate at different excitation angle

6.2.3 Understanding circular plate resonance: FFT (Fast Fourier Transform)

In order to have a better understanding of the circular plate's resonance, an FFT analysis was done using LabVIEW. This analysis enables us to find out the active frequencies of vibration, and more importantly, which one of these frequency components is more dominating at a particular configuration. The block diagram of the LabVIEW VI (Virtual Instrument) file used to analyse these FFTs is shown below:

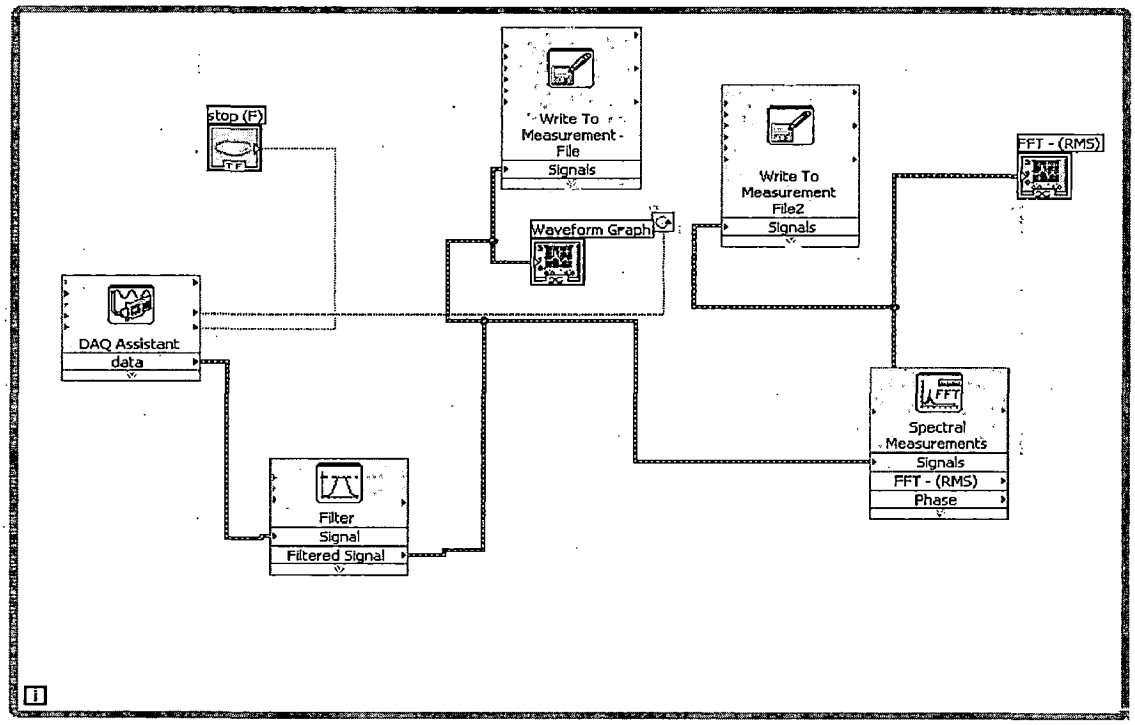

Figure 6.14: Block diagram of VI file used to analyses FFT of waveforms

The possibilities that can be examined are three: a general non resonance excitation, a resonance excitation with noise component involved and a resonance excitation without noise involved. All the three cases are presented one by one in the following figures:

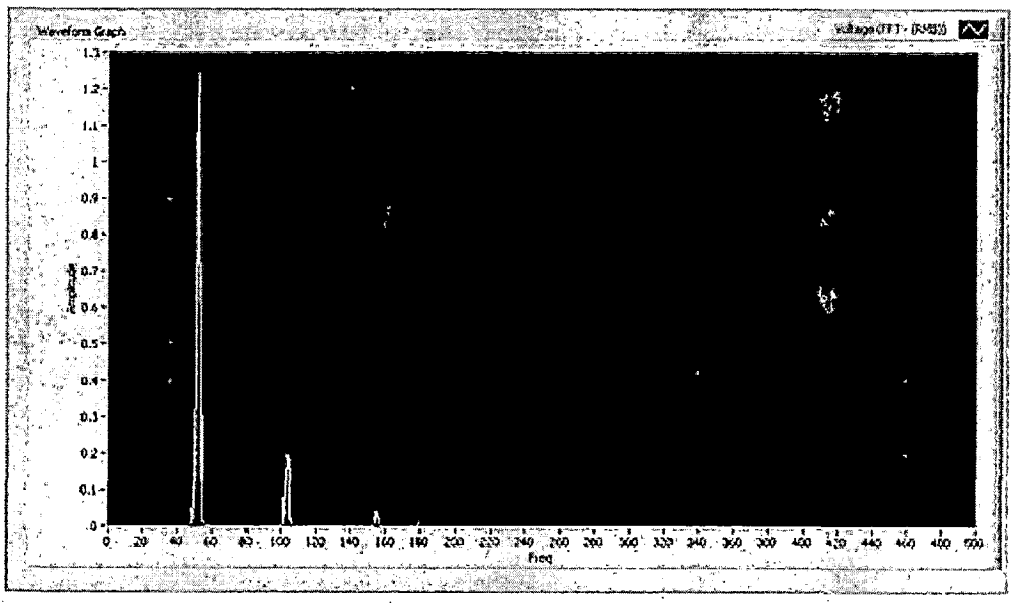

Figure 6.15: FFT for a general non resonance excitation

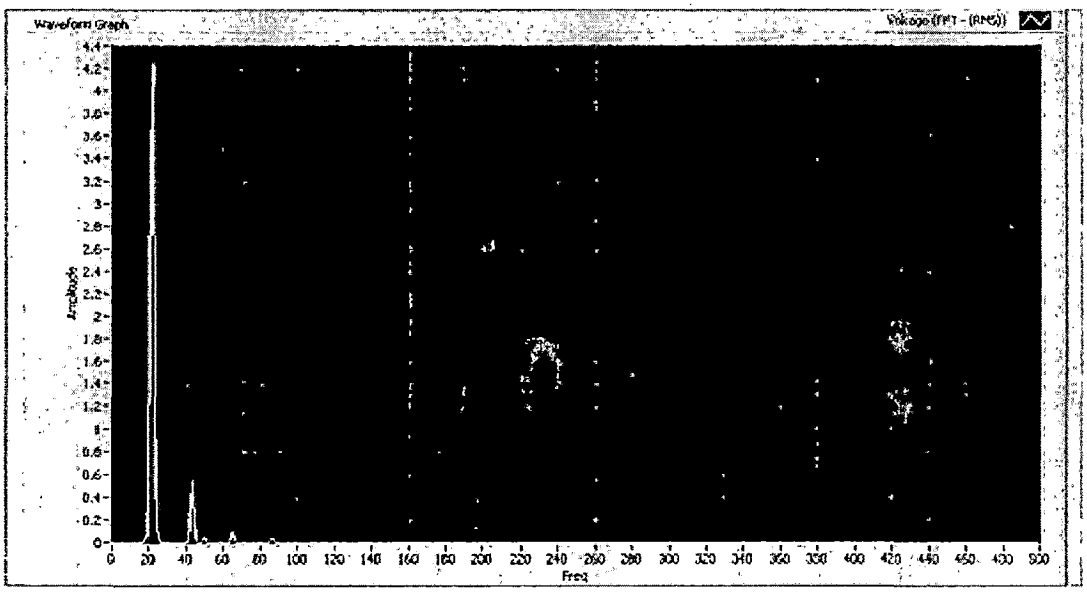

Figure 6.16: FFT for a resonance at which no noise emission occurs

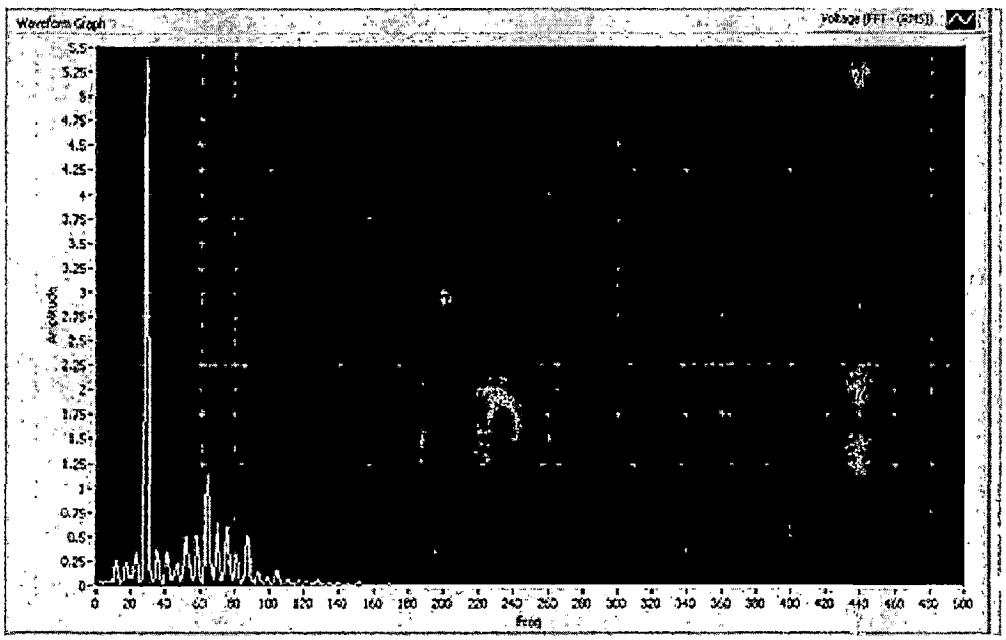

Figure 6.17: FFT for a resonance at which noise is emitted

From figure 6.15, it can be seen that at a general excitation frequency, the exciting frequency is the dominating frequency, while the other prevalent components are linear multiples of this frequency only.

Even at a resonance frequency, dominating frequencies are the applied frequency and its multiples. But some other frequency components also assume importance. This is evident from Figure- 6.16.

Figure 6.17 shows the frequency spectrum when noise is emitted at resonance. A large number of random frequency components start dominating and leading to unnecessary acoustic radiation. However, the most dominating component even in this case is the applied frequency only.

The experimental setup consists of a piezo voltage amplifier and a data acquisition card. The aluminum beam/circular plate with bonded piezoelectric sensors and actuators is excited by a function generator. The sensor reading is taken and stored in a computer using the LabVIEW software using a DAQ hardware interface.

Based on experimental study following conclusions are drawn:

7.1 Cantilever beam

(1) For proportional feedback control method, vibration reduction was observed to lie in the vicinity of 50 % experimentally. This was in tune with the fact that theoretically also, it was predicated that about 50 % vibration reduction should be achieved.

(2) It was noticed that controlling action reaches a maximum value at resonance frequencies. That is, as frequency of excitation is increased, vibration reduction increases as resonance approaches. At resonance, it reaches a peak value. Beyond resonance, it starts declining again.

The explanation for the phenomenon stated above is that a resonance, the amplitude of vibration becomes so large that the detrimental effect of the fixed component of instrument error present becomes negligible. At other frequencies, owing to smaller magnitudes of vibration amplitude, this component has measurable detrimental effect on the vibration reduction achieved.

(3) The vibration controlling action of cantilever beam is better with double pair PZT patches configuration than single patches configuration. It is observed that the vibration suppression increases as the coverage area of the actuator increases.

7.2 Circular plate

(1) Controlling action through proportional feedback control method was observed to lie around 50%, though significant deviations were observed from this median value.

The fact that about 50% controlling action was achieved for both cantilever and circular plate might give the illusion that similar amount of control is achieved. But in reality, the cantilever beam was much thicker than the circular plate. Hence, it is not possible to make a direct comparison of the percentage vibration reductions in each case. Based on the fact that the circular plate was much thinner, it can be judged that better control exists for cantilever beam.

(2) It was observed that instead of happening at a single frequency, resonance occurs over a range of frequencies. Further, this range varies with the angular separation between the point of excitation and the sensor placement.

This might be due to the fact that mode shapes that are struck are non symmetrical with respect to the relative placement of the sensor and the point of excitation.

(3) At some natural frequencies, resonance is accompanied by noise emission. It was observed that at such frequencies, percentage vibration reduction decreases substantially all of a sudden. In contrast, at natural frequencies at which resonance occurs without noise emission, percentage vibration reduction doesn't exhibit any untoward decrease. The reason for such a phenomenon remains unclear.

(4) The vibration controlling action of circular plate is better with double pair PZT patches configuration than single patches configuration. It is observed that the vibration suppression increases as the coverage area of the actuator increases.

(5) The relation between controlling action and the angular separation between point of excitation and sensor placement is inversely proportional. The vibration controlling action is reduces due to increase in the angle between point of excitation and sensor/actuator pair placement.

(6) FFT (Fast Fourier Transform) analysis of the waveform generated by the sensor PZT patch at various frequencies was done. It was found that in the absence of noise component, the dominating frequencies are the applied frequency and its multiples. When acoustic radiation is also emitted, a large number of random frequency components also become active.

8.1 Scope of Future Work

(1) PID feedback control method may be investigated experimentally to achieve even better control. This may be achieved in two ways:

i. A higher model of the NI Data Acquisition Card (6221 or higher) may be purchased. This would enable PID control using virtual instrumentation on LabVIEW software.

ii. A physical circuit may be built which achieves PID control of a current waveform. This method is much simpler and cost effective. However, a major limitation is accuracy and precision of control.

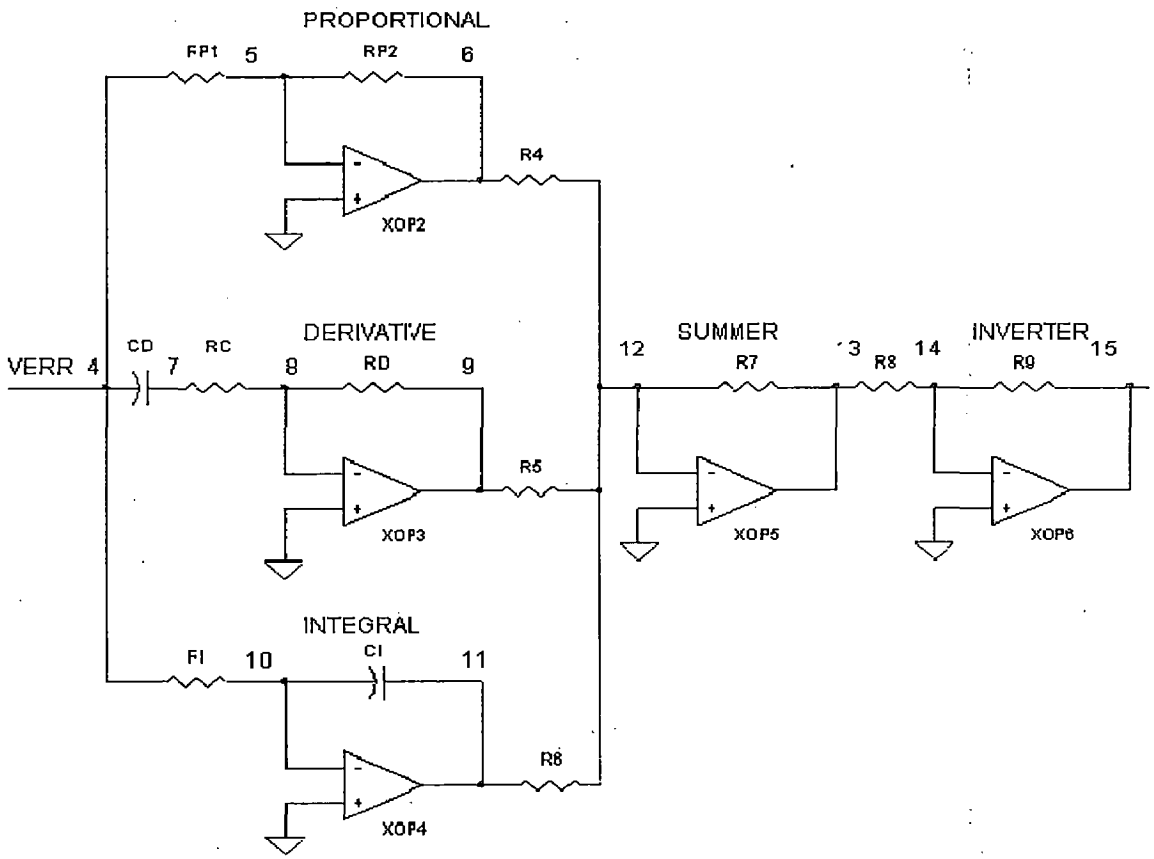

Figure 8.1: Circuit diagram for a PID circuit

In the above circuit diagram,

$$V_{out}(t) = \frac{R_{P2}}{R_{P1}} V_{in}(t) + \frac{1}{R_I C_I} \int V_{in}(t)\,dt + R_D C_D \frac{dV_{in}(t)}{dt}$$

(2) The phenomenon of reduction in controlling action due to noise emission for circular plate may be studied in more detail. Attempts can be made to explain this phenomenon in more detail, and possibly to quantify it as a function of the decibels (dB) of noise emitted.

(3) Now that active vibration control has been demonstrated for a static circular plate, the next possibility that can be considered is that of a rotating circular plate. This case finds immense applications in real life engineering problems. In fact, with suitable modifications, the rotating circular plate can be converted to a scaled model of rotating rotor blades, which resemble those in helicopters or wind generators.

(4) Similar analysis can be performed for change in the operation mode, i.e. use of piezo sensing and actuation system can be completely replaced with the help of a computer with input output interface device or PZT can be replaced with other sensing device like MFC.

[1]. Akella Padma, Chen Xin, Cheng Weiying, Hughes Declan and T Wen John, "Modeling and control of smart structures with bonded piezoelectric sensors and actuators", *journal of Smart Material and Structure, Vol 3*, 1994, pp 344-353.

[2]. Akhras Georges, "Smart Materials and Smart Systems for the Future", *Canadian Military Journal*, Autumn 2000, pp 25-32.

[3]. Al-hazmi Mohammed W., "Finite Element Analysis of Cantilever Plate Structure Excited by Patches of piezoelectric Aotuators", *Institute of Electrical and Electronics Engineers, Inc Vol 978-1-4244-1701-8/08*, 2008, pp 809-814.

[4]. Barrault Guillaume, Halim Dunant, Hansen Colin and Lenzi Arcanjo, "High frequency spatial vibration control for complex structures", *Applied Acoustics, vol 69*, 2008, pp 933–944.

[5]. Brennan M J, Day M J, Elliot S J and Pinnington R J, "The active vibration control", *International Union of Theoretical and Applied Mechanics, Symposium, University of Bath, UK,* 1994, pp 263-274.

[6]. Bronowicki A J, McIntyre L J, Betros R S and Dvorsky G R , "Mechanical validation of smart structures", *journal of Smart materials and structures, vol 5*, 1995, pp 129-139.

[7]. Crawley E. F. and Lazarus K. B.,"Induced Strain Actuation of Isotropic and Anisotropic plate", *AIAA Journal, vol 29*, 1991, pp 944-952.

[8]. Crawley E F and Luis Javier de, "Use of piezoelectric actuators as elements of integrated structure", *AIAA Journal, vol 25*, 1987, pp 1373-1385.

[9]. Damaren Christopher J, "Optimal location of Collocated Piezo-actuator/sensor Combinations in Spacecraft Box Structures", *Journal of smart Materials and Structures, Vol 12*, 2003, pp494-499

[10]. Dhuri K D and Seshu S., "Favorable locations for Piezo Actuators in Plates with good Control Effectiveness and Minimal Change in System Dynamics", *Journal of Smart Materials and Structures, Vol 16*,2007,pp 2526-2542

[11]. Dimitriadis E K, Fuller C. R and Rogers C. A, "Piezoelectric Actuators for Distributed Vibration Excitation of Thin Plates", *journal of Vibration and Acoustics, Vol 113*, 1991, pp 100-106

[12]. Fei Juntao and Fang Yunmei, "Active Feedback Vibration Suppression of a Flexible Steel Cantilever Beam Using Smart Materials", *Proceedings of the First International Conference on Innovative Computing, Information and Control (ICIC1C'06)*, IEEE, 2006, pp 1-4.

[13]. Halim Dunant and Cazzolato Ben S, "A multiple-sensor method for control of structural vibration with spatial objectives", *journal of sound and vibration, vol 296,* 2006, pp 226-242.

[14]. Halim Dunant and Moheimani S O Reza, "An optimization approach to optimal placement of collocated piezoelectric actuators and sensors on a thin plate", *Mechatronics, Vol 13*, 2003, pp 27-47.

[15]. Han J.H., Rew K.H. and Lee In, "An experimental study of active vibration control of composite structures with a piezo-ceramic actuator and a piezo-film sensor", *journal of Smart material and structure, vol 6,* 1997, pp 549-558.

[16]. Hiramoto K, Doki H and Obinata G, "Optimal sensor/actuator placement for active vibration control using explicit solution of algebraic Riccati equation", *Journal of sound and vibration, Vol 229*, 2000, pp 1057-1075.

[17]. Hu Yan-Ru and Ng Alfred, "Active Robust Vibration Control of a Circular Plate structure using Piezoelectric Actuators", *43rd American Institute of Aeronautics and Astronautics /ASME/ASCE/AHS/ASC Structures, Structural Dynamics, and Materials Conference,* 22-25 April 2002. Denver, Colorado.

[18]. Hwang Woo-seok, Hwang Woonbong, and Park Hyun Chul, "Vibration Control of laminated Composite Plate with Piezoelectric sensor/actuator: Active and Passive Control Methods", *Journal of Mechanical System and Signal Processing, Vol 8(5),* 1994, pp 571-583.

[19]. Karagulle H., Malgaca L. and Oktem H. F., "Analysis of Active Vibration Control in Smart Structures by ANSYS", *Journal of Smart Materials and Structures, Vol 13*, 2004, pp 661-667

[20]. Keir John, Kessissogolu Nicole J and Norwood Chris J, "Active control of connected plates using single and multiple actuators and error sensors", *Journal of sound and vibration, Vol 281*, 2004, pp 73-97.

[21]. Kovalovs E.A., Barkanov S. and Gluhihs."Active Control of Structures using Macro-fiber Composite (MFC)", *Functional Materials and Nanotechnologies (FM&NT 2007), Journal of Physics: Conference Series, Vol 93*,2007, 012034

[22]. Kumar Ramesh K. and Narayanan S., "Active Vibration Control of Beam with Optimal Placement of Piezoelectric Sensor/ Actuator pairs", *Journal of Smart Materials & Structures, Vol 17*,2008,pp 1-15.

[23]. Kurpaa Lidia, Pilguna Galina and Amabilib Marco, "Nonlinear vibrations of shallow shells with complex boundary: R-functions method and experiments", *journal of Sound and Vibration, vol 306*, 2007, pp 580–600.

[24]. Lee Y Y and Yao J, "Structural Vibration suppression using the piezoelectric sensors and actuators", *Journal of Vibration and Acoustics, Vol 125*, 2003, pp 109-113.

[25]. Mehrdad Ghasemi-Nejhad, Russ Richard and Pourjalali Saeid, "Manufacturing and testing of active composite panels with embedded piezoelectric sensors and actuators", *Journal of intelligent material systems and structures, vol 16*, 2005, pp 319-333

[26]. Moita Jose M. Simoes, Soares Cristovao M. Mota and Soares Carlos A. Mota, "Active Control of Forced Vibrations in Adaptive Structures using a Higher Order Model", *Journal of Composite Structures, Vol 71*, 2005, pp 349-355.

[27]. Nagaia K, Maruyamaa S, Muratab T and Yamaguchi T, "Experiments and analysis on chaotic vibrations of a shallow cylindrical shell-panel", *journal of Sound and Vibration, vol 305*, 2007, pp 492–520.

[28]. Obe O. Ibidapo, "Optimal actuators placements for the active control of flexible structures", *Journal of mathematical analysis and applications, Vol 105*, 1985, pp 12-25.

[29]. Park Gyuhae, Ruggiero Eric and Inman Daniel J, "Dynamic testing of inflatable structures using smart materials" , *journal of Smart Material and Structure, vol 11*, 2002, pp 147–155.

[30]. Peng X.Q, Lam K.Y, and Liu G R, "Active Vibration Control of Composite Beams with Piezoelectric: A Finite Element Model with Third Order Theory", Journal of Sound and Vibration, Vol 209(4), 1998, pp 635-650.

[31]. Qiu Jinhao and Haraguchi Masakhazu, "Vibration control of a plate using a self-sensing piezoelectric actuator and an adaptive control approach", *Journal of intelligent material systems and structures, vol 17*, 2006, pp 661-669.

[32]. Qiu Zhil-cheng, Zhang Xian-min, Wu Hong-xin and Zhang Hong-hua,"Optimal Placement and Active Vibration Control for Piezoelectric Smart Flexible Cantilever Plate", *Journal of Sound and Vibration, Vol 301*,2007,pp 521-543.

[33]. Quek S T, Wang S Y and Ang K K , "Vibration control of composite plate via optimal placement of piezoelectric patches", *Journal of intelligent materials and structures, vol 14*, 2003, pp 229-245.

[34]. Reddy J. N., "On Laminated Composite Plates with Integrated Sensors and Actuators", *Journal of Engineering Structures, Vol 21*, 1999, pp 568-593

[35]. Reddy J.N., "Theory and Analysis of Elastic Plates", *Taylor & Francis, Philadelphia, PA 19106, ISBN 1-56032-705-7*, 1998, pp 179-247.

[36]. Sekouri EI Mostafa, Hu Yan-Ru and Ngo Anh Dung, "Modeling of a Circular Plate with Piezoelectric Actuators", *Journal of Mechatronics, Vol 14*, 2004, pp 1007-1020

[37]. Sethi Vineet and Song Gangbing, "Multimodal Vibration Control of a Flexible Structure using Plezoceramics", *Proceedings of the 2005 IEEE/ASME, International Conference on Advanced Intelligent Mechatronics, Monterey, California, USA,* 24-28 July, 2005

[38]. Smithmaitrie P, Tzou H S, "Micro-control actions of actuator patches laminated on hemispherical shells", *journal of Sound and Vibration, vol 277*, 2004, pp 691–710.

[39]. Thomson B.S., Gandhi M. V. and Kasiviswanathan S, "An Introduction to Smart Materials and Structures", *Materials and Design, Vol 13*, 1992,pp 3-9

[40]. Tiersten H.F., "Linear Piezoelectric Plate Vibrations", *Plenum Press, New York,* 1969, pp 33-36,51-61

[41]. Tzou H S, "A new distributed sensor and actuator shell theory for intelligent shell", *journal of Sound and Vibration, vol 153,* 1992, pp 335-349.

[42]. Van H Nguyen, Mai-Duy N and Tran-Cong T, "Free vibration analysis of laminated plate/shell structures based on FSDT with a stabilized nodal-integrated quadrilateral element", *journal of Sound and Vibration, vol 313,* 2008, pp 205–223.

[43]. Wang S.Y., Quek S.T. and Ang K K, "Dynamic Stability Analysis of Finite Element Modeling of Piezoelectric Composite plates", *International Journal of Solids and Structures, Vol 41,* 2004, pp 745-764

[44]. Wang S. Y.,Tai K., Quek S T, "Topology Optimization of Piezoelectric Sensors/Actuators for Torsional Vibration Control of Composite plates", *Journal of Smart Materials and Structures, Vol 15,*2006, pp 253-269

[45]. Yue H H, Deng Z Q and Tzou H S, "Optimal actuator locations and precision micro-control actions on free paraboloidal membrane shells", *Communications in Nonlinear Science and Numerical Simulation, vol 13,* 2008, pp 2298–2307.

[46]. Zhang Yahong, Niu Hongpan, Xie Shilin and Zhang Xinong, "Numerical and experimental investigation of active vibration control in a cylindrical shell partially covered by a laminated PVDF actuator", *journal of Smart Material and Structure., vol 17,*2008, pp 12-24.

[47]. http://www.hk-phy .org

[48]. http://www.smart.tamu.edu

[49]. http://www.azom.com

[50]. http://www.physikinstrument.com

[51]. http://www.virtualskies.arc.nasa.gov

[52]. http://www.physicsmail.org